SNE SIMULATION NOTES EUROPE

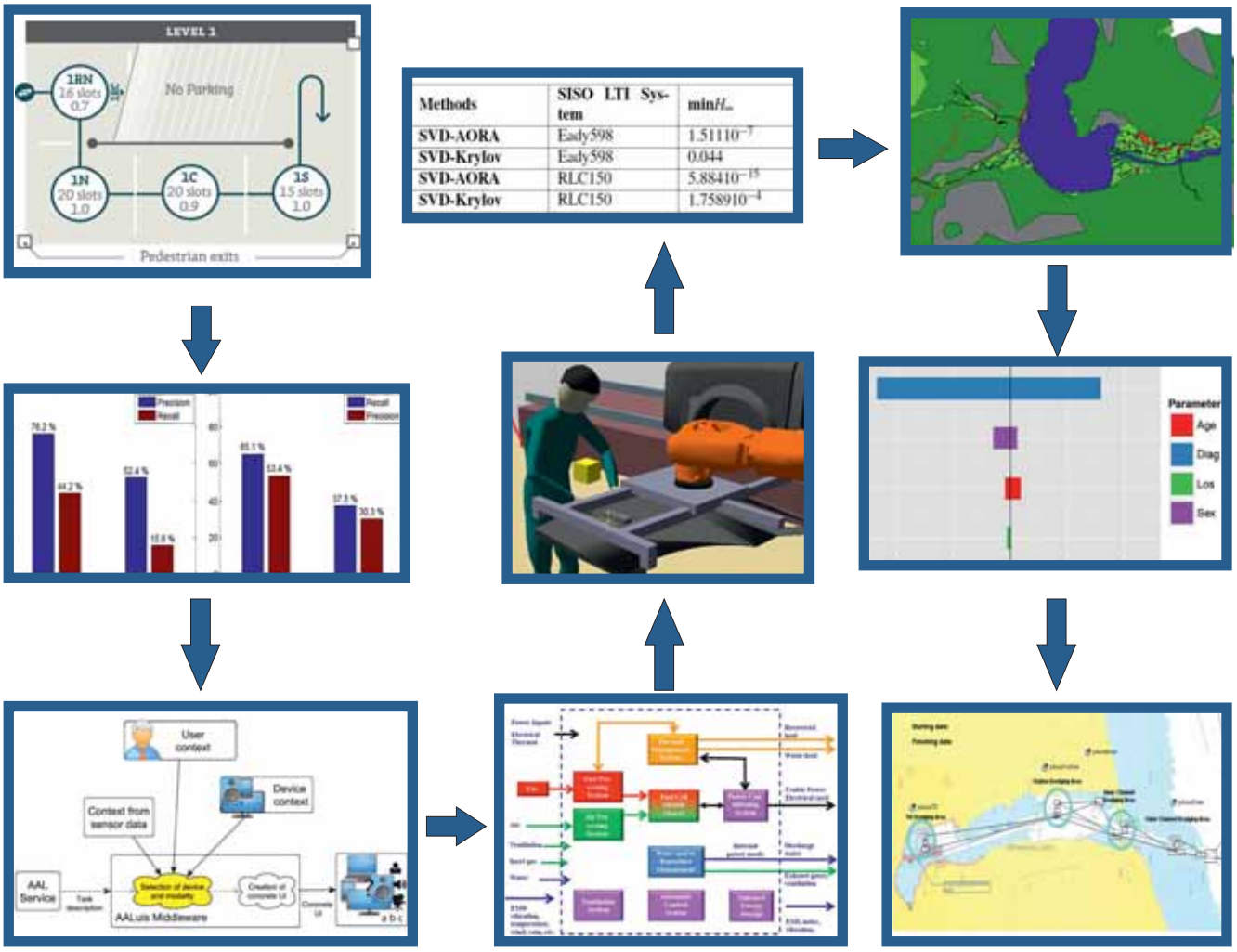

Volume 26 No.1 March 2016 doi: 10.11128/sne.26.1.1032

Journal on Developments and Trends in Modelling and Simulation

Membership Journal for Simulation Societies and Groups in EUROSIM

Print ISSN 2305-9974
Online ISSN 2306-0271

ARGESIM

EUROSIM 2016

9th EUROSIM Congress on Modelling and Simulation

City of Oulu, Finland, September 12 – 16, 2016

EUROSIM Congresses are the most important modelling and simulation events in Europe. For EUROSIM 2016, we are soliciting original submissions describing novel research and developments in the following (and related) areas of interest: Continuous, discrete (event) and hybrid modelling, simulation, identification and optimization approaches. Two basic contribution motivations are expected: M&S Methods and Technologies and M&S Applications. Contributions from both technical and non-technical areas are welcome.

Congress Topics The EUROSIM 2016 Congress will include invited talks, parallel, special and poster sessions, exhibition and versatile technical and social tours. The Congress topics of interest include, but are not limited to:

- Intelligent Systems and Applications
- Hybrid and Soft Computing
- Data & Semantic Mining
- Neural Networks, Fuzzy Systems & Evolutionary Computation
- Image, Speech & Signal Processing
- Systems Intelligence and Intelligence Systems
- Autonomous Systems
- Energy and Power Systems
- Mining and Metal Industry
- Forest Industry
- Buildings and Construction
- Communication Systems
- Circuits, Sensors and Devices
- Security Modelling and Simulation
- Bioinformatics, Medicine, Pharmacy and Bioengineering
- Water and Wastewater Treatment, Sludge Management and Biogas Production
- Condition monitoring, Mechatronics and maintenance
- Automotive applications
- e-Science and e-Systems
- Industry, Business, Management, Human Factors and Social Issues
- Virtual Reality, Visualization, Computer Art and Games
- Internet Modelling, Semantic Web and Ontologies
- Computational Finance & Economics
- Simulation Methodologies and Tools
- Parallel and Distributed Architectures and Systems
- Operations Research
- Discrete Event Systems
- Manufacturing and Workflows
- Adaptive Dynamic Programming and Reinforcement Learning
- Mobile/Ad hoc wireless networks, mobicast, sensor placement, target tracking
- Control of Intelligent Systems
- Robotics, Cybernetics, Control Engineering, & Manufacturing
- Transport, Logistics, Harbour, Shipping and Marine Simulation

Congress Venue / Social Events The Congress will be held in the City of Oulu, Capital of Northern Scandinavia. The main venue and the exhibition site is the Oulu City Theatre in the city centre. Pre and Post Congress Tours include Arctic Circle, Santa Claus visits and hiking on the unique routes in Oulanka National Park.

Congress Team: The Congress is organised by SIMS - Scandinavian Simulation Society, FinSim - Finnish Simulation Forum, Finnish Society of Automation, and University of Oulu.
Esko Juuso EUROSIM President, Erik Dahlquist SIMS President, Kauko Leiviskä EUROSIM 2016 Chair

Info: eurosim2016.automaatioseura.fi, office@automaatioseura.fi

Editorial

Dear Readers – *SNE Volume 26 (2016) comes along with an extension but sharpening of orientation, and with minor changes in publication structure. Simulation itself has developed further on, with enhancements towards model-based design, computational complex systems and model-based analysis of big data – 'new' subjects of interest for SNE – but at concentrating on the simulation circle and not only on one part. SNE publishes four issues a year, but for many years third and fourth issue have been combined to a double issue; from 2016 on, SNE will have four separate issues, with more pages than the years before.*
This issue, SNE26(1), the first issue of SNE vol.26, shows this broad and enlarging variety of simulation. The title page is a graphical list of content, guiding through multifaceted topics of simulation: modelling garage parking, model-based human activity pattern recognition , model-base IO device selection for ambient environments, semulations of fuel cells, simulation-based planning of human-machine-collaboration, model order reduction for efficient simulation, agent-based simulation for virtual experimental archaeology, microsimulation of burden of mental diseases, and network-based simulation for equipment selection in water construction –

I would like to thank all authors for their contributions, and the editorial board members for review and support, and the organizers of the EUROSIM conferences for co-operation in post-conference contributions. And last but not least thanks to the Editorial Office (please note change of address of the Editorial Office) for layout, typesetting, preparations for printing, and web programming for electronic publication of this SNE issue.

Felix Breitenecker, SNE Editor-in-Chief, eic@sne-journal.org; felix.breitenecker@tuwien.ac.at

Contents SNE 26(1)

SNE doi: 10.11128/sne.26.1.1032

SNE Contact & Info

SNE Print ISSN 2305-9974, SNE Online ISSN 2306-0271

→ *www.sne-journal.org*
✉ *office@sne-journal.org, eic@sne-journal.org*

✉ SNE Editorial Office, Andreas Körner
ARGESIM / Math. Modelling & Simulation Group,
Vienna Univ. of Technology /101,
Wiedner Haupstrasse 8-10, 1040 Vienna , Austria

SNE Simulation Notes Europe

WEB: → *www.sne-journal.org*, DOI prefix 10.11128/sne

Scope: Technical Notes, Short Notes and Overview Notes on developments and trends in modelling and simulation in various areas and in application and theory; benchmarks and benchmark documentations of ARGESIM Benchmarks on modelling approaches and simulation implementations; modelling and simulation in and for education, simulation-based e-learning; society information and membership information for EUROSIM members (Federation of European Simulation Societies and Groups).

Editor-in-Chief: Felix Breitenecker, Vienna Univ. of Technology, Math. Modelling and Simulation Group
✉ *Felix.Breitenecker@tuwien.ac.at,* ✉ *eic@sne-journal.org*

Layout / Administration: A. Körner, A. Mathe, J. Tanzler, C. Wytrzens, et al.; ✉ *office@sne-journal.org*

Print SNE: Grafisches Zentrum, Vienna Univ. of Technology, Wiedner Hauptstrasse 8-10, 1040, Vienna, Austria

Online SNE: ARGESIM /ASIM, address below

Publisher: ARGESIM Arbeitsgemeinschaft Simulation News
c/o Math. Modelling and Simulation Group,
Vienna Univ. of Technology / 101, Wiedner Hauptstrasse 8-10,
1040 Vienna, Austria; *www.argesim.org,* ✉ *info@argesim.org*
on behalf of ASIM *www.asim-gi.org* and EUROSIM
→ *www.eurosim.info*

SNE Editorial Board

SNE - Simulation Notes Europe is advised and supervised by an international scientific editorial board. This board is taking care on peer reviewing and handling of *Technical Notes*, *Education Notes*, *Short Notes*, *Software Notes*, *Overview Notes*, and of *Benchmark Notes* (definitions and solutions). At present, the board is increasing (see website):

SNE Aims and Scope

Simulation Notes Europe publishes peer reviewed contributions on developments and trends in modelling and simulation in various areas and in application and theory, with main topics being simulation aspects and interdisciplinarity.
Individual submissions of scientific papers are welcome, as well as post-conference publications of contributions from conferences of **EUROSIM** societies.

SNE welcomes also special issues, either dedicated to special areas and / or new developments, or on occasion of vents as conferences and workshops with special emphasis.

Furthermore **SNE** documents the **ARGESIM Benchmarks** on *Modelling Approaches and Simulation Implementations* with publication of definitions, solutions and discussions (*Benchmark Notes*). Special *Educational Notes* present the use of modelling and simulation in and for education and for e-learning. **SNE** is the official membership journal of **EUROSIM**, the Federation of European Simulation Societies. A News Section in **SNE** provides information for **EUROSIM** Simulation Societies and Simulation Groups.

SNE is published in a printed version (Print ISSN 2305-9974) and in an online version (Online ISSN 2306-0271). With **Online SNE** the publisher **ARGESIM** follows the **Open Access** strategy, allowing download of published contributions for free – identified by a DOI (Digital Object Identifier) assigned to the publisher **ARGESIM** (DOI prefix 10.11128).

Print SNE, high-resolution **Online SNE**, full **SNE Archive**, and source codes of the *Benchmark Notes* are available for members of **EUROSIM** societies.

Author's Info. Authors are invited to submit contributions which have not been published and have not being considered for publication elsewhere to the **SNE** Editorial Office. Furthermore, SNE invites organizers of EUROSIM conferences to submit post-conference publication for the authors of their conferences.
SNE distinguishes different types of contributions (*Notes*):

- *Overview Note* – State-of-the-Art report in a specific area, up to 14 pages, only upon invitation
- *Technical Note* – scientific publication on specific topic in modelling and simulation, 6 – 10 pages
- *Education Note* – modelling and simulation in / for education and e-learning; 6 - 8 pages
- *Short Note* – recent development on specific topic, max. 6 p.
- *Software Note* – specific implementation with scientific analysis, 4 – 6 4 pages
- *Benchmark Note* – Solution to an ARGESIM Benchmark; commented solution 4 pages, comparative solutions 4-8 pages

Further info and templates (doc, tex) at **SNE's** website.
www.sne-journal.org

Modeling Garage Parking

Oliver Ullrich[1*], Charaf Azzouzi[1], Benjamin Brandt[1],

Daniel Lückerath[2], Naphtali Rishe[1]

[1]School of Computing and Information Sciences, Florida International University, ECS 243C, 11200 SW 8th St, Miami FL-33199, USA; *oullrich@cs.fiu.edu*

[2]Institut für Informatik, Universität zu Köln, Weyertal 121, 50931 Köln, Germany

Simulation Notes Europe SNE 26(1), 2016, 1-8
DOI: 10.11128/sne.26.tn.10321
Received: March 11, 2016 (Selected ASIM STS/GMMS 2016 Postconf. Publ.)
Accepted: March 20, 2016;

Abstract. Described is a simulation model of cruising for garage parking, intended both for the calibration and evaluation of real-time parking recommendation methods, and as a base for predictive guidance to available parking. The model combines the event-based and agent-based simulation approaches to represent the parking garage and the driver behavior. It is validated by simulating a real-world parking garage and comparing the model's output with observations. The validation results show the model's capability to predict a garage's state over the course of an operational day, even though specific results are not yet precise enough for the intended use.
After an introduction to scope and aims, the paper shares some background on garage parking and related work, followed by a description of the simulation model, and its validation based on a representation of a real-world parking garage.

Introduction

With a significant part of inner city traffic consisting of drivers cruising for parking (on average 30%, see [1]), and with ever growing parking garages containing 2,000 or more individual parking slots (see figure 1), computer based systems providing predictive recommendations to find available parking in these major structures are significantly beneficial to users, and also improve resource utilization for infrastructure providers. One way to predict availability of parking slots is by simulation, starting out from the real-time state of the garage. Even if a parking guidance system is not predictive, but only considers real-time information, its strategies have to be carefully calibrated and evaluated before their application in the field. Another use of a garage parking model is therefore to evaluate recommendation strategies in a simulated environment.

Figure 1: A parking garage with approx. 2,000 parking spaces on six levels.

This paper presents a simulation model of cruising for parking in parking garages, which will serve both as a prediction model, and as a virtual testbed for calibrating and evaluating garage parking guidance algorithms. The model applies a combination of two simulation approaches: while the basic mechanics, e.g. the arrival of cars, are modeled in an event-based fashion (see [2]), the agent-based paradigm (see [3]) is utilized for modeling the drivers' decision making behavior.

The paper continues with sharing some background of garage parking modeling and related work (section 1), followed by the presentation of the simulation model (section 2), representing both the parking garage and the individual driver's behavior. Then, the model's output is validated based on a real-world example (section 3). The paper closes with a summary of the lessons learned and a short outlook on future work (section 4).

1 Background

1.1 Garage Parking

The term garage parking refers to the process of entering a building at least partially designated for car parking, finding and navigating to an available parking slot, leaving the car unoccupied at that slot for a while, and then de-park by finding the shortest or most convenient path from the parking slot to a vehicular exit. As the intended application for the developed model is to test recommendation algorithms which are concerned with reducing the time spent cruising for available parking, the last part of the process, de-parking, is beyond the scope of this paper and will not be discussed further. The described buildings are often referred to as parking garages, but also as multistorey car parks, parkades, or parking structures.

Garage parking, together with parking lot parking, is often described by the more general term off-street parking. This contrasts with on-street parking with its diverse modes, e.g. parallel parking, angular parking, perpendicular parking.

The parking garage usually consists of a number of connected levels, which are themselves composed of a number of areas. Each area contains a set of parking slots fit for individual cars. The readers will know this decomposition from their own experience: "I parked my car in a slot on level 3, in area C."

Vehicular access to the parking garage is granted, often at the ground floor, by entry and exit lanes, which are usually unidirectional. Pedestrians access the garage via elevators or stairways, or on the ground floor by doorways. Pedestrian access ways are usually bidirectional.

1.2 Related work

Corresponding to its importance in planning and design of public spaces, on-street parking has seen a lot of research attention, both in general modeling (see e.g. [4], [5], [6], [7], [1], [8], [9], [10]) and in simulation modeling (see [11], [12], [13], [14], [15], [16]). Most of the more recent simulation models are at least partially agent-based (see [11], [12], [14], [15]). Dieussaert et al. (see [12]) and Horni et al. (see [14]) combine agent-based modeling with the cellular automata paradigm, while Gallo et al. (see [13]) construct a multi-layer network supply model. Some authors (see [12], [15]) utilize the described models to evaluate pricing and other policy considerations, while others (see [11], [13], [14], [16]) apply them to analyze technical methods to reduce cruising time and thereby traffic in general.

Only a few models (see [17], [11], [12], [8]) consider off-street parking: Asakura and Kashiwadani (see [17]) apply a model to examine the effect of different types of on-street and off-street parking availability information on overall system performance, but do not examine the drivers' behavior inside of individual parking lots. Benenson et al. (see [11] and also [6]) develop a spatially explicit model of parking search and choice, with simulated drivers cruising through an artificial or real-life city center model, giving them both on-street and off-street parking options. Dieussaert et al. (see [12]) also are interested in the traffic patterns generated by cruising for parking. They model on-street parking as well as parking lots and garages, but consider parking lots and garages as simple sinks, not modeling their interior. Van der Waerden et al. (see [8]) develop a simple cellular automata based sub-model for choosing parking spaces inside a parking lot, but clearly set their focus on modeling traffic patterns resulting from the whole, city-wide process of traveling and parking.

None of the described models considering off-street parking is detailed enough for the evaluation of garage parking recommendation systems.

2 Modeling Garage Parking

An agent-based model usually includes two components (see [3]): the agents themselves, and the environment they interact with.

The agents are usually self-contained and autonomous; they have attributes whose values change over the course of a simulation run. Their behavior is determined by a set of rules, and they interact dynamically with other agents and the environment they exist in. In more complex models, agents are often goal-directed and adaptive, and may even be heterogeneous. Individual agents usually only interact with a local subset of the environment and other agents, and therefore consider only local information.

In addition to their communication with their set of neighbors, agents interact with their environment. This information might provide only basic information, e.g. the agent's position in the environmental model. It may also provide more detailed information, e.g. the capacity and real-time rate of occupancy of parking garage areas. While in many cases the environment might be

modeled as an attributed graph structure, it sometimes is built as a complex simulation itself, e.g. based on cellular automata.

In the proposed model (which is based on a simpler model described in [18]), drivers and their cars are modeled as agents adhering to a set of rules and acting on local information, while the parking garage is modeled as an attributed neighborhood graph, and constitutes the agents' environment.

2.1 Modeling parking garages

The parking garage is modeled as an attributed graph $G(A,E)$ representing the garage's layout and the internal neighborhood relations. A node $a \in A$ represents an area of the parking garage, an edge $e(a_i,a_j) \in E$ with $a_i, a_j \in A$ represents a direct connection between two areas a_i and a_j which is traversable by car. If all lane segments in the parking garage are two-way, the garage can be modeled as an undirected graph. If some or all segments only allow for one-way traffic, a directed graph can be established. As it is the garage planner's basic objective to ensure reachability of each parking area, the graph consists generally only of one connected component.

Each node $a \in A$ is attributed by its total number of parking slots z_a, the number of currently occupied slots $o_a(t)$ at time t, by extension also the number of free slots $f_a(t) = z_a - o_a(t)$ at time t, and the average time r_a a car needs to traverse and search the area. The recommendation methods to be tested (see [19]) explicitly consider only these areas, and do not depict individual parking slots. Therefore, a spatially explicit modeling of these individual slots is not necessary.

Each edge $e(a_i,a_j) \in E$ is attributed by a time r_e a car needs to move from area a_i to area a_j. In cases where areas are directly adjoining, $r_e = 0$ can be assumed.

In this simplified model we assume an infinite traversal capacity for nodes and edges, therefore ignoring congestion resulting from multiple cars cruising the same area.

The garage's entry lanes are modeled as special nodes $a_e \in A_e \subset A$ with $z_{a_e} = 0$, which serve as sources for the transient car agents. As is customary in discrete modeling (see [2], pp. 209-210), interarrival times are approximated with an exponential distribution with an arrival rate of $\lambda_{a_e}(t)$. The distribution parameter is established for each entry lane a_e and each period t by input data analysis. Technically, the agents are generated by the event-based framework at each entry node at appropriately distributed simulation times.

Figure 2 shows a simplified layout of a parking garage level, while figure 3 shows the corresponding partial model graph.

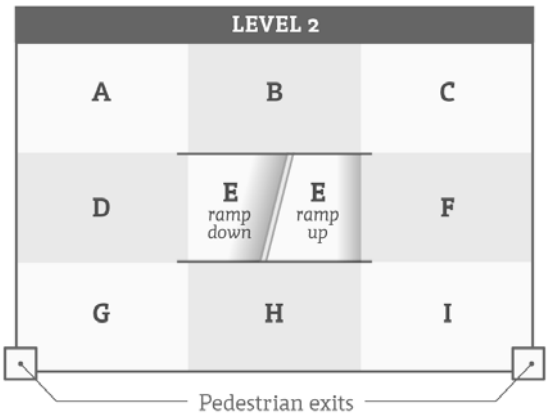

Figure 2: Simplified parking garage level with two pedestrian exits, two bi-directional ramps, and nine areas.

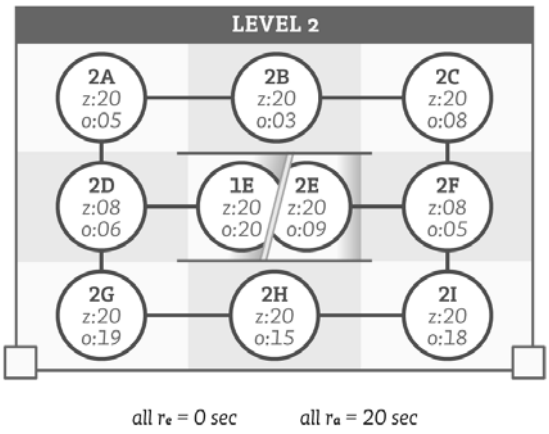

Figure 3: Partial model graph of a parking garage level.

2.2 Modeling driver behavior

Agents enter the model from one of the entry lane nodes $a_e \in A_e$, and in the course of the simulation move iteratively from node a_i to node a_j along edge $e(a_i,a_j) \in E$. On any given node $a_i \in A$ the agent, after spending a time of r_{a_i} searching the area for available parking, has to take two decisions: It has to decide whether to park in the current area (parking decision), and, if not, where to go next (routing decision).

To enable the agents to take these decisions, the model considers a number of aspects:

Basic routing: To avoid moving in an infinite loop, an agent administers a counter $v(a_i)$ representing the number of times an area a_i has been visited by that agent. If an agent always chooses one of the routing options a_j with the lowest $v(a_j)$, every loop will eventually be broken. In addition, as cars are rarely seen to turn on the spot in a parking garage, agents can never move onto the area they just left.

Attractiveness: The model assumes that a driver prefers to park in a slot which is as attractive as possible. The model therefore assumes an order of attractiveness on a parking garage's areas: $1.0 \geq c(a_{i_1}) \geq \ldots \geq c(a_{i_n}) \geq 0.0$ (see figure 4). Agents prefer areas with greater values of $c(a_i)$ to areas with lower attractiveness. Attractiveness orders are individual to classes of drivers, i.e. customers with distinct destinations. For example, during the day 40% of customers might desire to park as close to a supermarket as possible, while 60% might be attracted by parking slots near a hospital. These distributions could change over the time of day, e.g. when the hospital closes for the evening, but a neighboring cinema starts to attract parking visitors in another region of the parking garage. As these classes of preferences are generally shared by many drivers, only a few different orders of attractiveness represent all drivers' intentions for any given garage.

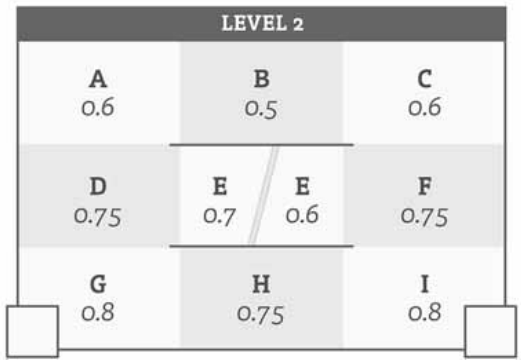

Figure 4: Parking garage level with attractiveness values.

Real-time availability: Drivers also consider real-time availability: if they observe that no spaces are available in a specific area, they are not attracted to it. Obviously, without technical measures the drivers cannot have total knowledge of the current state of the garage, but can look ahead only locally. To model this, we assign a look-ahead set $L_{a_i} \subseteq A$ for any current area a_i. An agent has access to $c(a)$ and $f_a(t)$ only if $a \in L_{a_i}$.

Classes of parking decals: Some parking providers offer different classes of parking decals, with some classes having more options then others: at a university campus, administrative and faculty/staff might be allowed to park at any given area, while students might only park at labeled student parking. A business park's parking provider might distinguish executive, employee, and visitor parking. This is modeled by assigning each agent a decal class, and by assigning each slot to one of these classes. The number of slots visible to an agent is then defined by that class. Non-compliant parking is thus not permitted to the agent.

Long-term experience and expectations: Instead of having to explore an area's attractiveness while driving through a specific garage, a driver with long-term experience already knows the attractiveness of each area, and can also estimate the individual areas' occupancy to a certain degree. These experience and expectations can be modeled by extending the look-ahead set to the whole graph, and by replacing the exact knowledge $f_a(t)$ by a "guessing function" $h_a(t) = f_a(t) \pm random$ which includes a small random component. The agent now knows the attractiveness of each area, and has imprecise knowledge of the areas' availability.

Based on these considerations, and starting out from the current position a_i as root, an option tree is constructed. This is accomplished by considering all neighboring areas a_j reachable from a_i via an edge $e(a_i, a_j) \in E$, and from thereon iteratively to succeeding neighbors with a maximum depth of d (see figure 5). The branch starting with the area last visited is removed from the tree, adhering to the no-turn-around rule.

For each node a_j in the option tree, a *conditional attractiveness* $g(a_j)$ is calculated: if $a_j \in L_{a_i}$ and $h_{a_j}(t) > 0$ then $g(a_j) = c(a_j)$, else $g(a_j) = 0$. Thus, if the agent assumes an area to have zero slots currently available, it is not at all attracted to that area. In a next step, for each immediate neighbor a_j of a_i an *assumed utility* $u(a_j)$ is

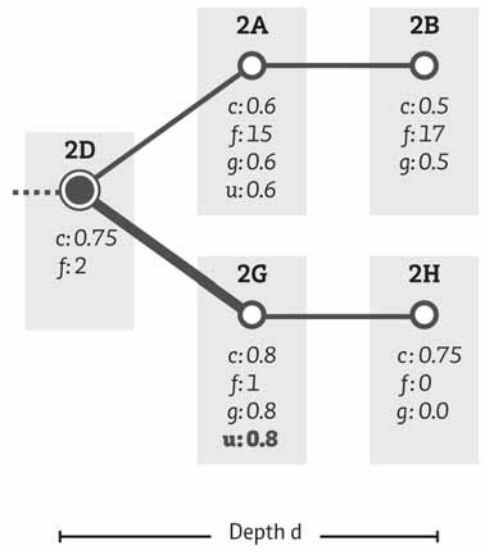

Figure 5: A simplified option tree, with the selected option being highlighted.

calculated by assigning $u(a_j) = \max_{a \in T_{a_j}} g(a)$, with T_{a_j} being the partial option tree with root a_j (again see figure 5).

At each simulation step, the agent takes a parking decision, followed by a routing decision if necessary. To take a *parking decision*, it selects the a_* with the maximum $u(a_*)$ out of the current area a_i's immediate neighbors. If $f_{a_i}(t) > 0$ and $c(a_i) \geq u(a_*)$, the agent decides to park at the current area a_i. If not, it moves on with the routing decision.

To take the *routing decision*, the agent only considers the options with the lowest $v(a)$. From these, the agent selects the option a_j with the maximum $u(a_j)$. It moves to that area via edge $e(a_i, a_j)$, completing the movement after a time of $r_{e(a_i,a_j)}$.

If all areas have been visited, i.e. all $v(a) > 0$, and no available parking slot has been found, the agent concludes that the parking garage is full, stops searching, and is subsequently removed from the simulation.

3 Validation

3.1 Modeling Florida International University's Parkview Housing Garage

The Florida International University (FIU) Parkview Housing Garage provides students living in adjacent dorms with 282 parking slots on three levels. Access to the garage is controlled; students swipe an identity card for the entry and exit barriers to open. The building consists of 16 areas with an average of 17.6 slots. Its layout is translated to a model graph as described in section 2.1 (see figure 6), with the attractiveness values being assigned by considering the areas' distances to both the vehicular entry and the pedestrian exits in accordance with information gathered from local experts. The traversal time for each area $a \in A$ is set to an average of $r_a = 10\,sec$. As all areas are immediately adjacent, the time necessary to move between areas is set to $r_e = 0$ for all $e \in E$. The agents' interarrival times are modeled based on a typical day's observed entry events per hour. By correlating the registered entry and exit events over a longer period, the average parking duration (and its standard deviation) based on entry times is modeled. As Housing Garage parking is only available to students living nearby, a high degree of experience can be assumed. The agents' look-ahead set is therefore extended to include the whole model graph.

The model was implemented utilizing an in-house event-based modeling and simulation framework. To validate the model's results, the individual areas' occupancy was measured in the Parkview Housing Garage over the course of two weeks at 10:00, 13:00, 17:00, and 20:00.

3.2 Results and Discussion

The described model was applied to simulate 100 operational days, with output measurement beginning after a 72 hour initialization phase. A simulation run generates approx. 1,700,000 events of nine event types. An average operational day thus consists of approx. 17,000 events, with the majority of these considering searching areas and moving through the graph (see figure 7).

The simulation's results are shown in table 1 and figure 8. At 10:00, the average number of simulated cars is 1.7% higher than the average number of observed cars. The average deviation of simulated to observed occupancy ratios is 8.7%. The other measuring points at 13:00, 17:00, and 20:00 show comparable results: On average, 2.5 more agents (1.4%) are simulated than cars were observed, while the average occupancy ratio over all areas and all measurement points deviates by 9.1%.

The model's validation shows its capability to predict a garage's state over the course of an operational day, even though specific results with their deviation of 9.1% are not yet precise enough for a feasible recommendation system. One major weakness of the de-

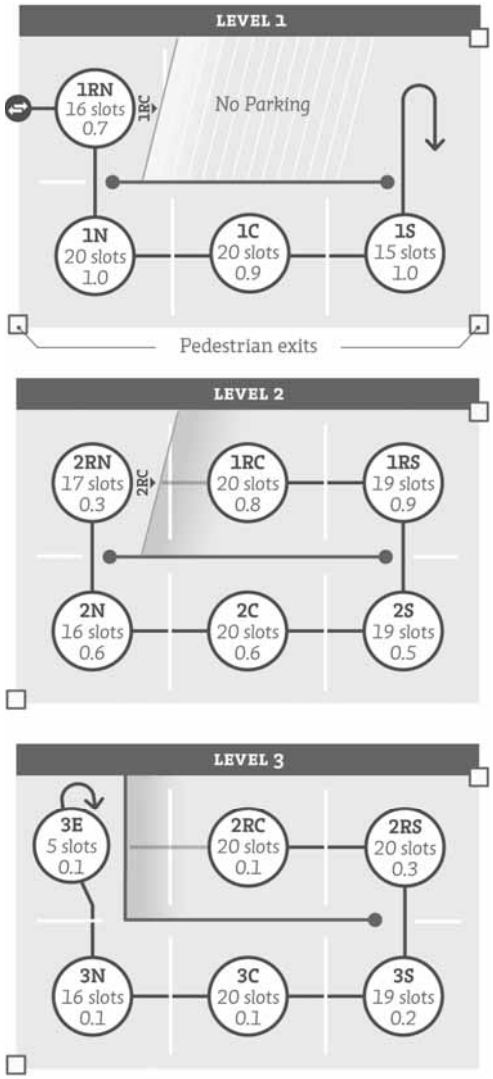

Figure 6: FIU Housing Garage: Model graph and attractiveness levels.

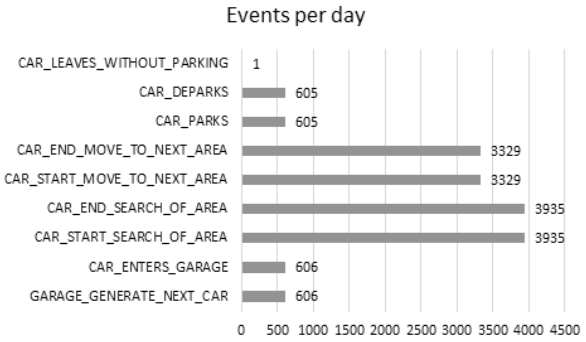

Figure 7: Number of simulation events per operational day.

Time	Obs. cars	Sim. cars	Dev. n/o cars	Deviation occupancy
10:00	194.5	197.9	1.7%	8.7%
13:00	164.5	161.7	1.8%	9.8%
17:00	164.2	166.5	1.4%	8.1%
20:00	169.3	176.4	4.2%	9.9%
Average	173.1	175.6	1.4%	9.1%

Table 1: Validation results.

scribed validation process is that the occupancy measurement was executed on different days than the registration of entry and exit events. There was therefore no way to calculate the number of cars already present in the garage at the start of the registration period. Currently, FIU's parking data collection is being converted from batch processed reports to real-time data streams, in addition to replacing the parking garage's card swiping mechanisms with license plate recognition cameras at entry and exit lanes. As these new data streams will be continuously available, occupancy rates can be measured for periods with available entry and exit events. By utilizing these improved data sources, higher quality input data distributions can be modeled. We therefore expect the model's precision to be improved significantly.

4 Conclusions

This paper presented an agent-based simulation model of cruising for parking in parking garages. Beyond the parking structure's layout and attributes, the model considers basic routing, an order of attractiveness on the garage's areas, local knowledge of real-time availability, different classes of decals, and a driver's long-term experience and expectations regarding attractiveness and expected availability. The model's validation shows its general capability to predict a garage's state over the course of an operational day based on layout data, attractiveness values, interarrival times, and parking durations. All these values can be easily collected for controlled access garages.

After further validation based on improved data streams, the model will be applied to the evaluation of parking recommendation methods. It will also be extended to accept real-time input data, and then be utilized as a base of a predictive parking information and recommendation system.

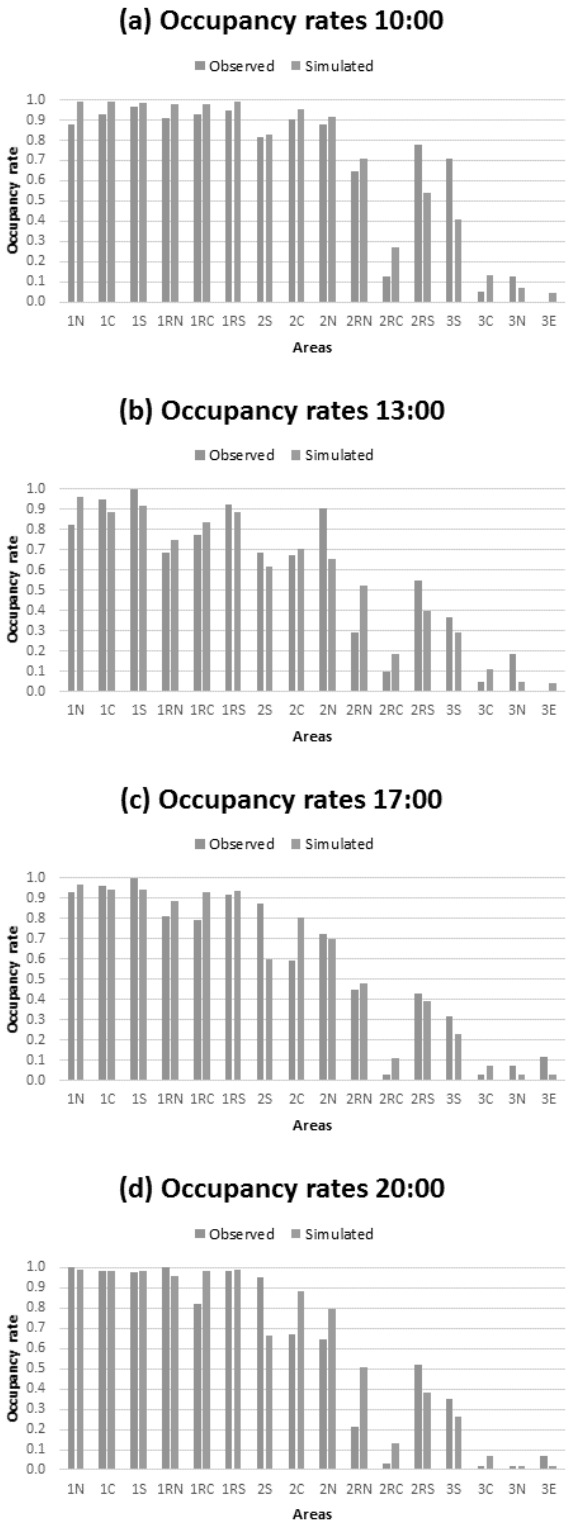

Figure 8: Validation results.

Acknowledgement

The authors wish to thank the FIU Department of Parking and Transportation for sharing access to their data streams, and for tolerating our repeated raids of their Parkview Housing Garage.

This material is partially based upon work supported by the National Science Foundation under grants I/UCRC IIP-1338922, AIR IIP-1237818, SBIR IIP-1330943, III-Large IIS-1213026, MRI CNS-0821345, MRI CNS-1126619, CREST HRD-0833093, I/UCRC IIP-0829576, MRI CNS-0959985, and FRP IIP-1230661 and U.S. Department of Transportation under a 2013 TIGER grant.

References

[1] Shoup DC. Cruising for parking. *Transport Policy*. 2006;13(6):479 – 486.

[2] Banks J, Carson JS, Nelson BL, Nicol DM. *Discrete-Event System Simulation*. Pearson, 5th ed. 2010.

[3] Macal MC, North JM. Tutorial on agent-based modelling and simulation. *Journal of Simulation*. 2010; 4(3):151–162.

[4] Ayala D, Wolfson O, Xu B, DasGupta B, Lin J. Pricing of parking for congestion reduction. In: *GIS: Proceedings of the ACM International Symposium on Advances in Geographic Information Systems*. 2012; pp. 43–51.

[5] Ayala D, Wolfson O, Xu B, Dasgupta B, Lin J. Parking slot assignment games. In: *GIS: Proceedings of the ACM International Symposium on Advances in Geographic Information Systems*. 2011; pp. 299–308.

[6] Levy N, Martens K, Benenson I. Exploring cruising using agent-based and analytical models of parking. *Transportmetrica A: Transport Science*. 2012; 9(9):773–797.

[7] Shoup DC. *The High Cost of Free Parking*. Chicago: Planners Press. 2005.

[8] van der Waerden P, Timmermans H, Borgers A. PAMELA: Parking Analysis Model for Predicting Effects in Local Areas. *Transportation Research Record: Journal of the Transportation Research Board*. 2002;1781:10–18.

[9] Xu B, Wolfson O, Yang J, Stenneth L, Yu P, Nelson P. Real-time street parking availability estimation. In: *Proceedings - IEEE 14th International Conference on Mobile Data Management (MDM)*, vol. 1. Milan, Italy. 2013; pp. 16–25.

[10] Young W, Weng T. *Simulation Approaches in Transportation Analysis, Springer Operations Research/Computer Science Interface Series*, chap. Data and Parking Simulation Models. Kitamura, R. and Kuwahara, M. 2005;.

[11] Benenson I, Martens K, Birfir S. PARKAGENT: An agent-based model of parking in the city. *Computers, Environment and Urban Systems*. 2008;32(6):431 – 439.

[12] Dieussaert K, Aerts K, Steenberghen T, Maerivoet S, Spitaels K. SUSTAPARK: an agent-based model for simulating parking search. In: *Proceedings of AGILE International Conference on Geographic Information Science*. 2009; .

[13] Gallo M, D'Acierno L, Montella B. A multilayer model to simulate cruising for parking in urban areas. *Transport Policy*. 2011;18(5):735–744.

[14] Horni A, Montini L, Waraich RA, Axhausen KW. An Agent-Based Cellular Automaton Cruising-For-Parking Simulation. In: *Proceedings of the 13th International Conference on Travel Behaviour Research*. Toronto, Canada. 2012; .

[15] Martens K, Benenson I. Evaluating Urban Parking Policies with Agent-Based Model of Driver Parking Behavior. *Transportation Research Record*. 2008; 2046:37–44.

[16] Saltzman RM. An Animated Simulation Model for Analyzing On-Street Parking Issues. *SIMULATION*. 1997;69(2):79–90.

[17] Asakura Y, Kashiwadani M. Effects of parking availability information on system performance: a simulation model approach. In: *Proceedings of Vehicle Navigation and Information Systems Conference, 1994*. 1994; pp. 251–254.

[18] Ullrich O, Brandt B, Lueckerath D, Rishe N. A Simple Model of Cruising for Garage Parking. In: *Proceedings of ASIM-Workshop STS/GMMS - ARGESIM Report 51*. Lippstadt, Germany: ARGESIM/ASIM Pub. TU Vienna. 2016; pp. 223–229.

[19] Ullrich O, Rishe N. *US Patent 14/660,283*. 2015;.

Human Activity Pattern Recognition based on Continuous Data from a Body Worn Sensor placed on the Hand Wrist using Hidden Markov Models

Sarah Fallmann[1,2*], Johannes Kropf[2]

[1]Department of Analysis and Scientific Computing, Vienna University of Technology, Wiedner Haupstraße 8-10, 1040 Vienna, Austria;
[2]Health & Environment Department, AIT Austrian Institute of Technology GmbH, Wiener Neustadt, Austria;
[*]*sarah.fallmann.fl@ait.ac.at*

Simulation Notes Europe SNE 26(1), 2016, 9-16
DOI: 10.11128/sne.26.tn.10322
Received: November 20, 2015; Revised: January 10, 2016;
Accepted: January 15, 2016;

Abstract. The work concentrates on combining discrete and continuous data in an algorithm to detect complex activity patterns.With the InvenSense MotionFit™ Software Development Kit (SDK) accelerometer and gyrometer data are recorded with the MPU-9150 sensor.[1] The raw data consisiting of processed daily acticities are preprocessed via a shifted window and different features are calculated. Afterwards activity recognition is done in MATLAB using the PMTK3 toolbox from Murphy *et al.* [2], where the classification algorithms are continuous Hidden Markov Models (cHMM).

Introduction

Activity pattern recognition analysis based on continuous sensor data using the MPU-9150 sensor is used to recognize daily activities in an everyday life environment. Activity recognition is currently a subject of intensive research, because of it's importance in many different fields. The motivation of this work lies in specific in the growing generation of older adults, and the need to provide them a secure and appropriate living standard. The continuous sensor data are used to recognize activities with a basic machine learning algorithm.

The demographic changes lead to more people suffering from Alzheimer's and Parkinson's disease. The challenge of the increasing number of dementia patients can be approached by Ambient Assisted Living Technologies like activity recognition, as some tasks of care givers can be eliminated or can be performed easier. This includes, among other things, sensors which control kitchen appliances like stoves, and guarantee the appropriate usage due to activity recognition. [3]

Human activity recognition based on accelerometer and gyrometer sensor data is an important task in the field of AAL technologies. The work focuses on the recognition of complex daily activities like tooth brushing, dinner preparation, changing clothes and others. The annotated data is recorded with the MPU-9150 sensor and the InvenSense MotionFit™ Software Development Kit (SDK). Supervised classification algorithms, namely continuous Hidden Markov Models (cHMM), are used to detect different daily activities.

The current attempts to detect human behavior and activity can be classified by the type of the sensors used (1) body worn sensors, (2) video cameras and (3) domotic sensor networks. [4] This work concentrates on body worn sensors. The data gained from body worn sensors consist of accelerometer and gyrometer data.

1 Related Work

There are many research studies over human activity recognition in different settings.[5, 6, 7, 8, 9] Most of these works are based on acceleration data and tries to recognize daily activities like [5, 6, 7, 9]. The main difference between the works lies in the choice of parameters in the different steps of recognition, meaning preprocessing, feature extraction, and finally training and classification.

Each study uses different sample frequencies during preprocessing. Bao *et al.*[5] used a sample frequency of

76.25Hz, Ravi *et al.*[6] and Shoaib *et al.*[8] used 50Hz. To get a hint which frequency is accurate in daily activity recognition, but still doesn't need too much memory, Khusainov *et al.*[9] compared different sampling rates and inferred that most of the body movements are contained in frequency below 20Hz.

Shoaib *et al.*[8] record a combination of accelerometer, gyrometer and magnetometer data from a smartphone sensor and later six different activities with seven classifiers are analyzed. Shoaib *et al.*[8] show that the combination of accelerometer and gyrometer completes the system and gives better results during physical activity recognition. The feature calculation is kept as simple as possible with two time domain features. They handle four dimensions x, y, z and the magnitude $\sqrt{x^2+y^2+z^2}$ and compute mean and standard deviation. On top of the work from Shoaib *et al.*[8] the frequency domain features are included within this work and the aim is to find out the performance including more complex activities.

In [10] a feature dataset is provided. They recorded eight activities from a group of 30 persons with a sampling rate of 50Hz. All activities were performed twice with a smartphone on the waste recording the accelerometer and gyrometer data. They calculated a bundle of 561 features and experimented mainly with a multi-class support vector machine, showing an overall accuracy of 96% for test data consisting of 2947 patterns.[10]

This work is mainly based on Bulling *et al.* [11], where body-worn accelerometer and gyrometer sensors are recorded to detect hand gestures which where commonly used during daily activities. They recorded 12 activities and inbetween non-specific activities, so called 'NULL'-class, are performed. Data from two persons with three sensors placed on their arms in different heights are gathered. The sensor are placed on top of the right hand, outer side of the right lower and upper arm. The data comes from a three-axis accelerometer and a two-axis gyrometer, both recording annotated motion data at a sampling rate of 32Hz.[11]

2 Activity recognition

The activity recognition consists the following steps. First the sensor is placed and the raw data are recorded. Afterwards preprocessing is done, which means data segmentation and filters are applied. During feature extraction, features are calculated. Finally, the training and classification is done with a continuous Hidden Markov Model (cHMM).

2.1 Data

The InvenSense MotionFit^{TM} Software Development Kit (SDK) is used to record data. The MPU-9150 is a nine-axis MotionTracking device optimized to fulfill the purposes for wearable sensor applications.[1]

The MPU-9150 sensor is placed on the left hand wrist, with which the daily activities are mostly executed, because of sinistrality. The recording is done in different time units in a $59m^2$ flat. In table 1 common daily activities [12] are displayed, which are recorded in this study with a sampling frequency of 50Hz.

Table 1: List of recorded daily activities.

labels	activities	
1	NULL	
2	comb hair	
3	wash face	
4	wash hands	
5	brush teeth	electric/ non electric
6	make bed	
7	change clothes	
8	put blinds up/down	
9	prepare food	
10	eat with	folk/ spoon/ chopsticks
11	open/close window	
12	read newspaper/book	
13	putting shoes on	
14	drink from/with	straw/ mug/ cup

Each activity is saved with their 3-axis accelerometer and 3-axis gyrometer data. Inbetween all activities a 'NULL'-activity is performed, which consists of preparing the next activity and closing the preceding activity. The data gathering extends over days in many small sessions, which is the reason why the sessions are put together to one dataset later on.

Data segmentation is performed via annotation during recording, saving information over start and duration of the activity. The annotation is automated via an app, which allows the recording within specific time

units, which are determined by the user and the annotation of the data accords to the user's purpose.

2.2 Preprocessing

Only data which are recorded more than once are used for analysis. This is done with one of two methods. The first method cuts out 'read newspaper/read book', 'putting shoes on' and 'drink from/with straw/mug/cup' from the whole dataset, but the 'NULL'-classes between the activities remain in the dataset. The second method redefines those classes labels to the 'NULL'-class label.

Some other activities are put together to one: 'Tooth brushing electric' and 'Tooth brushing non electric' get label 5 as well as 'Eat with folk', 'Eat with spoon' and 'Eat with chopsticks', which are assigned to label 10. Each sensor records data in three dimensions and a fourth dimension, describing the magnitude $\sqrt{x^2+y^2+z^2}$, is added for each sensor.

In the preprocessing step the artifacts and noises are reduced by filters and the signal is prepared for later feature extraction.[11] The noise and artifacts are disturbances which can corrupt the human activity recognition. During the study median filter and a 3rd order low-pass Butterworth filter are tested. These filters are also used among others in [10]. The 3rd order low-pass Butterworth filter has a cutoff frequency of 20Hz. This rate is sufficient, as the frequency of human body motions is 99% below 15Hz.[10]

The application of the median filter causes a smoothing of the data compare figure 1. Butterworth filters are used to cut high frequencies. The functionality of a third order low pass Butterworth filter with 20Hz cutoff frequency for a data segment of the original dataset can be seen in figure 2. The original data is displayed in blue and the filtered data is displayed in red.

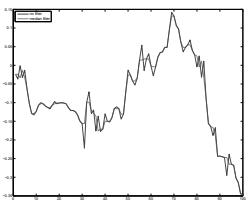

Figure 1: Median filter.

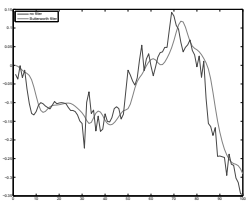

Figure 2: Butterworth filter.

2.3 Feature Mapping

In the feature extraction step the raw data are converted into features. This features are calculated for each annotated activity with a shifted window sized 50, containing 50 data vectors, and an overlap of 50%, which is the most significant value for overlap in past works.[13, 5] The mean, standard deviation, correlation [5, 6], energy [5, 6] and frequency domain entropy [5] are calculated for this data, as those are the most popular features for acceleration signals in activity recognition.[7]

The features can be divided into time domain features and frequency domain features. Time domain features are mean, standard deviation and correlation. Frequency domain features are energy and entropy. The energy and entropy calculation is much more expensive in comparison to the time domain features, because of the Fourier transformation (FFT).[8]

A periodic function in time is described with a direct current (DC) component. The DC component over the window is the mean value. Standard deviation is important for the reason of different range of values for different activities. Periodicity in the data is saved in the energy feature. Correlation between axes is useful to differentiate activities with translation in one dimension. As example, walking and stair climbing can be distinguished over correlation data.[5, 6]

In table 2 the calculation methods for the different features are depicted, where w is the window length and x_j are discrete FFT components. It is important to use a minimum number of features that allow good performance and at the same time minimize computational costs and memory.[11] Experimenting with the features get to the conclusion that entropy shows no improvement of the results. The best combination of features are mean, standard deviation and correlation.

2.4 Training

For activity recognition cHMMs are used. This is a supervised model which needs to get trained before operating.[11] Therefore the data has to be split into training and test data.

As some activities are not so common it is not possible to divide the data in usual 20% test data and 80% training data. Therefore one activity is cut out from each activity class, with the 'NULL'-class behind for the test data set. The remaining part is used as training data. An example for the structure of training and test data can be seen in figure 3 and 4.

Table 2: Features.

Features	calculation
mean	$\mu = \frac{1}{w}\sum_{j=1}^{w} x_j$ $x_j \ldots$ values
standard dev.	$\sigma = \sqrt{(\frac{1}{w}\sum_{j=1}^{w}(x_j-\mu)^2)}$
energy	energy= $\frac{1}{w}\sum_{j=1}^{w} \mid x_j \mid^2$
correlation	$cov(x,y) = \frac{1}{w}\sum_{j=1}^{w}(x_i-\mu_x)(y_i-\mu_y)$ $corr(x,y) = \frac{cov(x,y)}{\sigma_x\sigma_y}$
entropy	Frequency-domain entropy is calculated as the normalized information entropy of the discrete FFT component magnitudes of the signal.[5]

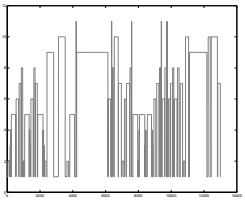

Figure 3: Training data.

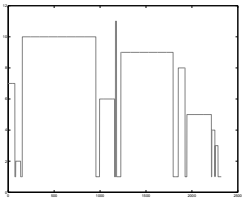

Figure 4: Test data.

The training needs a training set $\{(\mathbf{X}_i, y_i)\}_{i=1}^{N}$ consisting of N pairs of feature vectors $\mathbf{X}_i$ with corresponding labels y_i. In cHMMs the model parameters $\theta = (\pi, A, B)$ are learned by minimizing the classification error.[11] In this work the transition matrix A, can be calculated with the labeled training data as well as B, a list of pairs (μ, Σ) that define the distributions. Only π has to be guessed.

2.5 Classification

The classification consists of two steps. The first one maps a set of class labels to each feature vector of the test data with corresponding scores. In the second step the scores are used to calculate the maximum score and take the corresponding class label y_i as the classification output.[11]

2.6 Performance Evaluation

The classification of the activities can be either correct 'True Positive' and 'True Negative' or wrong 'False Negative' and 'False Positive'. The performance metric which is used for this model is a confusion matrix, with accuracy, sensitivity(=recall), specificity and precision.

The confusion matrix gives a breakdown of the misclassified activities by the model. The rows show the instances in each actual activity class and the columns show the instances for each predicted activity class. The values in one row are the results from the comparison of all ground truth instances, from the actual class, to the predicted class labels.[11] In table 3 a simple confusion matrix can be seen, where the last column describes the recall values, the last row the precision values and the last box describes the accuracy.

If the dataset is unbalanced, for example when the number of ground truth instances vary significantly, the overall accuracy is not representative for the whole classifier. A normalized confusion matrix inhibits this problem by using percentage of the total number of ground truth activity instances.[11] This problem occurs also in small scale during this study, that is the reason why all parameters are included in performance evaluation and no normalization is done.

Table 3: Simple confusion matrix.

	activity 1	activity 2	activity 3	recall
activity 1	11	2	0	84.62
activity 2	0	4	0	100
activity 3	1	0	5	83.33
precision	91.67	66.67	100	86.96

3 Validation

In the first attempt a validation with the provided data from Bulling *et al.* [11] and Anguita *et al.* [10] is accomplished to justify the use of continuous Hidden Markov Models (cHMM).

3.1 Bulling *et al.*[11]

In [11] data from 2 persons performing 12 activities are recorded: opening a window, closing a window, watering a plant, turning book pages, drinking

from a bottle, cutting with a knife, chopping with a knife, stirring in a bowl, forehand, backhand and smash. Additionally, a non-specific activity was performed called 'NULL'-class.[11] The inertial measurement unit (IMU) is placed on 3 positions, the upper arm, the lower arm and the hand wrist on the right side.[11] For evaluation, the hand position is used.

Provided data with a 32Hz sampling rate are used to calculate the features: mean, standard deviation, correlation and energy for all 7 axes. This 7 axes come from the 3-axes accelerometer and 2-axes gyrometer gathered data, including one axis for each sensor, representing the magnitude. This features are further used to calculate the cHMM model.

The calculated results from the cHMM are compared with the results in the paper from Bulling *et al.* [11]. This circumstances are shown in figure 5, where precision and recall is compared to the applied cHMM in this thesis using the same dataset. The same characteristic, namely lower precision than recall, can be seen. The different values between results of Bulling *et al.* [11] and this thesis are mostly caused by the number of features and the model used in [11]. They only calculated two features, mean and standard deviation and the classification algorithm uses a folding step.[11] In comparison this thesis takes into account the mean, standard deviation, energy and correlation features.

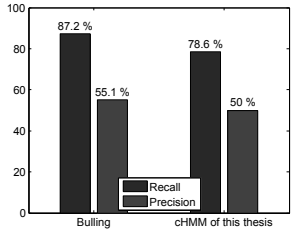

Figure 5: Precision and recall for sensor data from Bulling *et al.* [11] and this cHMM.

In [11] the precision lies by 87.2% using the sensor placed on the hand wrist. This relates to the results of an accuracy of 81.71% and good recall and precision values for each activity class in the confusion matrix. Therefore it follows, that the used cHMM is accurate.

3.2 Anguita *et al.*[10]

Anguita *et al.* gathered data from 30 volunteers, which followed a defined protocol of activities, consists of standing, sitting, laying down, walking, walking downstairs and upstairs. This data are collected via a Galaxy S II. smartphone on the waist, recording accelerometer and gyrometer data with a sampling rate of 50Hz and 5 seconds break between two activities.[10]

Only a part of the 561 features vector of the provided data is picked for evaluating the cHMM. The feature data is already noise reduced by median filter and 3rd order low-pass Butterworth filter with a 20Hz cut-off frequency and others.[10] In particular the data of mean, standard deviation and correlation is used for all three axes X, Y, Z.

The confusion matrix shows the precision in the last row, the recall in the last column and accuracy in the last box. In table 4 the confusion matrix of the cHMM is depicted. In table 5 the results of Anguita *et al.*[10] are reproduced. In contrast to the cHMM applied in this study, Anguita *et al.* used a multiclass Support Vector Machine (MC-SVM). The different accuracy can be attributed to the less used features, the usage of only one accelerometer and one gyrometer dataset, and the more complex MC-SVM model in [10].

Table 4: Confusion matrix of cHMM.

Walking	W.Upstairs	W.Downstairs	Sitting	Standing	Laying Down	
422	0	74	0	0	0	85.07
0	400	71	0	0	0	84.93
0	39	381	0	0	0	90.71
2	1	3	406	68	11	82.69
6	9	5	26	468	18	87.97
0	0	2	298	44	193	35.94
98.14	89.09	71.08	55.62	80.69	86.94	77.03

4 Experiments

In all experiments except 'Continuous/Discrete data', the activities which occur only once in the recording period are put in the 'NULL'-class activities. In 'Continuous/Discrete data' the once recorded classes are cut out of the whole dataset, leading to an one percent improvement. In real environmental applications this makes a small difference and therefore is not necessary.

Table 5: Confusion matrix of MC-SVM [10].

Walking	W.Upstairs	W.Downstairs	Sitting	Standing	Laying Down	
492	1	3	0	0	0	99.12
18	451	2	0	0	0	95.75
4	6	410	0	0	0	97.62
0	2	0	432	57	0	87.98
0	0	0	14	518	0	97.37
0	0	0	0	0	537	100
95.72	98.04	98.80	96.86	90.09	100	96

4.1 Training and test sets

Different sort of training and test data partitions are analyzed. For example, the test data includes the third repetition of each single activity class and takes either the 'NULL'-class behind or in front of each cut activity. Another approach uses the second repetitions, again with either the 'NULL'-class in front of the activities or behind. This results are compared to each other see figure 6, 7 and table 6. Out of the table, illustrating the changes in accuracy, specificity and sensitivity, the conclusion can be drawn, that the 3rd activities with 'NULL'-class behind, implies the best result.

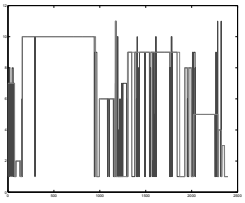

Figure 6: 3rd activities with 'NULL'-class behind.

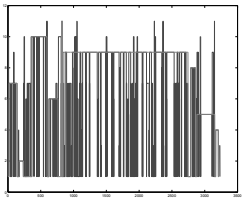

Figure 7: 2nd activities with 'NULL'-class in front.

Also different feature combinations are constructed and the accuracies are compared, leading to the most appropriate combination of mean, variance, correlation without the magnitude for the 3rd back data set.

4.2 Filters

In this section a median filter and a 3rd order low pass Butterworth filter with a corner frequency of 20Hz is used to remove noise, based on Anguita *et al.* [10].

Table 6: Accuracy, specificity and sensitivity for different sets.

Experiment	accuracy	specificity	sensitivity
3rd back	80.24	89.08	63.81
3rd front	79.84	88.35	61.25
2nd back	63.99	82.66	67.91
2nd front	64.67	85.48	56.18

For the best combination of features experimented above accuracy, specificity and sensitivity of filtered and non-filtered data are represented in table 7. If filters are applied, the sensitivity gets better, but the accuracy and specificity gets worse. Therefore filters seem unnecessary for this dataset.

Table 7: Accuracy, specificity and sensitivity for filtered and non filtered data.

Experiment	accuracy	specificity	sensitivity
no filter	80.24	89.08	63.81
filter	79.53	88.26	67.62

4.3 Accelerometer/Gyrometer

This experiment deals with analysis of accelerometer and gyrometer data on their own and combined. The outcomes of the accelerometer and gyrometer data on their own are further compared with the results of Bulling *et al.* [11].

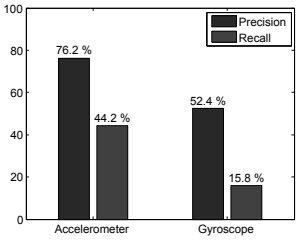

Figure 8: Precision and Recall by Bulling *et al.* [11].

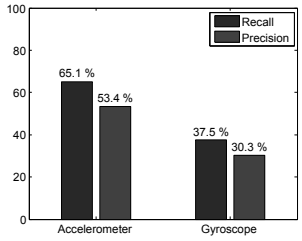

Figure 9: Precision and Recall of this study.

The single accelerometer dataset is more accurate than the single gyrometer dataset. This results coincide with those of Bulling *et al.* [11]. In [11] the gyrometer data on their own is also worse than the accelerometer

data on their own. These circumstances are illustrated in figures 8 and 9, where precision and recall are symbolized as blue and red bars. It can be noticed, that the results in the study of Bulling *et al.* [11] reach higher level of precision and lower level of recall than the results in this study. This is mostly caused by the greater dataset in [11]. The results in this study are not worse, but differ in activities as well as range and sort of recording.

The combination of accelerometer and gyrometer data is less accurate, combining accuracy, specificity, recall and precision therefore the conclusion can be drawn that gyrometer data is unnecessary in this case.

4.4 Extra cHMM

Activities are now divided in sub-activities with an extra cHMM. In specific, for each often misclassified activity-class, a cHMM is applied to divide the activities in sub-activities. The number of sub-activities depends on the number of states in the cHMM. Hence an iteration is done, constructing a 2-5-state cHMM, choosing the cHMM with highest accuracy.

For example the improvement by using the divided 'Tooth brushing' class comes from the case that electric tooth-brushing has a higher frequency.

The extra cHMM model is very sensitive. During the experiments only the parameter, for 'k'-fold cross-validation and the parameter, number of activity classes divided, are considered. But also a change in tolerance and of maximal iterations within the cHMM effects the outcome. The tolerance is always set to $1e^{-5}$ and the maximal iteration is set to 10.

In figures 10 the basic cHMM is shown, in contrast to figure 11, where the results for including sub-activities for tooth brushing, putting blinds up/down and prepare food are displayed, symbolized as Viterbi path (blue) correlating with the original labeled path (red). The results with sub-activities show a better fit to the original path. The experiments show that accuracy and specificity gets better, but do not justify higher runtime.

4.5 Continuous/Discrete data

The combination of continuous and discrete data is analyzed in this section. Test and training data get an additional column, consisting of the room number, describing the room where the activities are performed. The 'NULL'-class activities become half the room label from the previous activity and half the room label from the following activity. The process represents the usage of smart home sensors in combination with wearable sensors. An improvement of the results can be recognized. The outcomes in table 8 show that accuracy improves about 9% and sensitivity about 10%, while specificity stays nearly the same. This justifies the effort of collecting both data, continuous and discrete.

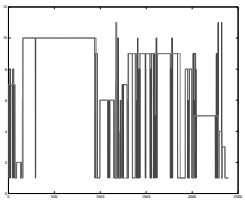

Figure 10: Basic cHMM.

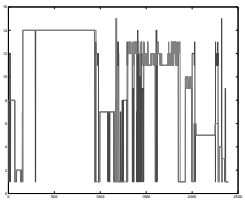

Figure 11: Extra cHMM.

Table 8: Accuracy, specificity and sensitivity for continuous and continuous & discrete data.

Experiment	accuracy	specificity	sensitivity
continuous	81.21	99.66	79.03
continuous & discrete	88.75	100	91.39

A great improvement can also be seen in the comparison of the Viterbi path (blue) and the original labeled path (red) in figure 12 and 13. Figure 12 shows results with continuous data and figure 13 with the combined dataset.

Overall the classes are not so likely misclassified as 'NULL'-class anymore, but one drawback is that the 'NULL'-class is much more likely misclassified as other activities.

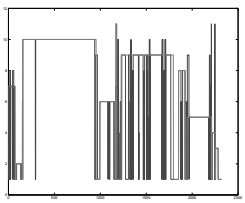

Figure 12: Continuous data.

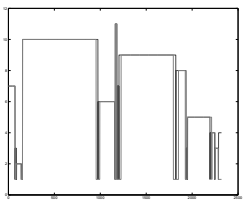

Figure 13: Con. & disc. data.

5 Conclusion and Outlook

Human activity recognition in Ambient Assisted Living (AAL) using a 3-axis gyrometer and a 3-axis accelerometer is performed. This raw data are preprocessed and split into test and training data sets. Later on features are extracted. Based on these features a continuous Hidden Markov model (cHMM) is constructed.

The cHMM model is validated with provided data and results from Bulling *et al.* [11] and Anguita *et al.* [10]. Afterwards different experiments were accomplished. The outcome shows, that using only accelerometer data with mean, variance and correlation leads to the best results. The conclusion is that gyrometer data are not necessary for good results and filters do not really contribute to significant improvement. The most important outcome is, that the combination of discrete and continuous data considerably improves the results.

The experiments have to be treated with caution, as the dataset is not big enough to get general statements and is only recorded from one person. Another drawback of the data is the recording sessions. It is recorded in different sessions with breaks inbetween, but still is applicable to real environments.

Research should focus on the combination of discrete data from binary sensors and continuous data from wearable sensors. This will lead to more robust and trustable models. A broader consideration, meaning a bigger dataset with more activities and people included, would lead to results which allow to imply more general statements.

References

[1] InvenSense Inc. MotionFit™ Wireless Developer Kit. http://invensense.com/mems/gyro/documents/PB-MPU-9150IMF%20MotionFit%20Wireless%20Developer%20Kit%20Product%20Brief.pdf. 2012. Accessed: 2015-02-06.

[2] Kevin M, Dunham M. Probabilistic modeling toolkit. https://github.com/probml/pmtk3. 2011. Accessed: 2015-08-13.

[3] Van Den Broek G, Cavallo F, Wehrmann C. *AALIANCE Ambient Assisted Living Roadmap*. Amsterdam, The Netherlands: IOS Press. 2010.

[4] Han JW, Pei J, Yan XF. From sequential pattern mining to structured pattern mining: a pattern-growth approach. *Journal of Computer Science and Technology*. 2004; 19(3):257–279.

[5] Bao L, Intille SS. Activity Recognition from User-Annotated Acceleration Data. In: *Pervasive*, edited by Ferscha A, Mattern F, vol. 3001 of *Lecture Notes in Computer Science*. Springer. 2004; pp. 1–17.

[6] Ravi N, Dandekar N, Mysore P, Littman ML. Activity Recognition from Accelerometer Data. In: *Proceedings of the 17th Conference on Innovative Applications of Artificial Intelligence - Volume 3*, IAAI'05. AAAI Press. 2005; pp. 1541–1546.

[7] Huynh DTG. Human Activity Recognition with Wearable Sensors. Ph.D. thesis, Universität Darmstadt, Darmstadt, Germany. 2008.

[8] Shoaib M, Scholten H, Havinga P. Towards physical activity recognition using smartphone sensors. In: *10th IEEE International Conference on Ubiquitous Intelligence and Computing, UIC 2013*. Los Alamitos, CA, USA: IEEE Computer Society. 2013; pp. 80–87.

[9] Khusainov R, Azzi D, Achumba IE, Bersch SD. Real-Time Human Ambulation, Activity, and Physiological Monitoring: Taxonomy of Issues, Techniques, Applications, Challenges and Limitations. *Sensors*. 2013;13(10):12852–12902.

[10] Anguita D, Ghio A, Oneto L, Parra X, Reyes-Ortiz JL. A Public Domain Dataset for Human Activity Recognition using Smartphones. In: *21th European Symposium on Artificial Neural Networks, Computational Intelligence and Machine Learning, ESANN 2013*. 2013; Bruges, Belgium.

[11] Bulling A, Blanke U, Schiele B. A Tutorial on Human Activity Recognition Using Body-worn Inertial Sensors. *ACM Computing Surveys*. 2014;46(3):33:1–33:33.

[12] Pendleton HM, Schultz-Krohn W. *Pedretti's Occupational Therapy - Practice Skills for Physical Dysfunction*, pp. 157–173. Elsevier Inc. Mosby. 2013;.

[13] Van Laerhoven K, Cakmakci O. What Shall We Teach Our Pants? In: *ISWC '00: Proceedings of the 4th IEEE International Symposium on Wearable Computers*. IEEE Computer Society, Washington, DC, USA: IEEE Computer Society. 2000; p. 77.

Automatic IO Device Selection for Ambient Environments

Brigitte Kupka[1*], Jonathan Steinhart[1], Miroslav Sili[1], Matthias Gira[1], Christopher Mayer[1,2]

[1]AIT Austrian Institute of Technology GmbH, Health & Environment Department, Donau-City-Straße 1, 1220 Vienna, Austria; *brigitte.kupka@ait.ac.at*

[2]Department of Analysis and Scientific Computing, Vienna University of Technology, Wiedner Haupstraße 8-10, 1040 Vienna, Austria

SNE Simulation Notes Europe SNE 26(1), 2016, 17-22
DOI: 10.11128/sne.26.sw.10323
Received: January 10, 2016; Revised: February 15, 2016;
Accepted: March 20, 2016;

Abstract. Active and Assisted Living (AAL) aims at providing services for elderly or disabled people in their homes using modern smart home technology and AAL software. The accessibility of user interfaces for such systems is of particular interest. This article proposes a model-based solution for selecting the best device and modality for user interactions of AAL services using the Ambient Assisted Living user interfaces (AALuis) framework. The best device and modality for a given situation depends on context information provided by the AAL system. An exemplary household was modeled as a Bayesian Network, incorporating a selection of devices and their modalities, together with relevant context information regarding the user and the environment. Each entity of the network is assigned with a probability. For devices and modalities these probabilities represent a measure of their suitability for output for the user, given the context. This model was then used to simulate different scenarios, in order to review the results of this selection mechanism.

Introduction

Active and Assisted Living (AAL) Environments use modern technology to provide services specifically tailored to elderly or disabled people and their caretakers [1]. Those services include telecare, telecommunications, comfort services and emergency prevention and detection [2]. They have, in general, the objective of promoting and maintaining physical and psychological health, and assistance in daily life. AAL middleware unites common household electronics and specialized smart home hardware components with AAL service software. AAL services are meant to be integrated into the live of the user as seamlessly as possible. Therefore the user interfaces (UIs) are of particular interest in AAL environments [3]. The project Ambient Asssisted Living User Interfaces (AALuis) [4] is concerned with the flexible creation of accessible UIs for AAL services.

The model-based Automatic IO Device and Modality Selection for AALuis has the objective of selecting the best device and modality combination for any AAL service, given the context. Context information, regarding the user, the devices and the environment is provided by the AAL framework and serves as a basis for the selection. A user interaction typically consists of input and output. This work is concerned with the selection mechanism for only the output part of UIs.

This paper first describes the problem of the Automatic IO Device Selection for AALuis and follows with a brief introduction to the chosen method, Bayesian Networks. Then, the modeling process is presented, followed by the results of evaluating this method for solving the given selection problem. Next, the results are discussed and finally the paper closes with a conclusion and a brief outlook on further topics of interest in this context.

1 Automatic Output Device Selection for AALuis

New devices, each with their individual features, are constantly being introduced. It is desirable to also make them available to AAL systems. However, AAL service developers cannot anticipate all device's possibilities and constraints regarding the UIs at design time. AALuis can help to use them to their full potential.
The idea of AALuis is to provide open AAL systems with innovative UIs. It frees service developers from

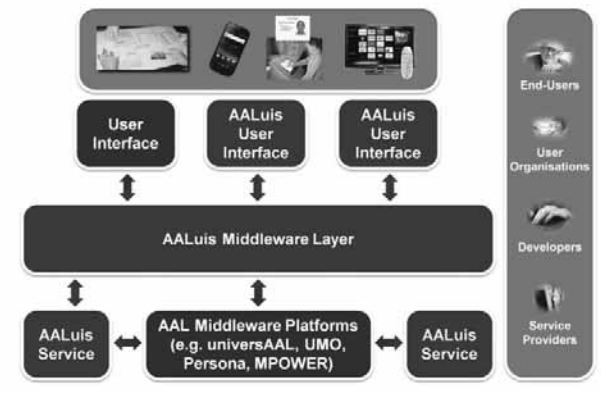

Figure 1: The AALuis middleware [4].

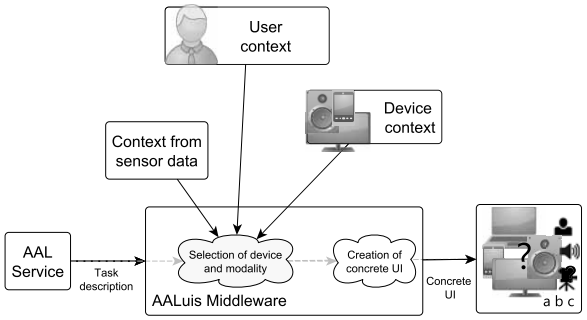

Figure 2: The device and modality selection problem in context of the AALuis UI creation process.

the task of designing the specific UIs, by linking the AAL system with the available devices and generating accessible interfaces for the services. The AALuis middleware operates from between another AAL middleware platform and the devices, as shown in Figure 1.

Each device supports one or more modalities. A modality is the communication channel used to transport a message between a human and a computer. Audio or text are output modalities, speech or text would be the corresponding input modalities [5].

AAL services initiating a user interaction contact the AALuis middleware with an abstract description of the task. It describes one user interaction and does not make references to a specific device or modality. During the following step AALuis shall automatically select the best combination of device and modality available, based on context and device information provided by the AAL middleware, and create an abstract UI description. On this basis, a concrete UI is created and sent to the selected device for rendering. Figure 2 shows this process and highlights the part of selecting a device and modality, which is the main focus of this article.

The context of an AAL system includes the user, the user's capabilities and constraints, personal preferences, the available devices, and the situational context, like surrounding noise, ambient light, temperature and current activities [6]. In different contexts, some modalities and devices might be preferable over others, for example, text output on a small device is not ideal for a person with visual limitations.

A number of additional requirements for the Automatic IO Device and Modality Selection for AALuis were identified. Input data from sensors, providing context information, might not be available at all times. Also, new devices can be added to a smart home at any time, others might become unavailable. Still, the selection mechanism has to produce a result every time.

Due to this flexible nature of the target systems, it is not possible to collect any training data for a classifier.

2 Bayesian Networks

Bayesian Networks were chosen as a method to solve the selection problem given the constraints stated above.

A Bayesian Network [7] is a directed acyclic graph and constitutes a compact representation of a probability distribution. The graph's nodes stand for discrete random variables and its edges represent causal relationships between them. Each node is assigned with the probability for each value the random variable can take.

Bayesian Networks can incorporate the subjectivist interpretation of probability, as opposed to the commonly known frequentist interpretation.

Traditionally, probability is based on the frequency at which certain events occur during repeated statistical experiments. There are situations however, where it is not possible to conduct an experiment multiple times in order to determine the frequencies of its outcomes. In the subjectivist interpretation of probabilities [8], probability is a numerical value, representing the degree of belief in the occurrence of an event A, given prior knowledge E (Evidence). This definition enables one to utilize expert domain knowledge and assign probabilities to events that are conditioned on E.

In a single Bayesian Network, both interpretations can be used conjointly.

2.1 Independence Assumption in Bayes Networks.

In a Bayesian Network, an edge connecting two nodes represents a causal relationship between them. Therefore, two nodes that are not connected are considered independent. This property is essential for using a Bayesian Network to compactly represent a probability distribution of n random variables. Expanding the definition of conditional probability $P(A|B) = \frac{P(A \cap B)}{P(B)}$ to multiple variables leads to the Chain Rule, shown in Equation 1, to calculate the joint probability distribution of the variables.

$$P\left(\bigcap_{k=1}^{n} A_k\right) = \prod_{k=1}^{n} P\left(A_k \middle| \bigcap_{j=1}^{k-1} A_j\right) \tag{1}$$

For two independent random variables the following holds: $P(A|B) = P(A)$.

This property, together with the assumption that there is no causal relationship between two not connected nodes, is utilized in a Bayesian Network, resulting in the Chain Rule for Bayesian Networks [8], shown in Equation 2.

$$P(A_1, ..., A_n) = \prod_{i=1}^{n} P(A_i | Pa_G(A_i)) \tag{2}$$

where $Pa_G(A_i)$ denotes the parent nodes of A_i in the graph G.

This means that after assigning each node of the Bayesian Network with the Conditional Probability of the represented random variable, given its parents, the Network contains all the information needed to calculate the joint probability function of all random variables.

2.2 Inference on Bayesian Networks

The states of some of the modeled random variables in a Bayesian Network can be observed in the real world. Using an inference algorithm, the graph structure can be exploited, to calculate the posterior probability of any random variable $P(A|E = e)$, given the observed evidence.

For this work, the junction tree algorithm by Shenoy and Shafer [9] was used for inference. This algorithm uses techniques of graph theory to convert the graph to a a simpler structure, the eponymous junction tree. After Evidence was observed, the probabilities in the model are updated. When the algorithm has completed, the probability of each single variable can be found through marginalization of a relatively small table. There is no need to calculate the entire joint probability distribution using the Chain Rule for Bayesian Networks, shown in Equation 2, to obtain the value for a single variable anymore.

3 Modeling

In order to solve the Output Device and Modality Selection for AALuis using a Bayesian Network, an example household was modeled as a template for any real household using AALuis. This section gives a brief introduction on the included elements and how they were combined in this model.

3.1 Elements of the Bayesian Network

Devices. For each known device, one node with the possible states *yes* and *no*, representing the subjective probability that the device is a good choice, was included. Each device has a parent node, indicating the device's current availability. Battery operated devices were additionally assigned a parent node, indicating the battery status of that device, with the possible values *low* and *OK*. In the modeled sample household, motion sensors provide the AAL middleware with information about the user's proximity to each device. To incorporate this information into the Bayesian Network, for each device node a proximity indicator was added as a parent. The subjective probability of every possible state of each node was assigned during the modeling process. These probabilities are used during inference, if the real value of the corresponding node was not observed. Figure 3 shows an example for a device called *smartphone*. Table 1 shows the corresponding conditional probability table for the device. It holds a probability for the values *yes* and *no*, for each possible state of the parent nodes.

For all entries, where the node *available* takes the value *no*, signaling that the device is currently not available to the system, the probability for the device node evaluating to *yes* was set to 0, thereby excluding the device from the selection process.

Modalities. Each modality supported by any of the known devices is represented as a single node in the

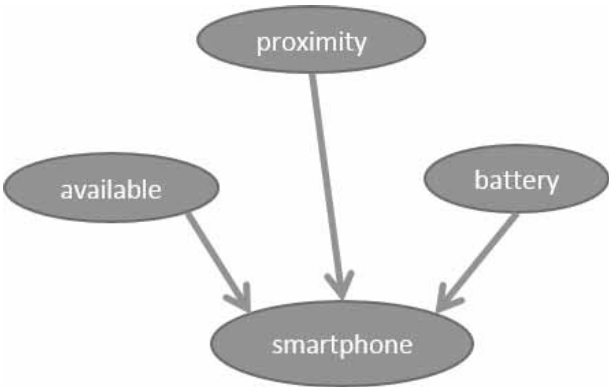

Figure 3: The nodes for a smartphone, with its properties battery status, availability and user's proximity.

available	battery	proximity	smartphone	
			yes	no
yes	OK	same room	1.0	0.0
		different room	0.5	0.5
	low	same room	0.1	0.9
		different room	0.1	0.9
no	OK	same room	0.0	1.0
		different room	0.0	1.0
	low	same room	0.0	1.0
		different room	0.0	1.0

Table 1: The Conditional Probability Table for the smartphone node of Figure 3.

Bayesian Network. The instance values *yes* and *no* represent how well the use of this modality would suit the current situation. The parents of a modality node are all the influencing factors from sensors or the user profile that have the potential of reducing the suitability of this modality.

User Profile and Sensor Data. For the modeled template household and AAL system, it was assumed that there was a user model, retrieving information about the user from a user profile. Four exemplary properties, indicating the user's abilities were included in the model: *hearing*, *visual acuity and sensitivity*, *field of vision* and *language reception*. Two items of sensor data were also included: *noise* and *ambient light*.

Result Nodes. Finally, for each possible combination of modality and device, a so called result node was added. It merges the probabilities of its parents so that the probability assigned to its value *yes* reflects the level of agreement for that combination, given the evidence. A minimal working example including only one device and one modality is shown in Figure 4.

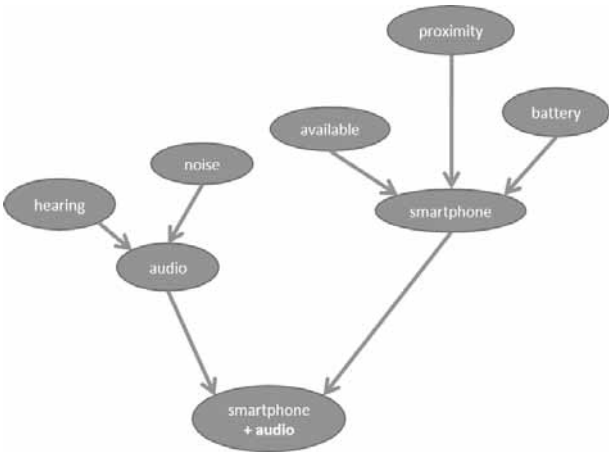

Figure 4: A minimal example of a household with only one device, which supports exactly one modality.

3.2 Inference on the model

When a selection is initiated by AALuis, evidence is set for all nodes which have been observed and inference can be performed. After completion, each result node is queried for the probability now assigned to its instance value *yes*. By ranking the result nodes according to their updated level of agreement, the best device and modality combination is found.

4 Results

To review the described approach's suitability to solve the Automatic IO Device Selection for AALuis, the example household was used to simulate different situations. Two example scenarios, will be presented below.

Scenario 1. A graphical summary of Scenario 1 is shown in Figure 5. It includes a user with good visual acuity and impaired hearing abilities. A TV is available in another room, and a touchtable is situated near the user. The level of noise is currently high, and the ambient light is of medium intensity. In this scenario, combinations using the touchtable are rated

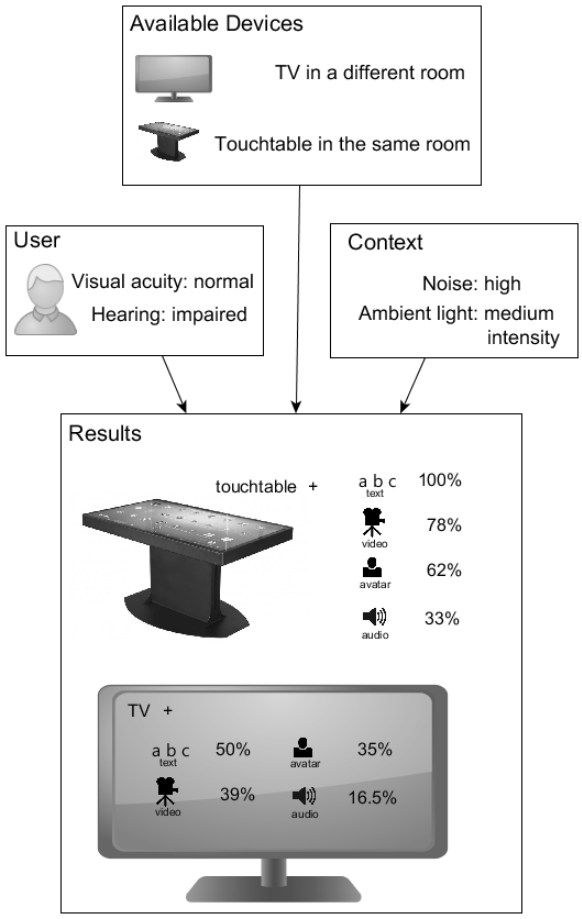

Figure 5: Scenario 1

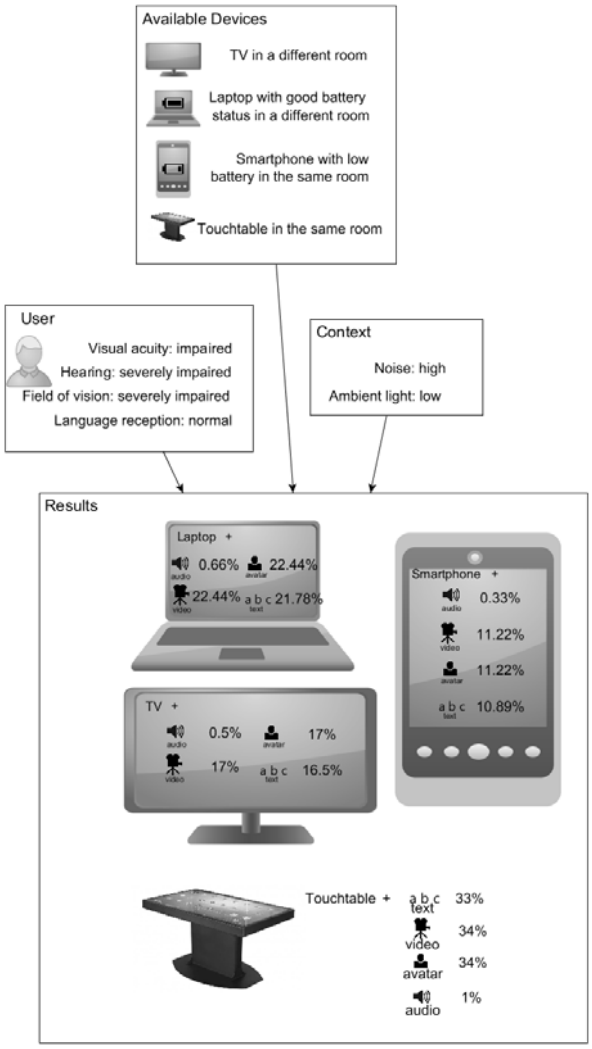

Figure 6: Scenario 2

overall higher than the options for the TV. The combination of touchtable and text output receives 100% agreement, while audio output on the TV receives only 16.5% agreement.

Scenario 2. The second scenario represents a user with severe impairments in hearing and their field of vision. Their visual acuity is also impaired, while the language reception was rated as normal. There are four devices present, including a TV in a different room, a laptop with good battery status in a different room, a smartphone with low batteries in the same room and a touchtable in the same room. The sensors report high noise and low ambient light. In this scenario, no result combination receives an agreement of more than 34%. Audio output on the smartphone scores only at 0.33%.

5 Discussion

This section will review the simulated scenarios presented above and provide a short interpretation of the individual results.

Scenario 1. Scenario 1 was shown in Figure 5. The results show that all modalities, including an audio component, namely audio, avatar and video, were penalized because the user was observed to have impaired hearing abilities. All combinations including the TV were rated significantly lower than the ones including the touchtable. This result is plausible because the TV

is in a different room. Output on this device would require the user to move closer to it, which should be avoided if possible.

Scenario 2. Scenario 2, shown in Figure 6, stands out because of the overall low agreement for all possible output combinations. The numerous negative influences present in this scenario influence all options heavily. This behavior, while being undesirable for successful user interactions, is in accordance with the concept applied during the modeling process. If one of the possible output combinations would receive a good score under these disadvantageous conditions, it would mean that none of the possible influences are connected to it. Regardless of the observed conditions, such a combination would always receive the exact same agreement level and possibly distort the selection mechanism. An occurrence like this could indicate that the model might not include causal relationships that should be considered.

The scenarios show that overall changes in the simulated input lead to plausible changes in the results. Single negative influences affect specific result combinations. The output of the selection mechanism in general reflects the intentions and assumptions that were the basis for the assignment of the probabilities for each node.

6 Conclusion and Outlook

The presented work described one possible approach to solve the Automatic Output Device Selection for AAluis with the use of Bayesian Networks. This method is capable of producing a result, even when the input data is incomplete, because it relies on the probabilities assigned during the modeling process in those cases. The use of subjective probabilities also eliminates the need for training data. If training data were obtained, it can easily be used to adjust the assigned probabilities.

The results confirm that Bayesian Networks in this setting produce satisfactory results in general. The specific probabilities assigned to the individual nodes however are crucial to the success of this method in real-world applications. To validate the assumptions made during the modeling process, the model has to be tested in a live setting by users belonging to the target audience of AAL systems.

Moreover, a successful user interaction typically consists of both output and input. So far, this work has only covered the selection of output device and modality. It remains to be seen, if the same method proves to be practical applied to the selection of an input device and modality, and if both parts can be joined in a meaningful way.

Acknowledgement

The project AALuis is cofunded by the AAL Joint Programme (REF. AAL-2010-3-070) and the following National Authorities and R&D programs in Austria, Germany and The Netherlands: bmvit, programm benefit, FFG (AT), BMBF (DE) and ZonMw (NL).

References

[1] Belbachir AN, Drobics M, Marschitz W. Ambient Assisted Living for ageing well–an overview. *e & i Elektrotechnik und Informationstechnik*. 2010; 127(7-8):200–205.

[2] Kleinberger T, Becker M, Ras E, Holzinger A, Müller P. Ambient intelligence in assisted living: enable elderly people to handle future interfaces. In: *International Conference on Universal Access in Human-Computer Interaction*. Springer. 2007; pp. 103–112.

[3] Mayer C, Zimmermann G, Grguric A, Alexandersson J, Sili M, Strobbe C. A comparative study of systems for the design of flexible user interfaces. *Journal of Ambient Intelligence and Smart Environments*. 2016; 8(2):125–148.

[4] Mayer C, Morandell M, Gira M, Hackbarth K, Petzold M, Fagel S. *AALuis, a user interface layer that brings device independence to users of AAL systems*. Springer. 2012.

[5] Obrenovic Z, Abascal J, Starcevic D. Universal accessibility as a multimodal design issue. *Communications of the ACM*. 2007;50(5):83–88.

[6] Dey AK. Understanding and using context. *Personal and ubiquitous computing*. 2001;5(1):4–7.

[7] Pearl J. *Probabilistic Reasoning in Intelligent Systems: Networks of Plausible Inference*. San Francisco, CA, USA: Morgan Kaufmann Publishers Inc. 1988.

[8] Koller D, Friedman N. *Probabilistic graphical models: principles and techniques*. MIT press. 2009.

[9] Shenoy PP, Shafer G. Propagating belief functions with local computations. *IEEE Expert*. 1986;1(3):43–52.

Cross-boundary Simulations of Fuel Cells

Szilárd Dombi[1,2], Walter Commerell[1], Hubert Mantz[1], Dr. Ferenc Lezsovits[2]

[1]University of Applied Sciences Ulm, Prittwitzstrasse 10, 89075 Ulm, Germany; *dombi@mail.hs-ulm.de*

[2]Budapest University of Technology and Economics

Simulation Notes Europe SNE 26(1), 2016, 23 - 26
DOI: 10.11128/sne.26.sw.10324
Received: March 11, 2016 (Selected ASIM STS/GMMS 2016 Postconf. Publ.); Accepted: March 25, 2016;

Abstract. Simulation software systems play an important role in Automotive Fuel Cell System simulations. However, a considerable number of simulation system types are available on the market, which poses a dilemma for researchers. The question this review paper aims to answer is the following: What is the most effective way to choose the appropriate simulation system?
The paper (1) presents an inventory of typical issues that researchers seek to address and (2) discusses software that can help them find the solutions. When an issue can be addressed using several simulation systems, a comparison is made between them. When an issue is so complex that it cannot be addressed independently with any one of the available software, viable software combinations are proposed and examined. In such cases, the output of a software is used as the input for another, and the cross-boundary connections between them are addressed.
Finally, the paper presents a brief overview of modelling possibilities and a tabulated summary of the findings.

Introduction

Fuel Cells constitute a promising technology for the future, for example, because of their favourable environmental impact, efficiency, power density, and low noise level.

There are different types of Fuel Cells, but in the automotive sector the Polymer Electrolyte Fuel Cell (PEFC) is the most common. The PEFC generates electric current from electrochemical reactions between hydrogen and oxygen with the by-product of heat and water.

1 Fuel Cell System

A Fuel Cell System (FCS), as shown on Figure 1, has several components, which are defined in IEC 62282-1:2005 [1]. These components work together to produce electric and thermal power from the inputs of hydrogen, air, water, and the system also requires electric and thermal power.

The main components of a FCS are the Fuel cell stack; the air processing system, which contains a humidifier and a compressor; the fuel gas supply; and the thermal- and water management systems. Furthermore, there are several peripheral components such as pumps, valves, and electrical devices. The fuel and the air are not part of the FCS; they are fed into it.

The FCS and its parts raise many questions that researchers try to answer with the help of different types of simulation software systems. This paper aims to investigate which simulation software system are the most suitable for addressing the researchers' issues.

2 Fuel Cell Simulation Software Systems

There are several types of Fuel Cell simulation software systems available on the market, but only a few of them are used for scientific research.

This does not mean that the others do not work properly. Nevertheless, this paper only discusses those types of Fuel Cell simulation software systems that are preferred by the scientific community.

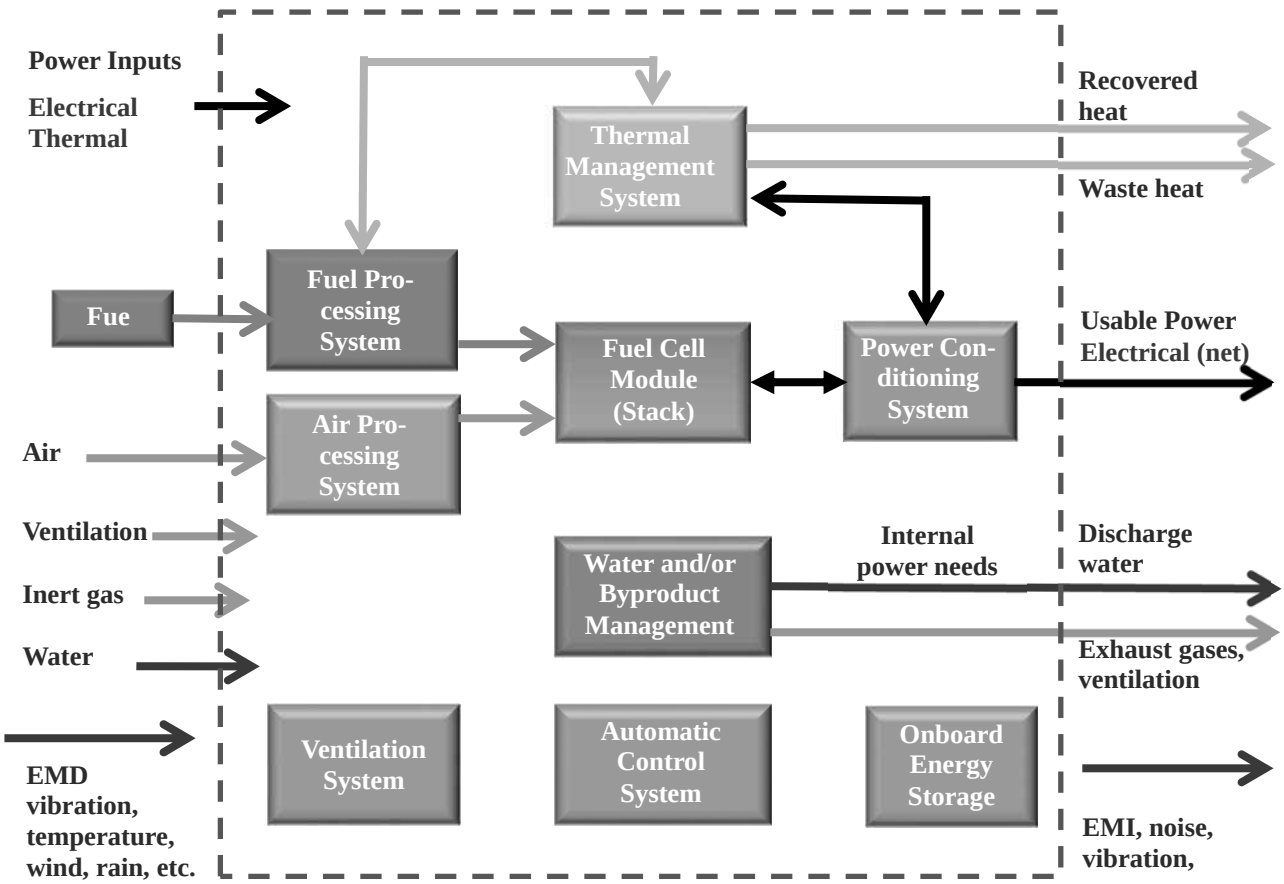

Figure 1. Fuel Cell System according to IEC 622882-1 [2]

These simulation software systems are:

- MATLAB®&Simulink®
- ANSYS Fluent
- AspenTech
- COMSOL Multiphysics

Each simulation software system has its own Fuel Cell specialised packages, which help making quick calculations.

Whereas these calculations may be sufficient sometimes, all of the packages have limitations that can only be solved by declaring equations and by setting up subsystems that are problem specific.

Cross-boundary Simulations are available between:

- MATLAB®&Simulink® and ANSYS Fluent by means of writing a journal file
- MATLAB®&Simulink® and COMSOL Multiphysics by means of MATLAB S-function and COMSOL Livelink
- MATLAB®&Simulink® and AspenTech Dynamics module by means of Control System Toolbox
- ANSYS Fluent and AspenTech by means of APECS [3]

ANSYS Fluent and COMSOL Multiphysics have been built for the same purpose; therefore, in their case there is no need for cross-boundary connection.

MATLAB®&Simulink® is mostly used for dynamic system simulations, ANSYS Fluent and COMSOL Multiphysics are suitable for Computational Fluid Dynamics, and AspenTech has been developed for chemical reactions and system optimizing.

3 Typical Questions

Some issues relate to an FCS as a whole whereas some others pertain to only a specific part of the system.

Issues
Stack operating conditions in different stack load points
Lower stack cathode pressure effect of FCS efficiency
Hydrogen consumption at different driving cycles
The effect of the compressor efficiency on the overall system efficiency
Stack idle operating conditions
Impact of the membrane resistance to the FCS peak efficiency
The impact of the compressor dynamic on the system dynamics

Table 1. Issues that can be addressed using MATLAB®&Simulink® [4]

Issues
Electrochemistry modelling
Current and mass conservation
Heat source problems
Liquid water formation and transport and their effects
Transient simulations
Leakage current

Table 2. Issues that can be addressed using ANSYS Fluent [5]

Issues
Fuel processing, hydrogen purification
Heat recovery, and water recovery
Steady-state material balances, heat integration
Dynamic analysis of heat-up, cool-down, power ramping
Safety analysis
Modeling of adsorption processes used to purify the fuel gas in the fuel conditioning section

Table 3. Issues that can be addressed using AspenTech [6]

Issues
Transport of charged and neutral species
Current conduction
Fluid flow, heat transfer, and the nature and driving forces of electrochemical reactions at planar and in porous electrodes
Design and optimization of the geometries and material choices of the system's electrodes, separators, membranes, electrolyte, current collectors and feeders with respect to performance, thermal management, and safety

Table 4. Issues that can be addressed using COMSOL Multiphysics [7]

4 Conclusion

In this paper, different kinds of simulation software systems have been reviewed. Tables 1-4 summarize the issues according to the simulation software systems with which they can be addressed.

None of the software can by itself provide the answers to all the questions, so for a complex analysis we need to use multiple software systems. Section 2 above presents the different feasible simulation software system combinations.

Acknowledgement

This work was supported by the DAAD (German Academic Exchange Service).

References

[1] Fuel Cell Technologies BSI Technical Committee GEL/105. DD IEC TS 62282-1:2005 *Fuel cell technologies - Part 1: Terminology*. BSI British Standards, 18 April 2005.

[2] Kabza A. *Fuel Cell Formulary*. Ulm, S. 19, 16. December 2015.

[3] http://www.colan.org/Catalog/ANSYS.html

[4] Kabza A. *Automotive Fuel Cell Systems*. Presentation, ZSW Ulm, S. 60, 10. December 2015.

[5] ANSYS, Inc. *ANSYS Fluent Fuel Cell Modules Manual*. Canonsburg, November 2013

[6] AspenTech. *aspen Fuel Cell Engineering Solution.* Brochure, Cambridge.

[7] www.comsol.com/batteries-and-fuelcells- module

ema – a Software Tool for Planning Human-Machine-Collaboration

Titanilla Komenda[1*], Wolfgang Leidholdt[2]

[1]Centauro GmbH, Gutheil-Schoder-Gasse 8-12, 1100 Wien, Austria; *komenda@centauro.at
[2]imk automotive GmbH, Amselgrund 30, 09128 Chemnitz, Deutschland

Simulation Notes Europe SNE 26(1), 2016, 27 - 32
DOI: 10.11128/sne.26.sw.10325
Received: January 10, 2016; Revised: March 5, 2016;
Accepted: March 15, 2016;

Abstract. Digital human models are already in use for validating manual work in terms of risk prevention and ergonomics. However, modelling different work activities is mostly very time-consuming and inefficient. This is because digital human models are considered as machines with more than 100 degrees of freedom to be specified for one pose. ema, however, the so called editor for manual work activities, treats its digital humans as virtual workers. By defining work instructions, the modelling process is much faster and more intuitive compared to efforts specifying individual poses. Furthermore, the implemented work instructions are more accurate and realistic as a result of theoretical development and empirical validation by means of motion capturing technologies. Newest work operations also allow the planning of human-machine-collaboration leading to the validation of interactive human-robot-scenarios. In this paper, features of ema are presented, including manual work modelling, time analysis and ergonomic evaluation.

Introduction

With the increasing digitalizing of product development processes more than 200 digital human models have been introduced on the market. Those models can be used for anthropometric as well as muscle stress analyses. A detailed register can be found in Mühlstedt [1] and Duffy [2]. The most significant digital models are Ramsis (Human Solutions), Human Builder (Dassault Systémes) and Jack (Siemens PLM). They are represented by an internal skeleton model and an envelope and have similar characteristics and functionalities in terms of evaluating human workspace. Ergonomic analyses is based on anthropometric data, i.e. percentiled body measurements, as well as on individual poses.

However, motion modelling is similar to this of machines, i.e. individual poses are obtained by manipulating specific degrees of freedom to desired target positions. In contrast to robots with only 6 degrees of freedom, this modelling approach is mostly very time-consuming and inefficient – considering the fact that those digital human models consist of 100 degrees of freedom and 50 segments on average. Furthermore, modelled human work activities do not refer to any standardized performance level and thus cannot be used to evaluating cycle time.

1 Developing ema

Facing the stated issues, the editor for manual work activities (ema) was developed by the imk automotive GmbH in cooperation with the Technical University Chemnitz, Volkswagen AG, the German MTM Association as well as Dassault Systémes [3]. The primary objective was to create a digital human model acting on the basis of a standardized process language in terms of work instructions. In addition, it should be used for evaluating cycle time requirements. After five years of brainstorming and development, the first version of ema was presented in 2011. Since then, ema is constantly being further developed.

1.1 Design Principles

ema uses a modular approach for describing and generating human work activities. The editor is based on so called complex operations representing an aggregation of single elementary movements originally formulated by the MTM-method. MTM is a predetermined motion time system that is used to analyse human work tasks based on five elementary movements, i.e. reach, grasp, move, position and release. Those elementary movements were empirically provided with standardised execution times dependent on influencing variables such as movement length or level of difficulty [4].

By applying highly automated algorithms for generating a workflow based on MTM, the modelling approach in ema is not only faster but also a premise on a standardised method.

1.2 Complex Operations

As mentioned before, ema uses complex operations for generating human work activities as a function of elementary movements. Thus, complex operations are aggregated single elementary movements in a logical sequence to fulfill a specific task. For instance, the operation 'get and place part' consists of the following single movements: steps forward – bend – hand to object – pick object – straighten body – object to body – step backward – turn – steps forward – bend – place object – release object – hand back – straighten body.

Complex operations are divided into 2 groups consisting of 36 human and 10 object operations. Human operations include picking and placing objects, using tools, grasping, manual screwing, visual control, waiting, walking, turning, sitting down, bending down, kneeling, etc. whereas object operations include moving, turning, waiting, establishing and resolving connections, inverse and forward kinematics. One major challenge in the development of ema was the definition and implementation of complex operations that can be found in various manufacturing environments. In the end, the team from imk succeeded in a logical separation of operations and an additional parameter setting for adjusting boundary conditions of individual tasks, e.g. the weight of the object to be handeled.

1.3 Empirical Validation

As there was no sufficient theoretical method that was able to fully describe the complexity of human motion generation, an empirical approach was applied to validate the implemented algorithms in ema. Therefore, a motion capturing system was used to record experienced operators from real production lines in an artificial testing environment. For each operation, external parameters that may influence task execution were systematically varied and recorded, e.g. working height, force direction, weight of handeled object, and body height of operator.

In this sense, the biomechanical correctness as well as a high accuracy of movements could be verified for the implemented modules in ema.

2 Workflow

Simulating human work activities in ema reduces the effort for modelling of up to 90 % compared to manual step-by-step simulation. While manipulating individual degrees of freedom for simulating 1 minute of human work requires about 230 minutes, only 25 minutes of effort are needed with ema.

The workflow for generating a simulation in ema can be divided into 3 steps: defining the scenario, modelling the behaviour and analysing the simulation. The individual steps are presented in more detail in the following.

2.1 Scenario Definition

Within the scope of defining the scenario, products and resources are implemented and positioned in the simulation environment. Products represent objects that are handeled as well as reference objects, whereas resources respresent human models, tools, machines, tables, containers, layouts, etc. Digital human models describing specific percentiles are selected from the comprehensive library. User defined geometries as well as collision objects are also either selected from the comprehensive library or imported through the CAD interface (Figure 1). At the moment, the comprehensive library consists of 360 objects. Furthermore, object characteristics are specified, such as weight or motion assignment.

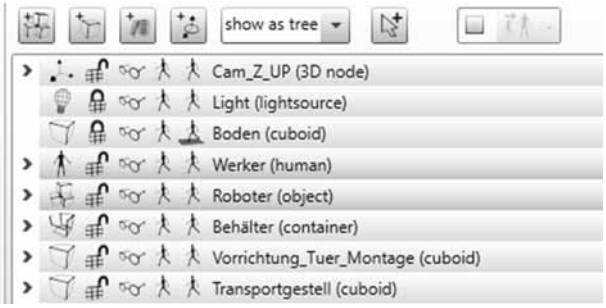

Figure 1: Object tree with library button.

2.2 Behaviour Modelling

After the scenario has been defined, the behaviour is modelled for each digital human model as well as for objects with previously assigned motion characteristics. The predefined complex operations are formulated to a task sequence by drag-and-drop (Figure 2). For each operation, parameters need to be specified, such as object to be handeled, automatic walk, target position or body posture.

Parameters like 'object to be handeled' or 'target position' can be easily set by selecting the required object or reference object in the 3D-environment. Thus, a complex operation is really formulated as a process language in terms of 'go and get the container and place

it on the shelf at the end of the hall'.

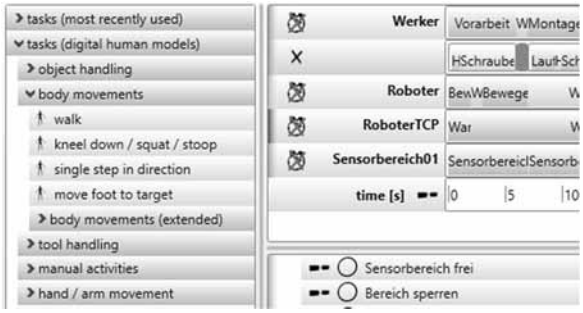

Figure 2: Task library and behaviour workflow

2.3 Analysis and Reporting

Basically, there are three analysing tools in ema with a focus on cycle time, ergonomics and motion path. Cycle time analysis corresponds to the MTM-method as each implemented human work activity is modelled complying with the standardised time of MTM. Thus, a comprehensive time analysis based on MTM-UAS (Universal Application System), an aggregated MTM-system, is available in ema (Figure 3).

UAS analysis

#	type	code	hand	TMU	c x f	TMU infl.
1	place	PA3		25.0	1 * 1	25.0
2	movement cycle	ZB1		10.0	1 * 15	150.0
3	body movement	KA		25.0	1 * 3	75.0
4	place	PA1		10.0	1 * 1	10.0
5	movement cycle	ZB1		10.0	1 * 5	50.0
6	place	PA1		10.0	1 * 1	10.0
7	movement cycle	ZB1		10.0	1 * 5	50.0
8	place	PA2		20.0	1 * 1	20.0
9	process time	PT		38.9	1 * 1	0.0
10	body movement	KA		25.0	1 * 2	50.0

Figure 3: Integrated MTM-UAS analysis

Furthermore, ema includes an ergonomic risk assessment according to NIOSH, OCRA (Occupational Repetitive Action) and EAWS (European Assembly Worksheet).

	Werker
information	50th percentile, male, German, 79kg, age: 40
whole body [pts]	**19.5**
postures [pts]	7.7
trunk rotating [pts]	7
trunk bending [pts]	2.7
far reach [pts]	1.7
postures sum [pts]	**19.5**

Figure 4: Integrated EAWS analysis

EAWS is a standardised tool for evaluating repetitive assembly tasks taking into account static postures, action forces, load handling and short, repetitive loads. Within the scope of the ergonomic risk assessment, joint angles and positions of the body segments are recorded throughout the entire simulation cycle, i.e. simulation time. Based on this data, each posture is categorised according to EAWS. However, information regarding action forces and object weights need to be specified manually. In the end, ema calculates a total risk score that is rated according to the traffic-light system green – yellow – red (Figure 4). Additionally, so called spaghetti diagrams visualising the motion paths, workflow reports as well as cycle time diagrams can be directly obtained from the simulation (Figure 5). All simulation results can be either saved as videos, screenshots or exported as Excel or CSV files.

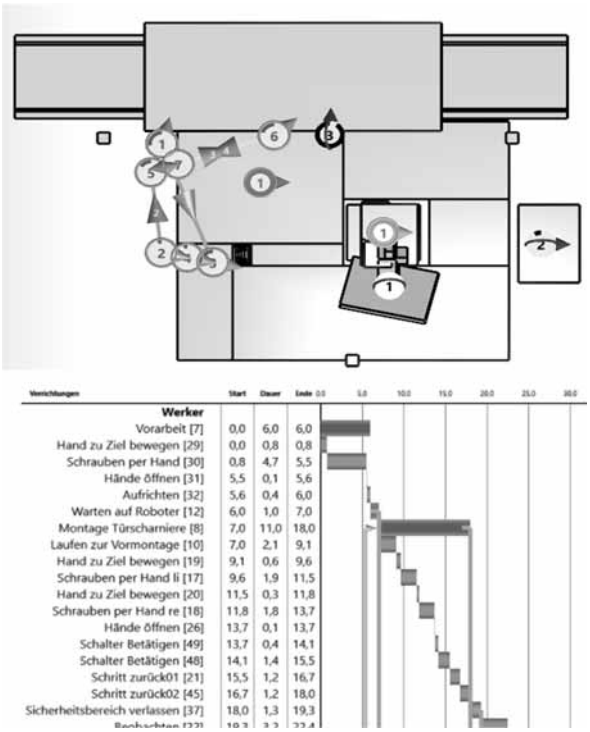

Figure 5: Spaghetti diagram showing motion paths (above) and cycle time diagram (below)

3 Planning Collaborative Work

With the introduction of human-machine collaboration, human workers are subject to a number of potential risks. Due to absent safety guards, humans work in the middle of highly dynamic enviroments where collision objects are not stationary any more. This leads to dangers arising from different sources, such as:

- planned and technological required collisions within the scheduled process, e.g. human-machine collaboration for a specific task within the collaborative space
- technical failure, e.g. collisions with out-of-control

objects
- machine dynamics, e.g. collisions with moved objects
- misbehavior, e.g. unattention, unintentional collision with objects

Those dangers challenge the planning and the design of collaborative working scenarios and make simulations prior to commissioning important than ever. ema, with its realistic human task modelling and its potential in incorporating also machine tasks, prepares a new era for validating human safety in the field of automation [5].

3.1 Design of collaborative scenarios

The design process for implementing collaborative working scenarios begins with a theoretical division of tasks between humans and machines and leads to the layout, tools and periphery design. Within the detailed planning phase, special tools for designing PLC-code, machine-code as well as human work activities are applied. As the following phase deals with the design and planning of scheduled collaborative tasks, a tool including PLC, machine and human tasks is urgently needed. Currently, research and development focuses on consecutive phases of generating misbehaviour and validating safety despite of misbehaviour – also as a basis for acceptance reports.

3.2 Analysing Regular Sequences

In order to efficiently analyse collaborative working scenarios, PLC, machine as well as human tasks need to be visualised in one simulation environment. Thus, the regular sequence of a collaborative work incorporates:

- Individual motions of the system, e.g. safety gate open – close
- Motion connections within the system, e.g. move machine only at closed safety gate
- Sensor reaction of the system, e.g. close safety gate only when light curtain is free
- Regular machine movement
- Sensor reaction of machine, e.g. force control
- Motion behavior of machine in case of sensor reaction, e.g. safety regulated stop
- Regular human motion
- Human motion for non-periodic tasks, e.g. tool change

3.3 Validating Safety at Misbehaviour

For validating safety at misbehaviour, the interaction between human misbehaviour and system reaction needs to be analysed. Furthermore, danger arising from excessive demand because of the system's dynamic needs to be taken into account. Even though, safety regulations are defined on the basis of risk assessments, human behaviour is analysed as a consequence of generated tasks. However, planning experience shows that validation requires an analytical approach.

Thus, misbehaviour can either result from FMEA (Failure Mode and Effects Analysis) or from random generators [6]. Both approaches have advantages and disadvantages in terms of objectivity and computation time. For instance, FMEA allows the analysis of a scenario with acceptable risk level where the robot moves an object with reduced velocity in close proximity to the human worker. The simulation of the scenario shows a collision between the object moved by the robot and the hand of the human worker (Figure 6). The next step would be a calculation and an evaluation of the applied and tolerable forces. There already exist tools for calculating forces during collision but those models are not yet implemented in ema. The physiological impact of collisions with the human body was already investigated by the BGIA in the past couple of years [7]. The results of this research are planned to be integrated in ema soon.

Even though, FMEA is an established method for failure analysis, the generation of misbehaviour is dependent on the engineer's imagination. In this sense, developers of ema are working on a so called numerical model for human behaviour which automatically generates collaborative scenarios [8].

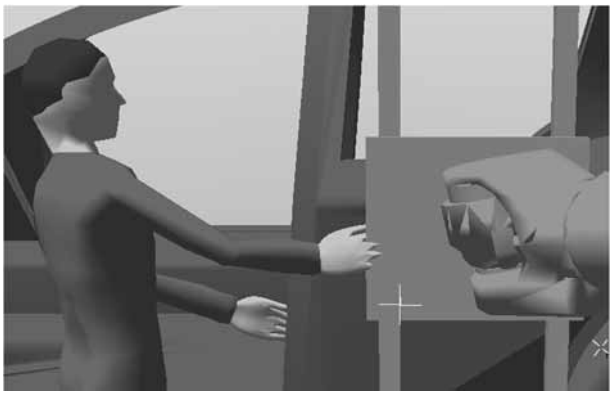

Figure 6: Collision between object and human body

For instance, the human worker is unconcentrated and enters the safety zone. The robot stops as fast as possible. The human worker is surprised by the reaction of the robot and almost falls over. The simulation of the scenario shows an unexected result, i.e. the human does not fall over as he reflexively supports himself on the workpiece (Figure 7).

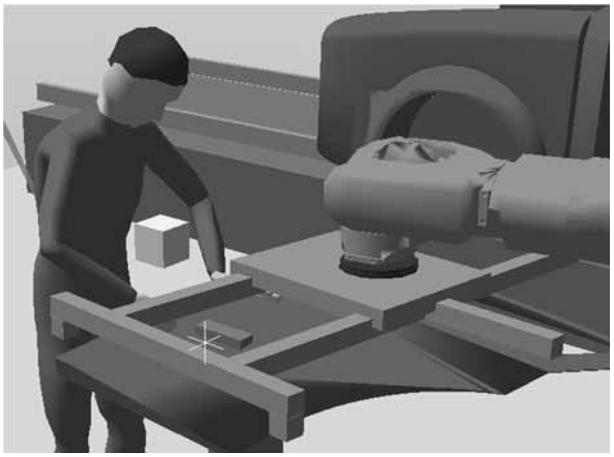

Figure 7: Simulation of misbehaviour

4 Discussion and Outlook

ema is an advanced simulation tool for intuitively generating and analysing human work activities. As the application of human-machine collaboration is of major interest now, ema was further provided with functionalities enabling the simulation of collaborative working scenarios.

Due to the development of universal exchange formats, ema not only comprises an interface for importing CAD data of machine objects but also for importing motion bevahviour in 3D space. Even though there exist exchange formats for geometries and motion data, logical connections to safety equipment are not yet integrated.

However, ema is able to simulate safety equipment on the basis of objects with their own active behaviour, i.e. sensors can be switched on and off. Furthermore, they are able to communicate to the system environment in case of specific events, e.g. human entering safety zones. This functionality expands ema to an event-based simulation system also allowing the validation of collaborative scenarios.

Even though ema is well-advanced in generating human activities, operations on moved objects in terms of following the moved object during task execution is not possible yet. For instance, objects moving on a conveyor belt or moved by a robot cannot be picked by the human worker during motion.

Furthermore, the integration of risk assessment analyses in terms of FMEA or random generators is still in focus of research and development. However, the examples show, that the integration of both methods is essential for the validation process.

References

[1] Mühlstedt, L. *Entwicklung eines Modells dynamisch-muskulärer Arbeitsbeanspruchungen auf Basis digitaler Menschenmodelle* [dissertation]. [Fakultät für Maschinenbau]. Technische Universität Chemnitz; 2012.

[2] Duffy, V.G. *Digital Human Modeling.* Orlando: Springer; 2011. 534 p.

[3] Fritzsche L., Leidholdt W., Bauer S., Jäckel T. und Moreno A. Interactive production planning and ergonomic assessment with Digital Human Models – Introducting the Editor for Manual Work Activities (ema). *IOS Press.* 2012: 4428-4432. doi: 10.3233.

[4] Bokranz, R. und Landau, K. *Handbuch Industrial Engineering: Produktivitätsmanagement mit MTM.* Schäffer-Poeschel; 2012. 1456 p.

[5] Leidholdt W. Simulation kollaborativer Arbeit von Mensch und Roboter – Die Sicherheit wird valide. In Schenk M., Herausgeber. Digitales Engineering zum Planen, Testen und Betreiben technischer Systeme. *18. IFF-Wissenschaftstage;* 2015 Juni; Magdeburg. Magdeburg: Fraunhofer IFF. 75-80.

[6] Leidholdt W. Die Simulation von Mensch-Roboter-Kollaboration – unabdingbar für die Prozessgestaltung. In Müller E., Herausgeber. Produktion und Arbeitswelt 4.0. Aktuelle Konzepte für die Praxis? *15. Tage des Betriebs- und Systemingenieurs;* 2014 Juni; Chemnitz. Chemnitz: Institut für Betriebswissenschaften und Fabriksysteme. 109-115.

[7] BGIA – Institut für Arbeitsschutz der Deutschen Gesetzlichen Unfallversicherung. *BG/BGIA-Empfehlungen für die Gefährdungsbeurteilung nach Maschinenrichtlinie. Gestaltung von Arbeitsplätzen mit kollaborierenden Robotern*. 2011. http://publikationen.dguv.de

[8] Leidholdt W., Wohlschläger C. Das Numerische Verhaltensmodell des Menschen – Simulation von Werkern unter erhöhter Beanspruchung. In Schenk M., Herausgeber. Tagungsband der 9. Fachtagung Digitales Engineering zum Planen, Testen und Betreiben technischer Systeme. *15. IFF-Wissenschaftstage;* 2012 Juni; Magdeburg. Magdeburg: Fraunhofer IFF. 229-233.

Note. At the moment, 4 editions of ema are available, i.e. Demo, Standard, Time&Ergo and Professional. The Demo edition is a fully featured software and can be installed for free. Compared to the Professional edition the only difference is in a watermark, a flag on each human model and in the only availability of the 5th female and 95th male percentile (Figure 8). The current version of ema is 1.6.0.0 including edition dependent functionalities like:

- Male and female digital human models representing the 5th, 50th and 95th percentile (Standard)
- Comprehensive task library for describing manual workflow (Standard)
- Comprehensive object library for different geometries, e.g. tables, shelves, containers, tools, etc. (Standard)
- CAD data interface for importing user defined geometries in Collada (.dae), JT (.jt), VRML (.wrl) and Wavefront (.obj) (Standard)
- Analysis tools, such as spaghetti diagrams, workflow reports including ErgoChecks and cycle time diagrams (Standard)
- Collision avoidance (Standard)
- Data interface for importing and exporting results as CSV or XLSX (Standard)
- Comprehensive ergonomic analysis based on the EAWS method (Time&Ergo)
- Comprehensive time analysis based on the MTM-UAS standard (Time&Ergo)
- Dynamic work station simulation including complex kinematic animation, e.g. robots (Professional)
- Motion capturing interface (Professional)
- Welding simulation (Professional)
- Assembly line balancing in terms of cycle variation analysis (Professional)

Centauro GmbH. The Centauro GmbH provides services in the field of simulating and analysing automation production lines. Currently, Centauro uses ema for planning human work activities within a research project – especially in the field of human-robot-collaboration – and is an essential partner for the further development of ema regarding task execution on moved objects.

Figure 8: User interface Demo edition. 1 menu bar, 2 tabs, 3 simulator, 4 task library, 5 behaviour workflow, 6 property settings, 7 3D settings, 8 3D view, 9 status area

SVD-AORA Model Order Reduction Method for Large-Scale Dynamic Linear Time Invariant System

Mohamed Kouki[1*], Mehdi Abbes[2], Abdelkader Mami[3]

[1]Université de Tunis El Manar, Ecole Nationale d'Ingénieurs de Tunis, Laboratoire d'Analyse et de Commande des Systèmes, BP 37, LE BELVEDERE 1002, Tunis, Tunisia; *koukimohammed@hotmail.com*

[2]Université de Carthage,Ecole Nationale d'Ingénieurs de Carthage, Laboratoire d'Analyse et de Commande des Systèmes, BP 37, LE BELVEDERE 1002, Tunis, Tunisia;

[3]Université de Tunis El Manar, Faculté des Sciences de Tunis, Laboratoire d'Analyse et de Commande des Systèmes, BP 37, LE BELVEDERE 1002, Tunis, Tunisia

Simulation Notes Europe SNE 26(1), 2016, 33-40
DOI: 10.11128/sne.26.tn.10326
Received: March 3, 2016; Revised: March 17, 2016;
Accepted: March 25, 2016;

Abstract. In this paper we present a joint model for order reduction for dynamic linear time invariant (LTI) system, which we call SVD-AORA (Singular Value Decomposition-Adaptive Order Rational Arnoldi). The SVD-AORA method is an extension of the SVD-Krylov based method. It is based on linear projection using two projection matrices (V and Z). The first matrix V is generated using the Krylov technique through the AORA method, the second matrix Z is generated using the SVD technique by the resolution of the Lyaponuv equation. After the resolution of the Lyaponuv equation, the solution obtained (The gramian observability matrix g_o) is decomposed using the SVD technique and thus we obtain the second projection matrix Z. The use of the AORA method enhances the numerical efficiency thanks to its relative lower computation complexity and the use of the SVD technique preserves the stability of the reduced system. The proposed method gives a reduced order model asymptotically stable, captures the essential dynamics of the original model and minimizes the absolute error between the original and the reduced one. The results of the proposed method are compared with other popular approach of order reduction in the literature which is the SVD-Krylov method. The reduced systems obtained by the proposed method have better performance compared to SVD-Krylov method. The method is explained through two numerical systems of different order.

Introduction

Technological world, physical and artificial processes are mainly written by mathematical models which can be used for simulation or for control. Among these models the LTI of high order. However, these high order models are difficult to manipulate and analyze because of the fact that the resolution of these models is indeed very demanding in computational resources, storage space, and mainely in CPU time. Hence the necessity of model order rection technique.. In the literature there exist different reduction methods of linear time invariant system (Arnoldi, Lanczos [1, 2, 3, 4],Rational Arnoldi [5],Rational Lanczos [6, 7], AORA [8], AOGRA [9], AORL [10], PRIMA [11],...); which performance differantly. Among these performances we can mention:

- A significantly reduced number of variables or states (required for description of a given model) compared to the original model,
- The simulation should be quick and does not require large memory space,
- The computational complexity associated with the evaluation of the reduced model should be significantly lower than the original model,
- Stability of reduced model must be guaranteed,
- Minimization of error between the original model and reduced one.

To Bring this performances, we depict in this paper the SVD-AORA method. This paper in organized as fol-

low: in section 3, basic tools are developed. In section 4, a description of SVD-AORA method is given with application in theoretical models. In section 5, a comparative study is presented. Section 6 concludes the work.

1 Preliminary

This section reviews some basic mathematical tools related to the linear dynamical system.

1.1 Moment matching

Let a state space representation of linear dynamical system be as [12, 13]:

$$\sum = \begin{cases} \frac{dx(t)}{dt} = Ax(t) + Bu(t) \\ y(t) = Cx(t) + Du(t) \end{cases} \quad (1)$$

The transfer function of linear system described as equation 1 is given by [14, 15]:

$$F(s) = C(sE - A)^{-1}B \quad (2)$$

If $F(s)$ is expanded as a power series around a given finite point $s_0 \in \mathbb{R}$, then we obtain [9, 8]:

$$F(s) = f_0 + f_1(s-s_0) + f_2(s-s_0)^2 + ... + f_{n-1}(s-s_0)^{n-1} \quad (3)$$

Where, n is the order of original system and the $f_k,\ for\ k = 0 : n-1$ coefficients present the moment matching of the dynamical linear system around the frequency s_0. The f_k coefficients are described by [10, 5]:

$$f_k(s_0) = C(s_0E - A)^{-(k+1)}B \quad (4)$$

1.2 Krylov Subspace

Let a frequency s_i be for $i = 1 : \hat{i}$, a matrix $\psi = (A - s_iE)^{-1}E$ and a vector $\xi = (s_iE - A)^{-1}B$. Then the Krylov subspace is obtained by [1, 2, 16, 17]:

$$\mathbb{K}(\psi, \xi) = \{\xi, \psi\xi, ..., \psi^{n-1}\xi\} \quad (5)$$

1.3 H_∞ error

Take a linear asymptotically stable system as in 1. The H_∞ norm is computed by this relation [18, 1, 19]:

$$H_\infty = sup_{w\in\mathbb{R}} \|F(jw)\|_2 \quad (6)$$

The reduced transfer function obtained by the use of model order reduction method is $\hat{F}(s) = \hat{C}(s\hat{E} - \hat{A})\hat{B}$. Then, the H_∞-norm error between the original system and reduced one is determined by the following relationship:

$$\| F - \hat{F} \|_{H_\infty} = sup_{w\in\mathbb{R}} \| f(jw) - \hat{f}(jw) \|_2 \quad (7)$$

2 SVD-AORA Model Order Reduction Method

The accuracy and the computational efficiency of the AROA and SVD-Krylov methods still insufficient in term of H_∞error minimization and the stability preservation of the reduced system. In this section we give a main mathematical problem formulation. Also, we present the main steps of the proposed method SVD-AORA and the results obtained by the use of two models.

2.1 Mathematical problem formulation

The mathematical problem consists on determining the state space parameters (order $k << n$) of the reduced model $\hat{\sum}$ from the state space parameters (order n) of the original model $\sum$ [1, 20, 12, 21] by using the proposed model order reduction method:

$$\sum = \begin{cases} \frac{dx(t)}{dt} = Ax(t) + Bu(t) \\ y(t) = Cx(t) + Du(t) \end{cases} \quad (8)$$

in which $A \in \mathbb{R}^{n\times n}$, $B \in \mathbb{R}^{n\times p}$, $C \in \mathbb{R}^{p\times n}$ and for simplicity we take $D = 0$, we obtain.

$$\hat{\sum} = \begin{cases} \frac{d\hat{x}(t)}{dt} = \hat{A}\hat{x}(t) + \hat{B}u(t) \\ \hat{y}(t) = \hat{C}x(t) + \hat{D}u(t) \end{cases} \quad (9)$$

such as, $\hat{A} \in \mathbb{R}^{k\times k}, \hat{B} \in \mathbb{R}^{k\times p}, \hat{C} \in \mathbb{R}^{p\times k}$.

2.2 Description of SVD-AORA Model Order Reduction Method

The SVD-AORA method is a joint method which benefits from both Krylov and Singular value decomposition technique. This method generates two projection matrices V and Z. The first projection matrix V is generated by using of the AORA technique. The second matrix is computed by the use of the SVD technique

and the matrix V is given according to this relation $Z = g_0 V (V^T g_0 V)^{-1}$, where g_o presents the Gramian observability matrix. The details of the SVD-AORA algorithm can be found in table 1 [21, 20, 6]:

Theorem 1 summarizes the principle of the proposed method .

Theorem 1: *Let a linear system as in 1 of order n and k expansion frequency $(k << n)$. Use the AORA algorithm to compute a first projection matrix V after a first k steps and the Lyaponuv technique to generate the observability Gramian matrix g_o. Then the second projection matrix Z is generated by the use of this relation:*

$$Z = WV(V^T WV)^{-1} \tag{10}$$

where the projection matrix W is a diagonal matrix, containing in the diagonal the first k singular values determined from the SVD decomposition of Gramian matrix.

2.3 Application

To test the SVD-AORA algorithm, we take two SISO models of different order (Eady of order 598 [22, 23] and RLC model of order 150 [24]). We present of each model the frequency response of the original model and the reduced one, the absolute error between the original model and reduced one and the poles distribution of the reduced model.

2.3.1 Model 1: Eady 598

The Eady model presents a mathematical model of atmospheric storm track (for example the region in the mid-latitude Pacific [22]). Its a SISO dynamical linear system of order 598 [22].

The figure 1 presents the frequency response of original system (Exact-598) and reduced one (SVD-AORA-16) of order 16. We notice a good correlation between the original and reduce one about the frequency range.

The absolute error variation between the original system and reduced one is shown in figure 2. We notice also from this result that there exist a good correlation between the original and reduced one.

The figure 3 depicts the poles distribution of the reduced system of order 16, we note that all poles are negative real part, which explain the preservation of stability.

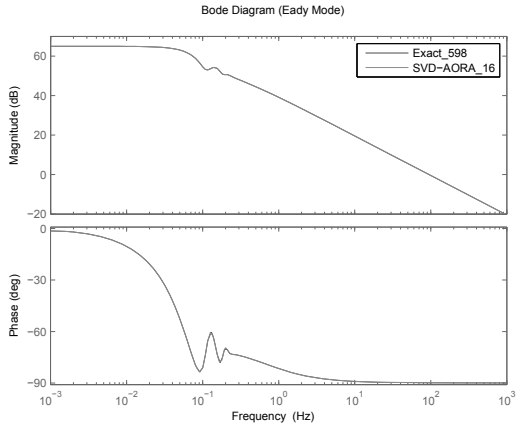

Figure 1: Frequency response of original system (Exact-598) and reduced one (SVD-AORA-16).

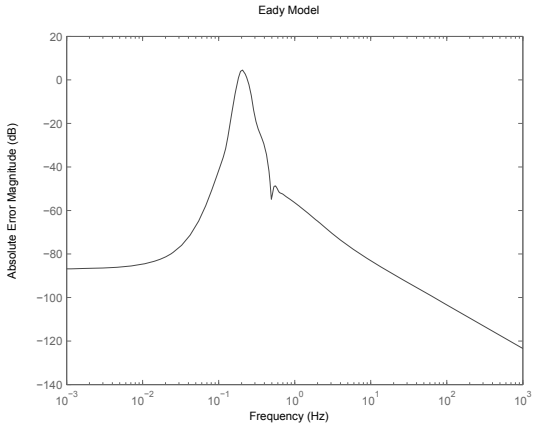

Figure 2: Absolute error between original model (598) and reduced one (16).

2.3.2 Model 2: N-RLC 150

The RLC model is a dynamical system with single-input/single-output [25, 26, 27, 11], it is very met in modeling of the electrical and electronic systems. The N-RLC model contains N chain of RLC circuit (where $R_N = 10k\Omega$, $C_N = 680\mu F$ and $L = 0.1H$ for $N = 1:50$). The electronic schematic of our N-RLC network is presented in figure 4:

The figure 5 depicts the frequency response of original system (Exact-150) and reduced one (SVD-AORA-12). We notice a good correlation between the original system and reduced one.

The figure 6 presents the absolute error variation between the original system and reduced one. We also

Table 1: SVD-AORA Model Order Reduction algorithm.

SVD-AORA Model Order Reduction algorithm:(Inputs:$A;B;C;D;S;k$; Outputs:$V;Z$)

(1): Define a frequency range S
$S = [s_1, s_2, ..., s_k]$ (with k $\ll$ n)
(2): Define a matrix ψ and a vector ξ for each expansion frequency s_i:
$\psi_i = -(s_i E - A)^{-1} E$ for i=1:k
$\xi_i = (s_i E - A)^{-1} B$ for i=1:k
(3): Compute the first projection matrix V using the AORA algorithm
$V = span\{\xi_1, \psi_2 \xi_2, ..., \psi_k^{k-1} \xi_2\}$
(4): Compute the gramian observability matrix g_o by solving the following Lyaponuv equation:
$A^T g_o + g_o A + C^T C = 0$
(5):Compute the singular value of the g_o matrix
$[U, W, T] = SVD(g_o)$
(6): Compute the second projection matrix Z through the following relation:
$Z = WV(V^T WV)^{-1}$
(7):The reduced system parameters can be defined by the congruences transformation
$\hat{E} = Z^T EV, \hat{A} = Z^T AV, \hat{B} = Z^T B, \hat{C} = C^T V$

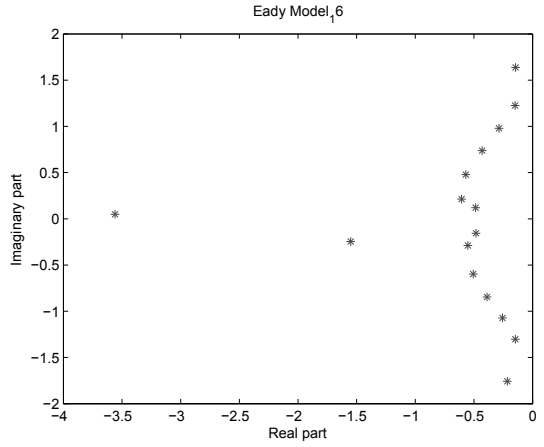

Figure 3: Poles Distribution of Eady reduced model with SVD-AORA method.

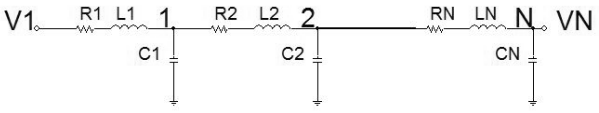

Figure 4: Chain RLC.

notice from the figure a good correlation between the original system and reduced one.

The poles distribution is depicted in the figure 7. We see that the all poles are negative real part, which explain the stability preservation of reduced system.

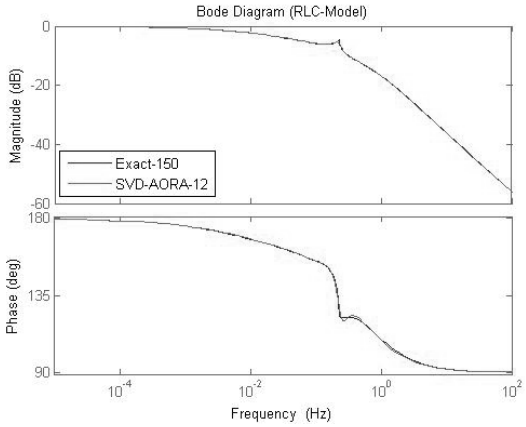

Figure 5: Frequency response of original system (Exact-150) and reduced one (SVD-AORA-12).

3 COMPARATIVE STUDY

In this section we present a comparative study between the SVD-AORA method and the SVD-Krylov one. Firstly, we present the frequency responses and the absolute error variations obtained by the tow methods. We depict also the poles distribution obtained by the SVD-Krylov method. Secondly, we give a comparative table containing the CPU-Time and the H_∞norm error for each method.

Figure 8 presents the frequency response of original system (order 598) and reduced one (order 16) obtained

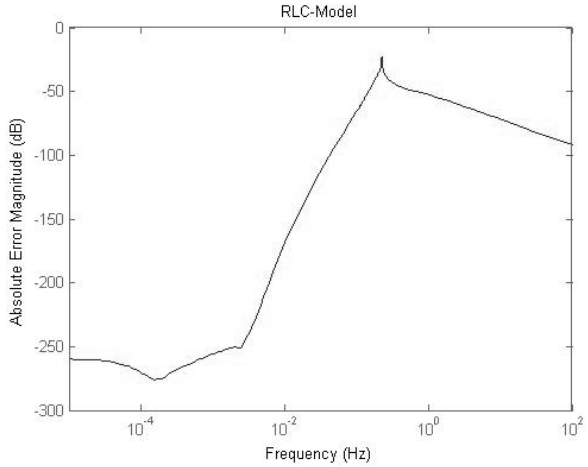

Figure 6: Absolute error between original system (150) and reduced one (12).

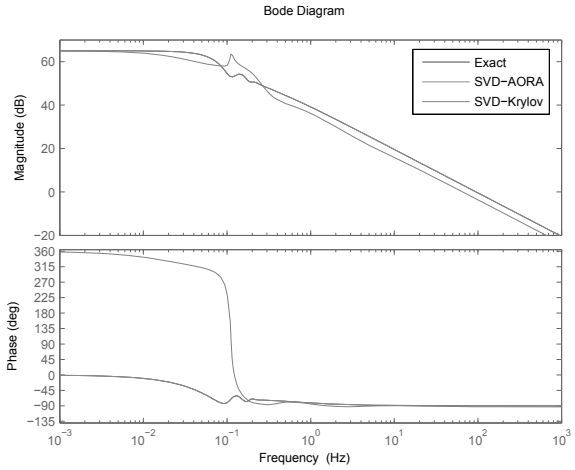

Figure 8: Frequency response of original system (Exact-598) and reduced one (16) with two methods.

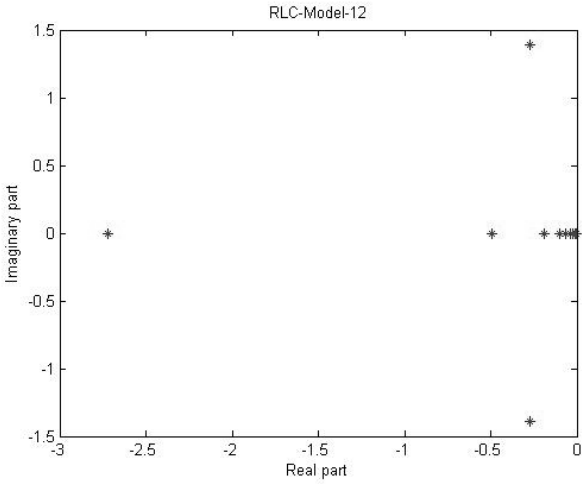

Figure 7: Poles Distribution of RLC reduced model (12) with SVD-AORA method.

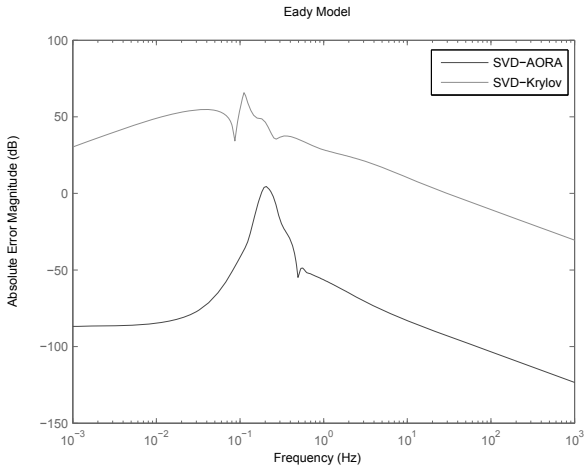

Figure 9: Absolute error between original model (598) and reduced one (16).

by the two methods. We notice a good correlation between the original system and reduced one for the result obtained by the SVD-AORA method.

We notice also from the figure 9 of the absolute error variation that the best result is obtained by the SVD-AORA method.

We note from the figure 10 of poles distribution obtained by the SVD-Krylov method the existence of positive real part poles, which explain the instability of reduced system.

Figure 11 shows the frequency response of original system (RLC-150) and reduced one (order 12) obtained by the two methods (SVD-AORA and SVD-Krylov). We note that the result obtained by the SVD-AORA method is very close to the original system which is not the case for the SVD-Krylov method.

Figure 12 shows the variation of absolute error between the original system and reduced one obtained according to the previous frequencies responses. The variation error between the original system and reduced one is very small near the low frequency and relatively small near the high frequency by the SVD-AORA method which is not the case for the SVD-Krylov method.

We note from the figure 13 of poles distribution ob-

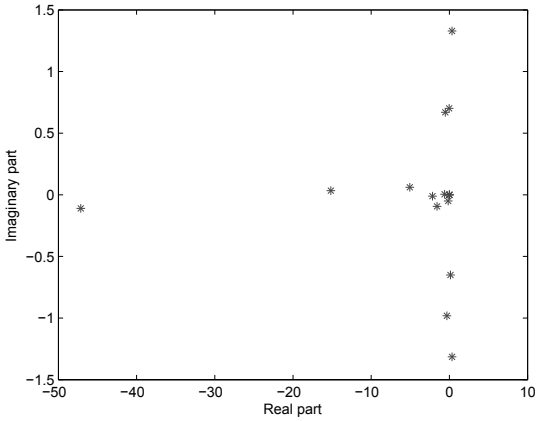

Figure 10: Poles Distribution of Eady reduced model (16) with SVD-Krylov method.

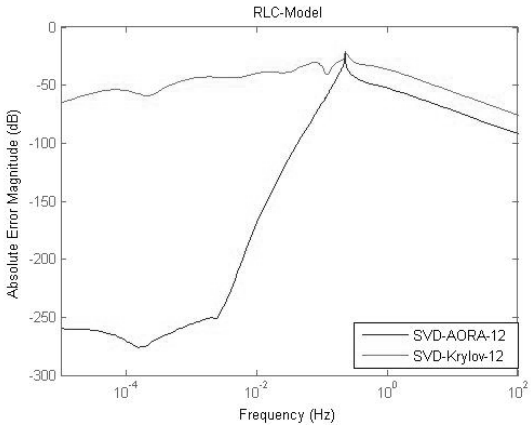

Figure 12: Absolute error between original model (150) and reduced one (12) with two methods (SVD-AORA-12 and SVD-Krylov-12).

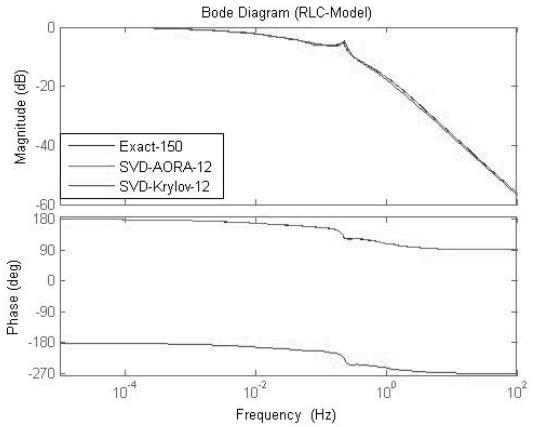

Figure 11: Frequency response of original system (Exact-150) and reduced one with two methods (SVD-AORA-12 and SVD-Krylov-12).

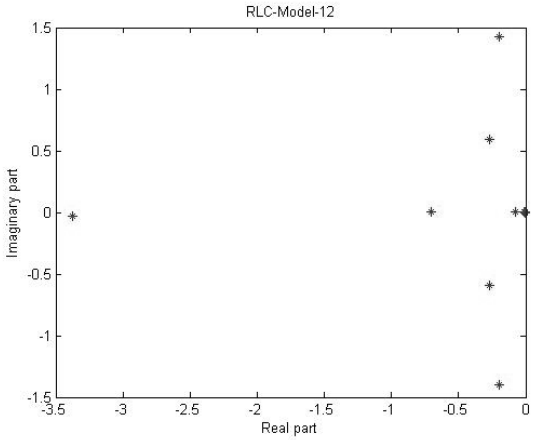

Figure 13: Poles Distribution of RLC reduced model (12) with SVD-Krylov method.

tained by the SVD-Krylov method that all the poles are negative real part, then the reduced system is stable. The table 2 contains the different values of H_∞ norm error and CPU-Time of each method. We note from the figures 8, 9, 11, 12 and from the table 2 that the best performance is obtained by the proposed method SVD-AORA.

4 Conclusion

A combined SVD-AORA method for dynamic linear time invariant model order reduction have been presented. The proposed method combine two techniques, which are the singular value decomposition and the Krylov. The Krylov technique is used in generation of first projection matrix, which is numerically efficiency. The singular value decomposition is used in computing the second projection matrix by the using of the Layponuv technique and the first projection matrix. Two models of different order were provided to prove why model order reduction via a combined techniques (SVD and Krylov) has the potential for significants improvement over existing combined method.

Table 2: H_∞norms and CPU-Time of each method.

Methods	SISO LTI System	minH_∞	maxH_∞	CPU-Time
SVD-AORA	Eady598	1.51110^{-7}	2.76010^{-5}	111.311s
SVD-Krylov	Eady598	0.044	6.693	98.755s
SVD-AORA	RLC150	5.88410^{-15}	4.34310^{-4}	13.023s
SVD-Krylov	RLC150	1.758910^{-4}	0.6290	11.823s

References

[1] Kouki M, Abbes M, Mami A. Arnoldi Model Reduction for Switched Linear systems. The 5th International Conference on Modeling, Simulation and Applied Optimization, Hammamet, Tunisia: IEEE. 2013; pp. 1–6.

[2] Kouki M, Abbes M, Mami A. Lanczos Model Reduction for Switched Linear systems. Proceedings in 2013 International Conference on Applied Mathematics and Computational Methods (AMCM 2013), 28-30 September, Venice. 2013; pp. 1–6.

[3] Frangos M, Jaimoukha I. Adaptive rational interpolation: Arnoldi and Lanczos-like equations. *European Journal of Control*. 2008;14:342–354.

[4] Barkouki H, Bentbib AH, Jbilou K. "An Adaptive Rational Block Lanczos-Type Algorithm for Model Reduction of Large Scale Dynamical Systems". *Journal of Scientific Computing*. 2015;67(1):221–236.

[5] Druskin V, Simoncini V. Adaptive rational Krylov subspaces for large-scale dynamical systems. *Systems and Control Letters*. 2011;60:546–560.

[6] Chu CC, Lai MH, Feng WS. MIMO Interconnects Order Reductions by Using the Multiple Point Adaptive-Order Rational Global Arnoldi Algorithm. *The Institute of Electronics, Information and Communication Engineers*. 2006;E89-C(6):792–802.

[7] Kouki M, Abbes M, Mami A. Lanczos Model Reduction for Switched Linear systems. In: *Proceedings in 2013 International Conference on Applied Mathematics and Computational Methods (AMCM 2013), 28-30 September*. 2013; pp. 1–6.

[8] Lee H, Chu C, Feng W. An adaptive-order rational Arnoldi method for model-order reductions of linear time-invariant systems. *Linear Algebra an its Applications*. 2006;415:235–261.

[9] Chu C, Lai M, Feng W. Mode-order reductions for MIMO systems using global Krylov subspace methods. *Mathematics and Computers in Simulation*. 2008; 79:1153–1164.

[10] Antoulas A. *Approximation of large-scale Dynamical systems*. Advances in Design and Control. 2005.

[11] Odabasioglu A, Celik M, Pileggi LT. PRIMA;Passive Reduced-Order Interconnect Macromodeling Algorithm. *IEEE Transactions on Computer-Aided Design of Integrated Circuits and Systems*. 1998; 17(8):645–654.

[12] Kouki M, Abbes M, Mami A. A Survey of Linear Invariant Time Model Reduction. *ICIC Express Letters,An International Journal of Research and Surveys*. 2013;7(3(B)):909–916.

[13] Zhang Y, Wong N. "Compact model order reduction of weakly nonlinear systems by associated transform". *International Journal of Circuit Theory and Applications*. 2015;29(6):1–18.

[14] Gugercin S, Sorensen D, Antoulas A. A modified low-rank Smith method for large-scale Lyapunov equations. *Numerical Algorithms*. 2003;32:27–55.

[15] Cullum J, Ruehli A, Zhang T. A Method for Reduced-Order Modeling and Simulation of Large Interconnect Circuits and its Application to PEEC Models with Retardation. *IEEE Transactions on Circuits and Systems*. 2000;47(4):261–273.

[16] Kouki M, Abbes M, Mami A. A survey of linear invariant time model reduction. *ICIC Express Letters,An International Journal of Research and Surveys*. 2013;7:906–916.

[17] Kouki M, Abbes M, Mami A. Non symmetric and global lanczos model reduction for switched linear systems. *International Journal of Mathematics and Computers in Simulation*. 2014;8:67–72.

[18] Gugercin S. An iterative SVD-Krylov based method for model reduction of large-scale dynamical systems. *Linear Algebra and its Applications*. 2008; 428:1964–1986.

[19] Kouki M, Abbes M, Mami A. *Complex System Modelling and Control Through Intelligent Soft Computations*, vol. 319, chap. Iterative Dual Rational Krylov and Iterative SVD-Dual Rational Krylov Model

Reduction for Switched Linear Systems, pp. 407–435. Springer International Publishing. 2015;.

[20] Kouki M, Abbes M, Mami A. Rational Arnoldi & Adaptive Order Rational Arnoldi for Switched Linear Systems. *Neural, parallel & scientific computations*. 2014;22:75–88.

[21] Kouki M, Abbes M, Mami A. SVD-AORA method for Dynamic Linear Time Invariant Model Order Reduction. 8th Vienna International Conference on Mathematical Modelling, Vienna, Austria: IFAC. 2015; pp. 695–696.

[22] Chahlaoui Y, Dooren P. A collection of benchmark examples for model reduction of linear time invariant dynamical systems. 2002. Http://niconet.NIC2.benchmarks.html/.

[23] Chahlaoui Y, Dooren P. *Dimension Reduction of Large-Scale Systems*, vol. 45 of *Lecture Notes in Computational Science and Engineering*, chap. A Collection of Benchmark Examples For Model Reduction of Linear Time Invariant Dynamical Systems,Technical Report, pp. 379–392. Springer Berlin Heidelberg. 2005;.

[24] Freund RW. *Model Order Reduction: Theory, Research Aspects and Applications*, vol. 13, chap. Structure-Preserving Model Order Reduction of RCL Circuit Equations, pp. 49–73. Springer Berlin Heidelberg. 2008;.

[25] Feldmann P, Fruend RW. Efficient Linear Circuit Analysis By Padé Aproximation via the Lanczos Process. *IEEE Transactions on Computer-Aided Design of Integrated Circuits and Systems*. 1995; 14(5):639–649.

[26] Popeea C, Jora B. Model Order Reduction with Disipativity Preservation. *Journal of Control Engineering and Applied Informatics*. 2004;6(1):27–33.

[27] Alam M, Nieuwoudt A, Massoud Y. Wavelet-Based Passivity Preserving Model Order Reduction for Wideband Interconnect Characterization. 8th International Symposium on Quality Electronic Design, San Jose, CA, USA: IEEE. 2007; pp. 1–6.

Agent-based Modelling and Simulation for Population Dynamics under Agricultural Constraints in Prehistoric Hallstatt: Hints for a Second Settlement

Johannes Tanzler[1*], Gabriel Wurzer[2], Kerstin Kowarik[3], Niki Popper[1,4], Hans Reschreiter[3], Martin Bicher[1,4], Felix Breitenecker[1]

[1]Institute of Analysis and Scientific Computing, Vienna University of Technology, Wiedner Haupstrasse 8-10, 1040 Vienna, Austria; **johannes.tanzler@tuwien.ac.at*

[2]Institute of Architectural Sciences, Vienna University of Technology, Treitlstrasse 3, 1040 Vienna, Austria

[3]Natural History Museum Vienna, Burgring 7, 1010 Vienna, Austria

[4]dwh GmbH, Simulation Services, Neustiftgasse 57-59, 1070 Vienna, Austria;

Simulation Notes Europe SNE 26(1), 2016, 41 - 46
DOI: 10.11128/sne.26.tn.10327
Received: November 20, 2015; Revised: March 3, 2016;
Accepted: March 10, 2016;

Abstract. This contribution is an outcome of a project cooperation between the Museum of Natural History Vienna and the Vienna University of Technology. The museum investigates since many years the prehistoric salt mines in Hallstatt, Austria, by classical archaeological methods, by experimental archaeology, and by modelling and simulation, which partly ca be seen as virtual experimental archaeology. This contribution continues investigations on modelling agricultural constraints for population size in prehistoric Hallstatt, presented in a previous conference publication.
As modelling and simulation approach agent-based simulation is used, as well for the mining process, and for the supply including food production, and for the environment.
First, the supply for the mining process is studied. The main focus is on the food production and its time consumption which is needed to feed all people working and living in prehistoric Hallstatt. This time consumption consists at one hand of the actual time used for seeding, mowing and harvesting and on the other hand more importantly of the time used for traveling to the fields and harvesting the goods. To simulate the traveling time an A* algorithm is used, also for the traveling time needed for the miners to get to the mine. Also the supply process of felling and transporting trees to the mine as well as chipping the wood to produce wood chips for lighting purposes is part of the simulation. Experiments with the model try to localize suitable areas for the prehistoric Hallstatt village with interesting outcome: the simulation 'suggests' a subdivision of the population into a village near the mine and another village at the location of today's Hallstatt.

Introduction

Hallstatt is famous for its prehistoric salt mine which is of great interest for archaeologists. The special interest comes along with very well conserved finds which results of the great conserving effect of salt and the collapse of the salt mine in the 13th century B.C. Some of these finds are very special tools and it is hard to understand in which way they were used. Not at last to get a better understanding of the way these tools were used a cooperation between the Museum of Natural History Vienna and the Vienna University of Technology was formed and this work is part of it. For instance a bronze pick which was investigated with the help of simulation in another project [1].

This work mainly focuses on the food production of the population of Hallstatt. It continues previous work on modelling agricultural constraints for population size in prehistoric Hallstatt, which studies how many people could have lived in Hallstatt if it is assumed that all food was produced locally [2]. The fields considered in this preliminary work are the same as used in this work. A result of this work is that 72 persons could have been fed of the food provided by these fields. This number of persons is used in the following as the population size. The population size is an essential parameter for this work because it directly influences the time needed to work on the fields.

The model which is used for this investigation is an agent-based one [3] and is implemented in Anylogic [4].

1 The Model

The basis for all agricultural production are the useable areas.

1.1 Areas

Because of the fact that this project is about prehistoric Hallstatt and its food production it would be desirable to know which areas they actually used and for which purpose. But unfortunately these data are not available so other data have to be used. The oldest data to get are data of the 19th century. At this time maps for tax purposes were created and these maps hold information about the usage of the fields. These maps have been digitalised and can easily be implemented as shapefiles [5]. Because no better data are available, these maps are used for this project.

There are several different types of areas declared but the ones used are 'grass', 'field' and 'garden'. The total size of the class 'field' is 13 hectare and is used for two different crops. Half of it is used for sorghum production and the other half is used for barley production.

The 'garden' has a total size of 16 hectare and its crop is beans. Actually the size of the class 'grass' is over 650 hectare, but this would be too much to be used by 72 persons, more precisely the meat which could be produced by this amount of grass would not guarantee a balanced nutrition. Therefore just the size of 100 hectare is supposed to be harvested. It also has to be said that no grazing is considered and all of these 100 hectare are mown and harvested.

Figure 1 shows the section of the map which is used for the simulation. The red areas are 'garden', the brown ones are 'field', the light green ones are 'grass', the dark green ones represent 'wood', grey is 'rock' and blue is 'water'.

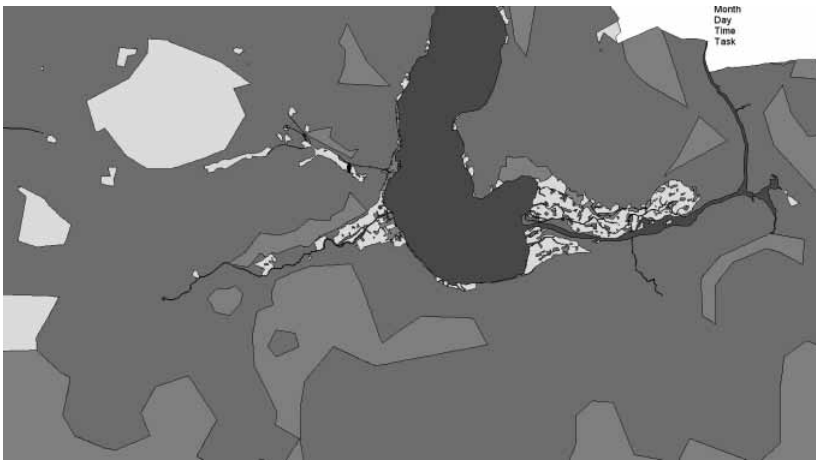

Figure 1: Used section of the map.

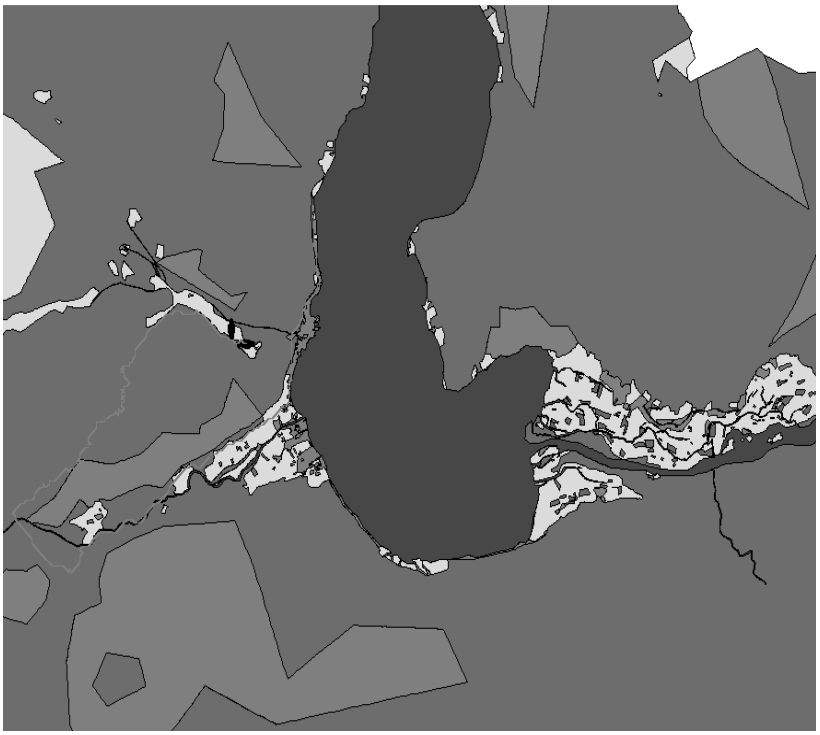

1.2 Calculation of the paths

Because of the sectional very steep terrain it is necessary to use a good algorithm for the calculation of the paths. Therefore the used algorithm is an A* algorithm.

The disadvantage of using a complex algorithm is that the calculation needs lots of time especially if a small grid is used. In this case a grid of 25 meters seems to be the best choice.

In Figure 2 a path from the village near the mine to a field near the lake is shown. It seems to be a loop way to the field, but actually this shows the steepness of the terrain because the A* algorithm takes into account that the traveling speed is faster if the path is not too steep.

The steepness can be better seen in Figure 3. Blue coloured areas are the deepest ones and the green ones are the highest.

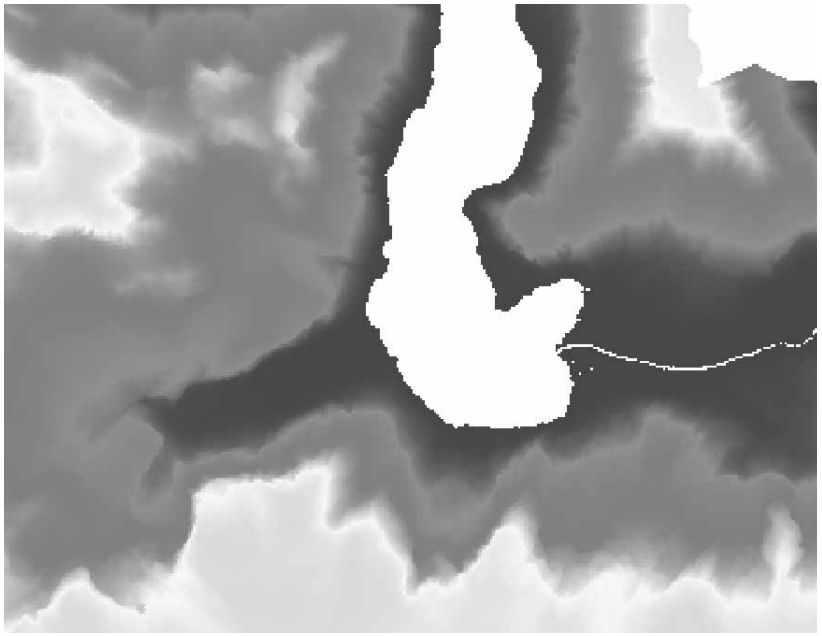

Figure 3: Depth model.

1.3 Population

Birth and death rates are basically gathered from the project 'Mining with agents' [6] and with these rates a population structure was calculated. As mentioned above the population size is taken from a prior work [1] and is 72.

Because of the calculated population structure not all of these 72 people are of an age which allows them to work. In this work it is assumed that persons younger than 6 years and persons older than 75 are not able to work. The following table shows the population structure and it can be spotted that 13 people are too young to work, no one is too old, what means that 59 persons are in an age where they can work.

[0;6)	[6;15)	[15;30)	[30;45)	[45;75)	[75; Inf)
13 Pers.	20 Pers.	21 Pers.	11 Pers.	7 Pers.	0 Pers.

Table 1: Population structure.

As mentioned before this model is an agent based model and each person which is able to work is represented as an agent. Persons who are too young or too old are not modelled because they have no influence on the model.

1.4 Working procedures

The level of detail of the models concerning the working procedures is not very high but this does not seem to be necessary or useful. These models are kept simple so if there are better data, maybe by using experimental archaeology, they can be implemented easily.

Seeding and mowing. For these two procedures parameters called 'timeMowingPerHectar' and 'timeSeedingPerHectar' are used to define the seeding and mowing rates. In view of these rates an agent seeds or mows in every time step, when it is located at the field and the field is ready for seeding or mowing, a specific area. The parameters 'timeMowingPerHectar' and 'timeSeedingPerHectar' are both equal to 10.

Harvesting. For harvesting a parameter called 'timeHarvestPerHectare' is used to represent the harvesting speed and is also 10. In this case the harvest speed is the same for each crop, even grass. But the most time consuming task concerning harvesting is not the harvesting itself but the transport of the goods to the home village of the agent because the physical highest load of each agent is set to 20kg.

Because of the time consuming task of transporting the crops the supposed yields of the crop plants are shown in Table 2.

	sorghum	barley	beans	grass
yield	341.269kg	760.049kg	510.773kg	3000kg

Table 2: Yields.

Wood production. This task is similar to harvesting but in this case another simplification is made, namely, all wood is gathered at one spot in the wood. The harvest rate of wood is set to 10kg per minute and the transport capacity is 50kg, in contrast to 20kg if carrying crop. A larger capacity is likely because there are finds that indicate a special method to drag wood.

Wood chip production. Wood which is dragged to the mine has to be chipped so it can be used for lighting purposes. This is also represented as a parameter called 'woodChipsPerMinute' which is set to 1kg.

Salt mining. The salt mining process itself is not modelled. The output of the salt mine is the time which is used in the mine. But every minute 0.5kg wood chips are used in the mine.

1.5 Scheduling of the workload

The seducing of the workload is highly dependent on the date especially concerning the agricultural tasks. In the following Table 3 the optimal points in time for the agricultural tasks are shown, the numbers in this table represent the days of the year.

	sorghum	barley	beans	grass
seeding/ mowing	110	90	100	180
harvesting	270	240	250	183

Table 3: Action time table.

When the optimal day for a specific task has come, all fields of the specific class are activated and then processed. To be more precise – an agent gets a task assigned in the morning, then goes to the location of the field and performs it. Afterwards the agent gets the next task and directly heads to the next field which has not been processed yet.

To minimize the walking time it is estimated how many people have to work on the specific field. If every field has enough workers assigned, the workload is empty and no more agents have to walk down to the fields and are free to do other work. Should it happen that the estimation was not good enough and the field is not processed when it is time to call it a day, the field is taken back to the workload and will be processed at the next day.

On days when there is no agricultural work to be done, the agents are assigned to work in the mine if there are enough woodchips in the stock to light the mine. Otherwise the task is to make wood chips, or if there is not enough wood, to manage to get some.

1.6 Second settlement

As described before, the village is assumed to be located close to the mine and almost all fields beside the grass fields are located in the valley. This raises the guess that it could have made sense to have a second settlement in the valley, which would mean that not that many people have to go down to the valley for the agricultural purposes. Also not all the crop has to be brought up the hill because the people living in the valley can take their food with them when going to work in the mine. The down side is, that the people in the valley, who work in the mine, have to go up the hill every morning.

The possibility of a second settlement is taken into consideration and is placed in the valley where Hallstatt is located today.

2 Results

The result of this simulation is mainly the time which can be used to be spent in the mine because with this inferences on the salt output can be drawn.

Although the time spend in the mine maybe is not the most meaningful output. It seems more useful to take a closer look at the time spent for harvesting and seeding because the most uncertain parameters are taken into account the most - namely the rate of chipping wood chips per minute and the amount of chips needed per minute.

2.1 Results one settlement

When taking a closer look at the time needed for seeding in Figure 4 it can be seen that the time used for seeding is about 459 hours.

The time theoretically used for seeding is the area of fields and gardens times the seeding speed which would be about 290 hours but in these 459 also the time for traveling to the areas and back is included.

It is also easy to see in Figure 4 that the time used for working is close to exactly 8 hours a day. This is possible because in the simulation if the worker comes home late from work, the overtime is credited to the next morning.

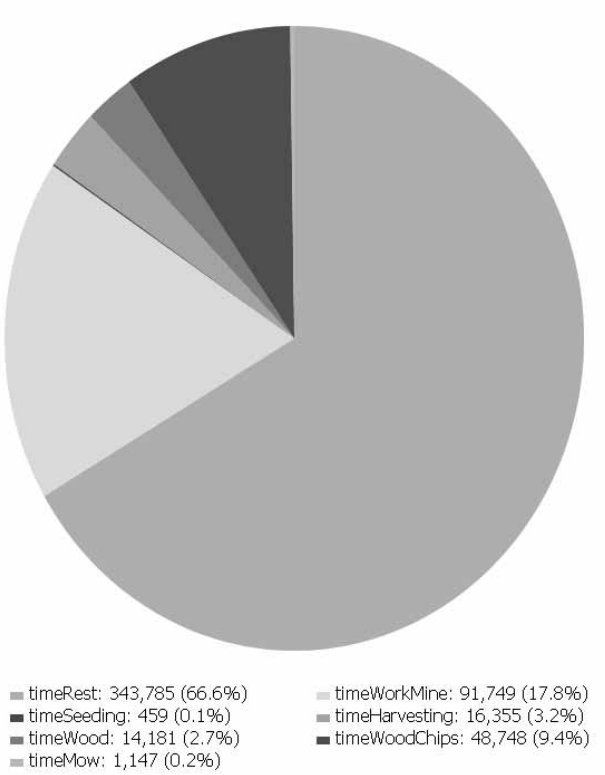

Figure 4: Time consumption.

Another thing to point out is that the time used for agricultural purposes seems quite low, especially if it is taken into account that a big area of 100 hectare grass has to be harvested.

2.2 Results two settlements

In this case the distribution of the people in the two settlements is studied.

Figure 5 shows that the more people live in the valley the shorter the time used for seeding is. Concerning the mowing time, the used time raises again when there are more than 45 people living in the valley. This is a result of the assumption that the people harvest the grass just in the valley and therefore they have to go around the lake to the right side of the lake to harvest grass and this path takes more time than going up the hill.

3 Conclusion

As the results have shown it really seems likely that there was a second settlement in the valley of Hallstatt. At the first look these results may look surprising but on the second look it is all about how often the people have to go up the hill.

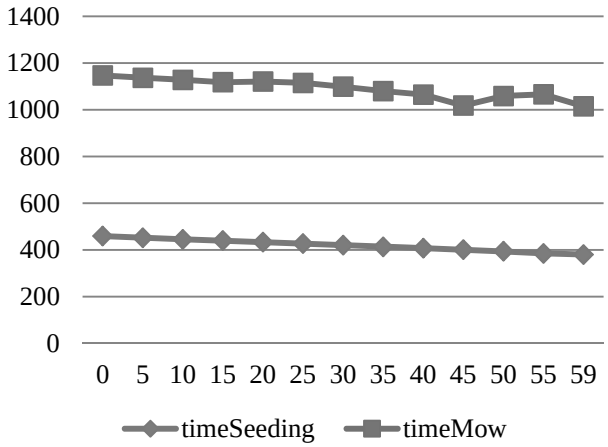

Figure 5: Time seeding and time mowing in dependence of the amount of people living in the valley.

The descending of the time consumption the more people live in the valley can be seen more dramatically in Figure 6.

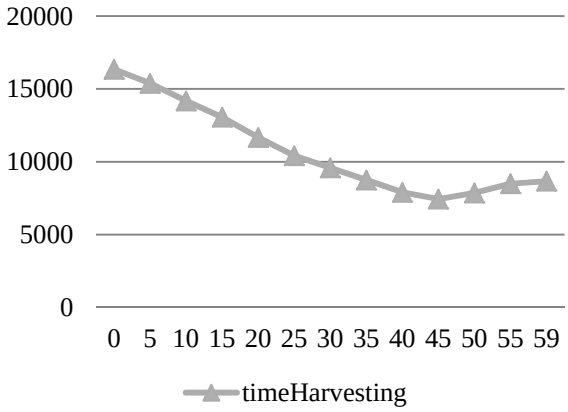

Figure 6: Time harvesting in dependence of the amount of people living in the valley.

If the amount of crop which can be transported at once could be raised a lot, it would be different at some point.

The fact that there are many more tasks which could be implemented and modelled more detailed, induces in doing so.

On the one hand it is questionable if also the results would get better on the other hand who can tell that they do not – the problem of validation in archeology.

References

[1] Heinzl B, Auer E, Slowacki B, Kowarik K, Reschreiter H, Breitenecker F. *Mathematical modelling for experimental archaeology: case studies for mechanical tools in hallstatt salt mines.* In: The 24th European Modeling and Simulation Symposium. 2012.

[2] Tanzler J, Pichler P, Kowarik K, Reschreiter H, Wurzer G, Bacher A, Breitenecker F. *Modelling agricultural constraints for population size in prehistoric Hallstatt.* ERK - International Electrotechnical and Computer Science Conference. 2013.

[3] Breitenecker F, Bicher M, Wurzer G. *Agent-based modeling and simulation in archaeology, chapter: Agent-Based Simulation in Archaeology: A Characterization.* [S.l.]: Springer, 2013.

[4] Grigoryev I. AnyLogic 6 in three days: a quick course in simulation modeling. AnyLogic North America, Hampton, NJ, 2012.

[5] *ESRI Shapefile Technical Description, An ESRI White Paper-July 1998.*

[6] Kowarik K, Reschreiter H, Wurzer G, Totschnig R, Rausch A. *Mining with Agents - Agent-based Modeling of the Bronze Age Salt Mine of Hallstatt*, Talk: Archäologie und Computer, Wien; 11-03-2008 - 11-05-2008; in: "Workshop 13 - Archäologie und Computer 2008", CD der Stadt Wien, Stadtarchäologie, Wien (2009), ISBN: 978-3-85161-016-1; 1 - 19.

Prediction of the Burden of Mental Diseases Using a Microsimulation Model

Andreas Bauer[1*], Christoph Urach[2], Felix Breitenecker[1]

[1]Department of Analysis and Scientific Computing, Vienna University of Technology, Wiedner Hauptstraße 8-10, 1040 Vienna, Austria; [*]*andreas.e101.bauer@tuwien.ac.at*

[2]dwh simulation services, Neustiftgasse 57-59, 1070 Vienna, Austria

SNE Simulation Notes Europe SNE 26(1), 2016, 47-52
DOI: 10.11128/sne.26.tn.10328
Received: January 20, 2016; Revised: February 12, 2016;
Accepted: March 5, 2016;

Abstract. This work aims to predict the burden of mental diseases to provide sufficient capacities for treatment. A microsimulation model is built to simulate the course of events of mentally ill patients. Three scenarios of simulations are defined to test the consequences of using differently detailed patient-level data on result quality. Significant differences in the results are encountered. The overall numbers and times of patients events are analyzed as well as the number of events per patient. The differences between the results for the different scenarios and for the various subpopulations regarding patient parameters are pointed out. For example, psychotic patients tend to have more readmissions. Further analyses regarding the connection between ambulant contacts and readmissions to the hospital are performed. Also, regional differences of Lower Austria compared to the entire Austrian population are analyzed. Finally, an intervention strategy with compulsory ambulant contacts is examined.

Introduction

The prediction of the burden of mental diseases is important to provide sufficient capacities in the hospitals. The overall number of readmissions to hospital is estimated as well as the numbers of events for subpopulations defined by certain patient characteristics to determine the required capacity and its change over time. Also, the influence of outpatient contacts to a psychiatrist on number and times of readmissions is examined.

The consideration of regional aspects is important for the accuracy of the simulation results. So, the situation of patients with mental diseases for Lower Austria is investigated in detail and compared with the situation of entire Austria.

The availability of patient data is often a problem. In these cases privacy protection only allows usage of k-anonymized data. So, it is not certain to get significant results with the given data. Differently detailed patient-level data based on the same set is used to analyze the effect on the quality of the outcome.

1 Survival Analysis

Methods from the field of survival analysis are used to build the statistical model behind the simulation model.

Survival analysis deals with the analysis of data of the time until the occurrence of a particular event. This kind of data is frequently encountered in medical research and referred as survival data.

Survival analysis mainly deals with the estimation of the survival function and the hazard function. The survival function $S(t)$ gives the probability that the events has not occurred until time t and the hazard function $\lambda(t)$ gives the instantaneous rate of occurrence of the event.

The cumulative hazard function Λ is defined as

$$\Lambda(t) = \int_0^t \lambda(x)dx. \tag{1}$$

The Nelson-Aalen estimate is an estimate for the cumulative hazard function Λ [1]. Let d_t and n_t denote the number of people that experience the event at time t respectively are at risk at time t. Let t_i denote the event times. Then Λ can be estimated by

$$\hat{\Lambda}(t) = \sum_{i:t_i \leq t} \frac{d_{t_i}}{n_{t_i}}. \tag{2}$$

1.1 Cox model

The Cox model is a model for the hazard function [2]. It assumes that the ratio of the hazards of different exposure groups remains constant over time. The hazard at time t for individual i with covariate vector X_i is assumed to be

$$\lambda_i(t) = \lambda_0(t)\exp(X_i\beta) \tag{3}$$

where λ_0 is an unspecified nonnegative function called baseline hazard function and β is a vector of regression coefficients.

Stratified Cox model. The stratified Cox model is an extension of the Cox model and allows for multiple strata [3]. The strata divide the subjects into disjoint groups and each subject is member of exactly one stratum. Each of which has a distinct baseline hazard function but common values for the coefficient vector β. The hazard for individual i belonging to stratum k is

$$\lambda_k(t)e^{X_i\beta}. \tag{4}$$

2 Model

2.1 Data

Two datasets are used in this work. Dataset *dataaut* consists of data of patients from Austria and dataset *datanoe* consists of data of patient from Lower Austria. Patient parameters are age, sex, length of stay in the psychiatric department and the diagnosis made during the initial stay at the hospital. Also times of readmissions, ambulant visits to a psychiatrist and deaths are included. It depends on the chosen scenario which events are actually considered in the model. The data samples are used for the parametrization and the sampling of the population of the simulation model.

2.2 Model description

The chosen model type is a microsimulation model. That means that it follows the bottom-up approach and every single individual is modeled. This approach is chosen because not only the cross-sectional analysis is important but also the longitudinal pathways of single individuals. Furthermore, this approach is suitable for the analysis of different policies and scenarios. Another reason is that the characteristics of the individuals are manageable with a bottom-up approach.

The events of a patient are expressed by state changes. The possible ways through the states are described by a transition matrix which can be interpreted as a directed acyclic graph. Every individual starts in state R (released after the first admission to hospital). If the most recent event of the patient was the ith readmission, the patient is in state A_i and if the most recent event was the ith ambulant psychiatrist visit, the patient is in state P_i. The dead patients are in state D. In order to calculate the times of the events respectively the probabilities for the events to occur the hazard and survival functions have to be modeled. The Cox model and the Nelson-Aalen estimate are applied to determine the according statistical models. The hazard functions for the transitions are estimated with a stratified Cox model. The strata represent the transitions [4].

The overall simulation time is fixed. The simulation starts for every patient with the day of the release from the first stay in a psychiatric department of a hospital. The simulation is executed in discrete time steps of one day.

The starting population is sampled from real data described in Section 2.1. It is modeled as a closed cohort, so there is no change in the size of the population except for deaths.

3 Simulations

3.1 Definition of scenarios

The given datasets of full records of patients are used to examine the consequences of using differently detailed patient-level data on result quality. Data at hand are often incomplete or contain only information about specific events due to data protection issues, loss of data and many other reasons. Three scenarios with different number and order of the readmissions that are used for the Cox model are defined. So, the scenarios only differ in terms of the parametrization. Each scenario is executed with and without ambulant contacts to psychiatrists.

In scenario 1, only the first readmission of each patient is considered and all the other readmissions that are available in the data are dismissed. In the simulation, the transition rates from any readmission state A_i to states A_{i+1}, P_{i+1} and D are assumed to be equal for all i. There are two versions of this scenario considering the visits to the psychiatrist, one with ambulant contacts ($1a$) and one without ($1b$).

In scenario 2, the first z readmissions of each patient are considered. All readmissions are considered independently from each other, even if they belong to the same subject. So, there is no order of the readmissions and every readmission is regarded as first readmission. Like in scenario 1, the transition rates from any readmission state A_i to states A_{i+1}, P_{i+1} and D are assumed to be equal for all i.

Between two consecutive admissions up to one contact to a psychiatrist is considered. Again, there are two versions of this scenario, one with contacts to the psychiatrist ($2a$) and one without any contacts ($2b$).

In scenario 3, the first z readmissions of each patient are considered with the same number z as in scenario 2 but in contrast to scenario 2 the readmissions are ordered. That means that for the first z readmissions the transition rates from a readmission state are independent. From the $(z+1)$th readmission on, the rates are assumed to be equal to the transition rates starting from state A_z. In scenario $3a$, at most one contact to a psychiatrist between two consecutive admissions is possible. Therefore, also the psychiatrist contacts are ordered. In scenario $3b$, no psychiatrist contacts are considered.

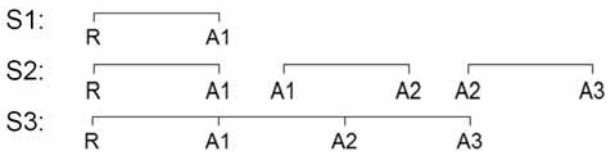

Figure 1: Schematic representation of the information needed in the three scenarios.

In Figure 1, the utilization of data in the three scenarios for a time line with three readmissions is presented.

3.2 Results

Simulations for single scenarios and comparisons of the matching scenarios that only differ in the inclusion of psychiatrist contacts and comparisons of all scenarios with and without contacts to a psychiatrist for populations from Austria and Lower Austria are carried out.

The simulation time is 2 years, because the majority of the readmissions, especially of the first readmissions, which are the most crucial events, happen within this period. A population of 18638 individuals is sampled from datasets *dataaut* and *datanoe*.

An exemplary result for scenario $1a$ is shown in Figure 2. The evolution of the distribution of patients over the states is shown. On the x-axis time is plotted, on the y-axis the percentage of each state is plotted on top of each other. The area under each curve is filled with a distinctive color. The states are coded with colors. Dark green represents state R, the readmission states are assigned to lighter shades of green, the psychiatrist states have shades of red and dark red represents the state death D.

The share of the patients in state R decreases almost exponentially. After two years about 50 percent are remaining in state R. The percentage of deaths increases almost linearly. At the end of the simulation around 3.4% of the population is dead.

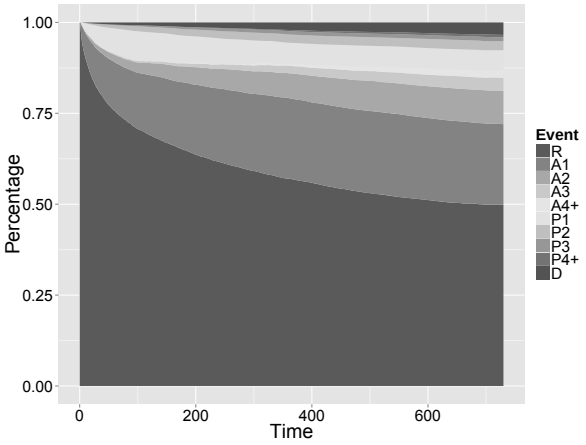

Figure 2: Evolution of patient over the states for scenario $1a$ for a population from Austria.

3.3 Comparison of scenarios

Patients with outpatient contacts to a psychiatrist (OPC) are compared with those without outpatient contacts (non-OPC). In Figure 3, the percentage of patients with readmissions is shown for both groups and all scenarios. Patients with ambulant contacts have a much higher percentage of readmissions, in scenarios $2a$ and $3a$ even twice as much as patients without ambulant contacts.

In Table 1, the percentages of patients with readmissions are compared for all scenarios. It can be seen that scenarios $2a$ and $2b$ have a higher percentage of readmissions. The reason is that the transition probability from state R to state A_1 is higher in scenario 2, because in scenario 1 only the first readmissions from the data are used to fit the rate from state R to A_1 while in scenario 2 all readmission times are treated as first readmission times. Since the times for the later read-

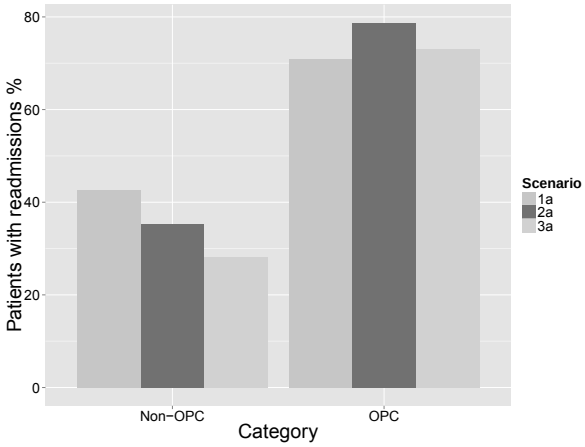

Figure 3: Comparison of the percentages of patients with readmissions between patients with and without outpatient contacts.

missions are shorter in average, the median of the first readmission times drops from 75 days for scenarios 1 and 3 to 63 days for scenario 2. This leads to a higher probability for entering state A_1 and having a readmission.

Scenario	1*a*	1*b*	2*a*	2*b*	3*a*	3*b*
Readmissions (%)	42	43	51	51	42	42

Table 1: Percentage of patients with readmissions.

In order to analyze the results in greater depth typical pathways of patients during the simulation are defined. In addition to the number of readmissions of a patient the times of these are taken into account to classify the pathways.

Nine typical, distinctive pathways are chosen to split the population in roughly equally sized classes. Only the class of patients with no readmission is much bigger than the others.

In Table 2, an overview of the classification for patients without ambulant contacts is given.

In Figure 4, the sizes of the classes for scenarios 1*b*, 2*b* and 3*b* are presented. Class 1 is not shown in the plot, because the number of patients without readmissions has already been analyzed and the focus is on patients with readmissions.

In scenarios 1*b* and 2*b* are more than twice as many patients in class 2 than in scenarios 3*b*. That means more individuals have exactly one readmission shortly after the release. This can be explained by the fact that

Class	Readmissions	Month of first readmission
1	0	–
2	1	1
3	1	2-6
4	1	7-12
5	1	13-24
6	2-4	1
7	2-4	2-6
8	2-4	7-24
9	> 4	any

Table 2: Classification of patient pathways.

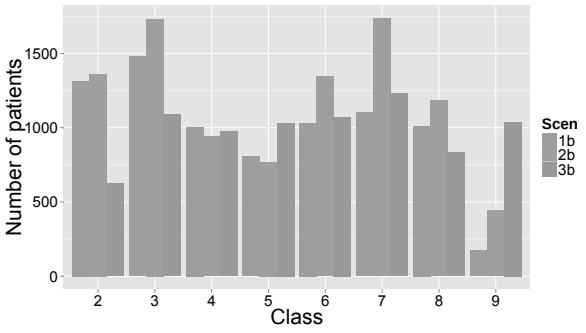

Figure 4: Size of classes for the scenarios without ambulant contacts.

in scenario 3*b* patients in average have more readmissions and in scenario 2*b* more patients have readmissions in general. The number of individuals with more than four readmissions is much higher in scenario 3*b*.

3.4 Intervention

An intervention strategy is examined to possibly reduce the number of readmissions. According to this strategy a compulsory visit to an ambulant psychiatrist 30 days after every admission to hospital is implemented. The question is, if this strategy can reduce the number of readmissions to hospital.

Type of Event	No intervention	Intervention
Readmissions	42.2	67.8
OPC	27.7	99.7
Deaths	3.9	3.6

Table 3: Comparison of percentages of the occurrence of events for scenario 3*a* with and without intervention.

In Table 3, the percentages of patients with readmis-

sions, ambulant psychiatrist contacts (OPC) and deaths are compared for scenario 3*a*. The percentage of patients with readmissions is much higher with the intervention strategy. This leads to the conclusion that an ambulant contact increases the probability for a readmission. The comparison of OPC and non-OPC patients in Figure 3 already hypothesizes this result. In the intervention scenario almost every patient visits a psychiatrist during the simulation. So, this strategy does not succeed in reducing the number of readmissions.

3.5 Comparison of simulations for Austria and Lower Austria

Results of the simulations for populations from Austria and Lower Austria are compared in terms of number and times of events. The evolutions of the patients distribution over the states for the two populations in scenario 3*a* are presented in Figures 5 and 6. The share of the patients in state *R* has a similar evolution for both simulations and decreases almost exponentially. About 50 percent of the patients from Austria are remaining in state *R* at the end of the simulation, about 47 percent of the other population. So, patients from Lower Austria have more readmissions, since the numbers for states P_i and *D* are very similar for both populations.

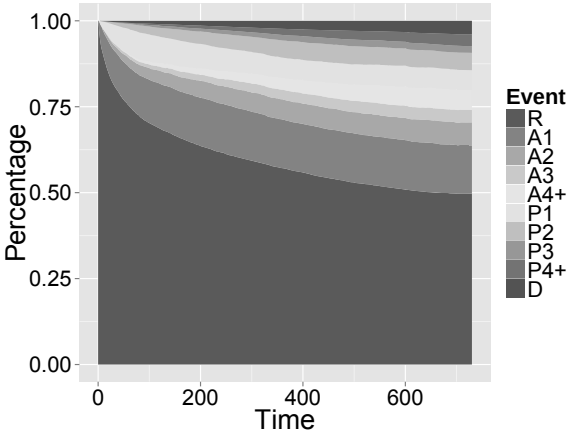

Figure 5: Evolution of the patients distribution over the states in scenario 3*a* for Austria.

The proportions of the two populations with readmissions, ambulant psychiatrist contacts (OPC) and deaths are displayed in Table 4. The population from Lower Austria has more events of every type. This can be linked to a higher percentage of psychotic patients in that population.

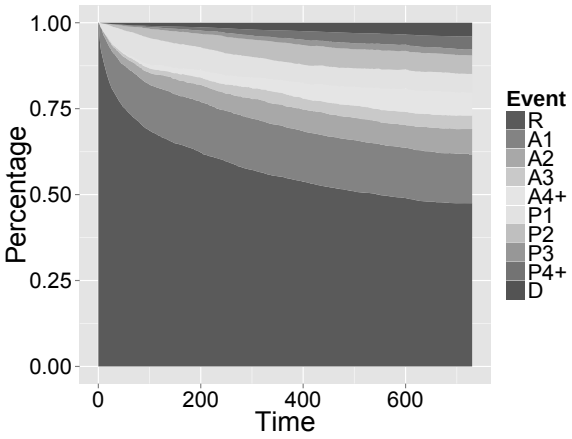

Figure 6: Evolution of the patients distribution over the states in scenario 3*a* for Lower Austria.

Type of Event	Austria	Lower Austria
Readmissions	42.2	44.8
OPC	27.7	28.6
Deaths	3.9	4.0

Table 4: Comparison of the percentages of the populations with readmissions, ambulant contacts and deaths.

3.6 Sensitivity analysis

The influence of the composition of the population on the number and times of readmissions is examined in the course of a sensitivity analysis.

Firstly, a base case with a random subpopulation sampled from dataset *dataaut* is considered. Starting from that population other populations are generated by changing only one parameter of all patients at a time while leaving the other parameters unchanged. 12 populations are generated: all male/female, all five years younger/older, length of stay 50% shorter/longer and all with each of the six diagnosis groups.

The number of patients with readmissions and the deviation of the number from the base case is calculated. In Figure 7, a tornado plot for the number of patients with readmissions for all populations is presented. This diagram is a bar chart with bars listed vertically and ordered by length. The vertical line at 0 marks the base case with no deviation. The bar for each parameter reaches from the deviation of the highest value to the deviation of the lowest value of the populations where that particular parameter is changed.

The populations with single diagnosis groups have the highest deviations ranging from has about 23% less

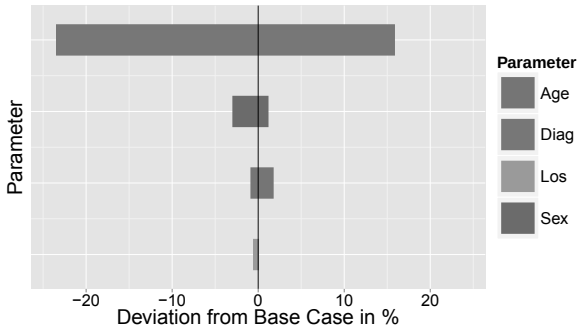

Figure 7: Tornado plot for number of patients with readmissions.

patients with readmissions than the base case to about 15% more. The male population has about 3% less readmissions than the base case, the female has 1.2% more. Also, the older population and the population with longer stays in hospital have a slightly higher number of readmissions compared to the younger patients and the population with shorter stays. All of these deviations are below 2%.

4 Conclusions

The microsimulation model is an appropriate tool to model the course of events of patients. Both the longitudinal analyses of the single patients as well as the cross-sectional analyses can be carried out with little effort.

In general, the results show an exponential decrease over time of the number of patients with no event. Nevertheless, about half of the patients have no readmissions during the simulation. The number of patients with one ambulant contact and no readmission has its peak after half a year and declines afterwards. So, many of these patients have a readmission soon after the visit to the psychiatrist. The percentage of patients with a particular number of readmissions is indirectly proportional to the number of readmissions.

The comparison of the results of different scenarios shows that in scenarios 2*a* and 2*b* the patients have more readmission than in the other scenarios. This is due to an overestimation of the number of readmissions because the order of the readmissions is not considered in these scenarios. So, the results of scenarios with a lower level of data detail show significantly varying results from scenario 3*a* which uses the most detailed data. However, scenario 3*a* requires data of entire patient histories which is rarely available due to data protection issues.

For a more detailed analysis, the population is split into classes defined by times and number of readmissions of patients. In comparison to the other scenarios, the readmissions of patients with only one readmission are later and the average number of readmissions per patients is higher in scenarios 3*a* and 3*b*.

The sensitivity analysis shows that the diagnosis of the population has a dramatic influence on the number of readmissions.

The proportion of patients with readmissions is much higher for patients with previous ambulant psychiatrist visit. Thus, ambulant contacts increase the probability for readmissions and are in most cases an indicator for a worsening of the condition of the patient. This also leads to the fail of the reduction of readmissions by the intervention strategy of compulsory visits to a psychiatrist after a certain time after the last admission.

The comparison of the populations of whole Austria and Lower Austria shows that more patients of the latter have readmissions and also ambulant contacts. This can be the result of the differing composition of the populations regarding the parameter distributions.

References

[1] Kirkwood BR, Sterne JAC. *Essential Medical Statistics*. Essentials. Wiley. 2003.

[2] Cox DR. Regression models and life-tables. *Journal of the Royal Statistical Society Series B (Methodological)*. 1972;34(2):187–220.

[3] Therneau TM, Grambsch PM. *Modeling survival data: extending the Cox model*. Springer Science & Business Media. 2000.

[4] Beyersmann J, Putter H. A note on computing average state occupation times. *Demographic Research*. 2014; 30(62):1681–1696.

Network-based Simulation in Water Construction – a Flexible Tool for Equipment Selection

Gerhard Höfinger*, Stefan Brunner

STRABAG Supply Chain Optimization, Central Technical Department Vienna, STRABAG AG, Donau-City-Straße 9, 1220 Vienna, Austria; *gerhard.hoefinger@strabag.com*

Simulation Notes Europe SNE 26(1), 2016, 55 - 58
DOI: 10.11128/sne.26.sn.10329
Received: October 20, 2015; Revised: February 10, 2016;
Accepted: March 10, 2016;

Abstract. A simulation model for the operation of barges and dredging platforms using AnyLogic was developed, allowing for optimization of equipment selection and cost calculation. The model is a discrete event model set up using AnyLogic's Enterprise Library. With a Monte-Carlo-approach applying the model, risks in cost and time planning can be quantified. Linking a generic version of the AnyLogic model with Excel and GoogleEarth, models for arbitrary water construction sites can be created and used by cost estimators without simulation modelling know how.

Introduction

Simulation is currently not very widely used in the construction industry. Reasons may, on the one hand, lie in the industry itself, which tends to be rather conservative. On the other hand, many projects have unique features and construction site layouts change with the progress of construction itself (imagine an assembly line that changes after every finished product), two factors which make the creation of simulation models difficult. Another challenge is the traditional way of developing a construction project, where final designs and construction methods for certain parts are only available after the start of construction.

At STRABAG's Central Technical Department in Vienna, a group of experts on mathematical modelling and simulation develops models for applications in the whole range of construction projects to secure the company's position as innovation leader in the construction industry.

It could be shown that simulation is a suitable instrument to examine the influence of certain phenomena on dredging, which is the process of earthworks under water. These phenomena, such as bad weather, technical defects, interruptions of supply, etc. on a dredging project, are outside the sphere of influence of the construction contractor, are mostly of a stochastic nature and can often have a significant impact on the cost of the relevant construction activity. Simulation supports in quantifying the influence of these factors and can therefore help reduce price risk for the construction contractor and its client. Some of the difficulties mentioned above are not present in this special kind of construction operation.

In the following, we present a flexible framework to dynamically generate simulation models of arbitrary harbour dredging projects with variable equipment fleets.

Figure 1: A dredging platform with a bucket excavator, bucket size 14m³.

1 Problem Formulation

In many harbors it is necessary to remove silt from basins and channels as part of the maintenance works or to increase the accessibility for larger ships.

Usually these works are carried out with dredging platforms (platforms which are fixed to the seafloor with stilts in the area of operation with a bucket excavator mounted on top, see Figure 1) and a fleet of barges which transport the material from the dredgers to spoil areas at some distance from the harbor entrance.

In addition to the dredgers and barges, tugs are needed to manoeuver the barges in the vicinity of the dredgers and to tow barges of the non-automobile type to the spoil areas and back to the dredgers. Modern tugs with enhanced maneuverability are used for moving the barges in the vicinity of the dredging platforms. Simpler and more inexpensive tugs are used to tow the barges to the spoil areas and back. Usually there are several dredgers, several dredging and spoil locations and a variety of barges and tugs involved in this kind of construction activity, see Figure 2.

Figure 2: Dredger in operation with two barges and a tug. The landing manoeuvre of the barges requires experienced captains in order to keep the disruption of digger usage short.

The equipment cost is essentially time based. However, a merely performance based approach does not lead to reliable results due to presence of phenomena influencing the construction process that are often interlinked and clearly outside the sphere of influence of the construction firm. These phenomena include but are not limited to: Unsuitable weather conditions, damage of barges or other equipment, necessary refuelling of the excavators, the passage of large ships, unsuccessful landing of barges, and the relocation of dredging platforms. All these items lead to a disruption of the construction process, reducing the degree of utilization of the dredgers, hence increasing total construction cost. The key to minimizing costs is maximizing the degree of capacity utilization of the dredgers as the most costly elements which is done by ensuring a continuous servicing of dredgers with barges.

Finding the right fleet composition for the barges is vital for achieving cost efficiency, especially because changing the fleet is very costly and time consuming. A sound simulation model enables the cost estimator to work with scenarios in order to find an 'optimal' fleet composition before the works start.

Compared to earthworks on land (as in conventional road construction), which can be optimized using linear programs (Bogenberger et al., 2013), the costs are higher and less units (barges, dredgers) are in use.

In order to create a more solid basis for cost calculation a framework for automatic simulation model creation was developed. The resulting model enables the user to carry out Monte-Carlo-analysis as well to further secure cost calculation results.

2 The Model

The nature of the problem described above suggests using discrete event simulation in order to quantify the bandwidth of the influence of the disruptions on the duration of a given construction project described before.
In summer 2013 a subsidiary of STRABAG was carrying out a dredging project in the harbour of Yuzhne, Ukraine.

Thus, activity reports of 3 dredging platforms for almost one year were available, making it possible to determine the probability distributions for the disrupting phenomena of interest. Data analysis, using R, has shown that a lognormal distribution is a suitable model for all these phenomena.

The simulation model was created using the simulation software AnyLogic (6.8.1), which had proven to be suitable for modelling construction related processes before in STRABAG's Central Technical Department (e.g. for tunnel construction, material supply in tunnel construction, material flow in a quarry, influence of construction activities on traffic, etc.).

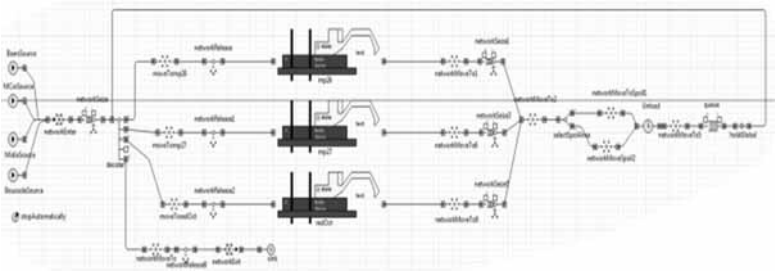

Figure 3: Modelling view in AnyLogic, showing the use of the Enterprise Library Network Blocks.

For the model presented in this paper a network based modelling approach was used, applying elements of AnyLogic's Enterprise Library, see Figure 3. Herein the locations, such as dredging and spoil sites and anchorage are the nodes and the routes along which the ships move are the vertices.

The network geometry is taken from a map of the relevant area. In the first phase of the research the network was literally drawn on a sea map of Yuzhne as can be seen in Figure 4.

Barges are entities that populate the network. The tugs are modelled as network resources, which means that the barges request the tugs in accordance with the task that has to be carried out and the network object itself provides the entities with the requested resource as soon as it is available.

The dredging platforms are modelled as Active Objects, located at certain nodes in the network. They consist of a workflow for incoming barges, modelled with objects of the Enterprise library and state charts, controlling the different modes of operation a dredger has, in detail a state of regular operation and all disrupting states as failures and disturbances.

A close to optimum disposition of the barges to the dredgers is crucial to minimize idleness of the excavators. Therefore, on site a human dispatcher controls the operation of the barges.

Figure 4: Map of the example region in Yuzhne, with the network used by the Enterprise Library Network blocks.

In the model, the dispatcher is represented by the 'Disponent' object, which iterates over all operational dredgers once a barge is unloaded at a spoil area and identifies the dredger with the least shipping space on the way and then sends the relevant barge to its dredging area. As in reality, the 'Disponent' object is called each time a barge has completed a task and a new destination for the respective barge has to be determined.

The events in the simulation are triggered by a random number generator using the frequency distributions and durations calculated from the reports of the dredgers. Parameters were calibrated using site data.

The validated model was then used to try a variety of different sets of equipment for the given project in order to find an optimal equipment configuration.

3 Validation

Similar to the real system the dredging platforms in the simulation model can create activity reports. This data was used to validate the model. The data of 30 days in the real system were compared to 30 simulated days. Simulation results match the real world results satisfactorily (see Table 1). Observing a longer timespan obviously leads to a better agreement with real world results.

	count		mean duration	
	real	sim	real	sim
loading	493	543	79,30	77,35
position change	57	38	56,43	58,32
repair	56	33	226,55	113,91
ship traffic	52	33	87,45	115,89
barge shortage	188	212	70,05	136,11
refueling	19	13	64,44	65,12
bad weather	27	39	416,35	661,14

Table 1: Comparison of a single simulation run with measured data.

4 Generalization

In order to allow application of the model to other construction sites of the discussed type, dependency of expert model developers had to be reduced. A tool had to be created which allows estimators without knowledge of modelling software to adapt the model to their respective construction project. Acceptance of this tool by estimators and simplicity of usage is crucial for introduction of simulation as a method for cost estimation and risk management.

In order to achieve this goal, object replication and connectivity features of AnyLogic were used. In a generic model, location of dredging sites, spoil areas, and ship routes are input via kml-files which are produced using GoogleEarth. Additional information on barges and dredgers are input via Microsoft Excel into standardized forms, which are partly created dynamically via VBA.

The Anylogic model reads the kml- and the Excel-file and sets up the model accordingly.

Training of estimators and application to new construction sites is part of an ongoing development project.

5 Monte Carlo Analysis

Recent dredging projects calculated without application of detailed models showed that the inherent risks of such a project were not accounted for sufficiently. The results were economically unsatisfying. It is assumed that normal operation could be quantified well using traditional ways of calculation with mean operation times. Risk factors added to the calculated costs are gained through experience. Of course, setting these factors is crucial, if they are to low, costs cannot be covered, in the other case, the projects are not won in the first place.

The calculated actual costs should nearly be the same for comparable companies. They use similar equipment, pay similar wages to workers and have similar management structures.

The ability to quantify of risks can therefore be the differentiating factor between the loosing and the successful bider.

In the model presented above, various stochastic elemts are present. Unfortunate combinations of their expressions can lead to significantly higher construction times (and therefore costs). Starting with a few hundred model runs of a Monte Carlo Analysis, the histogram of construction costs typically converges to a smooth curve, defining the distribution of the resulting construction costs. An example is depicted in Figure 5. Using this knowledge, the cost estimator can price for risk consciously, replicably, and in a project specific way.

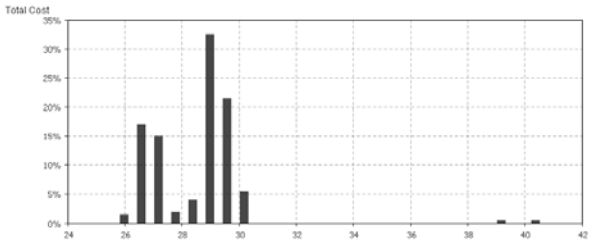

Figure 5: Histogram of simulation results (costs in Mio. €) from a Monte Carlo run with 200 iterations. The outliers can be explained by an unusual accumulation of condounders.

6 Conclusions

Simulation of logistic processes is currently not very widely used in the construction industry (an overview of existing approaches can be found in Günthner et al., 2012), despite the fact that many of its processes are predestined for simulation due to the circumstance that construction processes are very often so costly that real experiments cannot reasonably be carried out and external influences, which are hardly quantifiable, have an important impact on construction processes.

Yet it could be shown that simulation can be put to use for cost calculation and risk estimation, generating a significant benefit for the user. This project shows that highly flexible tools can be created in a way that estimators unfamiliar with modelling and simulation can use them.

Through application of simulation models in certain niches the degree of familiarity with and the trust in these instruments can certainly be increased. If we succeed in reproducing the complexity of large scale construction activities with semi- or fully automatized generated models, maybe also in connection with improved data models, it will be possible to facilitate a number of decisions with simulation models that can be generated quickly and inexpensively. Of course, in the future the majority of construction projects will still be satisfactorily planned and executed by experienced project managers. But more and more complex projects are harder and harder fully to perceive by a single human being. Therefore, prospects for simulation models in the construction industry are increasing and therewith the prospects for the players in the construction industry using the instrument of simulation. (Höfinger, 2014)

References

[1] Bogenberger C, Dell'Amico M, Hoefinger G, Iori M, Novellani S, Panicucci B. Earthwork Optimization Models for the Construction of a Large Highway System May *International Network Optimization Conference 2013.*

[2] Günthner WA, Borrmann A. *Digitale Baustelle – innovativer Planen, effizienter Ausführen*, Springer-Verlag, Berlin, 2011.

[3] Höfinger G. Chancen für die Simulation in der Bauwirtschaft, 2014, *WING Business*, 47/1, p. 10-12.

SNE Simulation News

EUROSIM Data and Quick Info

EUROSIM 2016

9th EUROSIM Congress on Modelling and Simulation

City of Oulu, Finland, September 16-20, 2016

www.eurosim.info

Contents

Simulation Notes Europe SNE is the official membership journal of EUROSIM and distributed / available to members of the EUROSIM Societies as part of the membership benefits.
If you have any information, announcement, etc. you want to see published, please contact a member of the editorial board in your country or the editorial office. For scientific publications, please contact the EiC.
This *EUROSIM Data & Quick Info* compiles data from EUROSIM societies and groups: addresses, weblinks, and officers of societies with function and email, to be published regularly in **SNE** issues.

EUROSIM
Federation of European Simulation Societies

General Information. **EUROSIM**, the Federation of European Simulation Societies, was set up in 1989. The purpose of **EUROSIM** is to provide a European forum for simulation societies and groups to promote advancement of modelling and simulation in industry, research, and development. → *www.eurosim.info*

Member Societies. **EUROSIM** members may be national simulation societies and regional or international societies and groups dealing with modelling and simulation. At present **EUROSIM** has 15 *Full Members* and 2 (3) *Observer Members*:

ASIM	Arbeitsgemeinschaft Simulation *Austria, Germany, Switzerland*
CEA-SMSG	Spanish Modelling and Simulation Group *Spain*
CROSSIM	Croatian Society for Simulation Modeling *Croatia*
CSSS	Czech and Slovak Simulation Society *Czech Republic, Slovak Republic*
DBSS	Dutch Benelux Simulation Society *Belgium, Netherlands*
FRANCOSIM	Société Francophone de Simulation *Belgium, France*
HSS	Hungarian Simulation Society; *Hungary*
ISCS	Italian Society for Computer Simulation *Italy*
LIOPHANT	LIOPHANT Simulation Club *Italy & International, Observer Member*
LSS	Latvian Simulation Society; *Latvia*
PSCS	Polish Society for Computer Simulation *Poland*
MIMOS	Italian Modelling and Simulation Association, *Italy*
SIMS	Simulation Society of Scandinavia *Denmark, Finland, Norway, Sweden*
SLOSIM	Slovenian Simulation Society *Slovenia*
UKSIM	United Kingdom Simulation Society *UK, Ireland*
KA-SIM	Romanian Society for Modelling and Simulation, *Romania, Observer Member*
ROMSIM	Romanian Society for Modelling and Simulation, *Romania, Observer Member*
RNSS	Russian National Simulation Society *Russian Federation, Observer Member*

EUROSIM Board / Officers. EUROSIM is governed by a board consisting of one representative of each member society, president and past president, and representatives for SNE Simulation notes Europe. The President is nominated by the society organising the next **EUROSIM** Congress. Secretary and Treasurer are elected out of members of the Board.

President	Esko Juuso (SIMS) *esko.juuso@oulu.fi*
Past President	Khalid Al.Begain (UKSIM) *kbegain@glam.ac.uk*
Secretary	Borut Zupančič (SLOSIM) *borut.zupancic@fe.uni-lj.si*
Treasurer	Felix Breitenecker (ASIM) *felix.breitenecker@tuwien.ac.at*
SNE Repres.	Felix Breitenecker *felix.breitenecker@tuwien.ac.at*

SNE – Simulation Notes Europe. SNE is a scientific journal with reviewed contributions as well as a membership newsletter for **EUROSIM** with information from the societies in the *News Section*. **EUROSIM** societies are offered to distribute to their members the journal **SNE** as official membership journal. **SNE** Publishers are **EUROSIM**, ARGESIM and ASIM.

Editor-in-chief	Felix Breitenecker *felix.breitenecker@tuwien.ac.at*

→ *www.sne-journal.org,*

✉ *office@sne-journal.org*

EUROSIM Congress. EUROSIM is running the triennial conference series **EUROSIM** Congress. The congress is organised by one of the **EUROSIM** societies.

EUROSIM 2016 will be organised by SIMS in Oulu, Finland, September 16-20, 2016.

Chairs / Team EUROSIM 2016

Esko Juuso EUROSIM President, *esko.juuso@oulu.fi*
Erik Dahlquist SIMS President, *erik.dahlquist@mdh.se*
Kauko Leiviskä EUROSIM 2016 Chair,
kauko.leiviska@oulu.fi

→ *www.eurosim.info*

✉ *office@automaatioseura.fi*

EUROSIM Member Societies

ASIM
German Simulation Society
Arbeitsgemeinschaft Simulation

ASIM (Arbeitsgemeinschaft Simulation) is the association for simulation in the German speaking area, servicing mainly Germany, Switzerland and Austria. ASIM was founded in 1981 and has now about 700 individual members, and 30 institutional or industrial members.

→ *www.asim-gi.org* with members' area

info@asim-gi.org, admin@asim-gi.org

ASIM – Inst. f. Analysis and Scientific Computing
Vienna University of Technology
Wiedner Hauptstraße 8-10, 1040 Vienna, Austria

ASIM Officers	
President	Felix Breitenecker *felix.breitenecker@tuwien.ac.at*
Vice presidents	Sigrid Wenzel, *s.wenzel@uni-kassel.de*
	T. Pawletta, *pawel@mb.hs-wismar.de*
Secretary	Ch. Deatcu, *christina.deatcu@hs-wismar.de*
Treasurer	Anna Mathe, *anna.mathe@tuwien.ac.at*
Membership Affairs	S. Wenzel, *s.wenzel@uni-kassel.de*
	W. Maurer, *werner.maurer@zhwin.ch*
	Ch. Deatcu, *christina.deatcu@hs-wismar.de*
	F. Breitenecker, *felix.breitenecker@tuwien.ac.at*
Universities / Research Inst.	S. Wenzel, *s.wenzel@uni-kassel.de*
	W. Wiechert, *W.Wiechert@fz-juelich.de*
	J. Haase, *Joachim.Haase@eas.iis.fraunhofer.de*
	Katharina Nöh, *k.noeh@fz-juelich.de*
Industry	S. Wenzel, *s.wenzel@uni-kassel.de*
	K. Panreck, *Klaus.Panreck@hella.com*
Conferences	Klaus Panreck *Klaus.Panreck@hella.com*
	J. Wittmann, *wittmann@htw-berlin.de*
Publications	Th. Pawletta, *pawel@mb.hs-wismar.de*
	Ch. Deatcu, *christina.deatcu@hs-wismar.de*
	F. Breitenecker, *felix.breitenecker@tuwien.ac.at*
Repr. EUROSIM	F. Breitenecker, *felix.breitenecker@tuwien.ac.at*
	A. Körner, *andreas.koerner@tuwien.ac.at*
Education / Teaching	A. Körner, *andreas.koerner@tuwien.ac.at*
	S. Winkler, *stefanie.winkler@tuwien.ac.at*
	Katharina Nöh, *k.noeh@fz-juelich.de*
Int. Affairs – GI Contact	N. Popper, *niki.popper@drahtwarenhandlung.at*
	O. Rose, *Oliver.Rose@tu-dresden.de*
Editorial Board SNE	T. Pawletta, *pawel@mb.hs-wismar.de*
	Ch. Deatcu, *christina.deatcu@hs-wismar.de*
Web EUROSIM	A. Körner, *andreas.koerner@tuwien.ac.at*

Last data update March 2016

ASIM Working Committee	
GMMS	Methods in Modelling and Simulation Th. Pawletta, *pawel@mb.hs-wismar.de*
SUG	Simulation in Environmental Systems Wittmann, *wittmann@informatik.uni-hamburg.de*
STS	Simulation of Technical Systems H.T.Mammen, *Heinz-Theo.Mammen@hella.com*
SPL	Simulation in Production and Logistics Sigrid Wenzel, *s.wenzel@uni-kassel.de*
EDU	Simulation in Education/Education in Simulation A. Körner, *andreas.koerner@tuwien.ac.at*
DATA	Working Group Data-driven Simulation in Life Sciences; *niki.popper@drahtwarenhandlung.at*
	Working Groups for Simulation in Business Administration, in Traffic Systems, for Standardisation, etc.

CEA-SMSG – Spanish Modelling and Simulation Group

CEA is the Spanish Society on Automation and Control and it is the national member of IFAC (International Federation of Automatic Control) in Spain. Since 1968 CEA-IFAC looks after the development of the Automation in Spain, in its different issues: automatic control, robotics, SIMULATION, etc. In order to improve the efficiency and to deep into the different fields of Automation. The association is divided into national thematic groups, one of which is centered on Modeling, Simulation and Optimization, constituting the CEA Spanish Modeling and Simulation Group (CEA-SMSG). It looks after the development of the Modelling and Simulation (M&S) in Spain, working basically on all the issues concerning the use of M&S techniques as essential engineering tools for decision-making and optimization.

→ *http://www.ceautomatica.es/grupos/*

→ *emilio.jimenez@unirioja.es*

simulacion@cea-ifac.es

CEA-SMSG / Emilio Jiménez, Department of Electrical Engineering, University of La Rioja, San José de Calasanz 31, 26004 Logroño (La Rioja), SPAIN

CEA - SMSG Officers	
President	Emilio Jiménez, *emilio.jimenez@unirioja.es*
Vice president	Juan Ignacio Latorre *juanignacio.latorre@unavarra.es*
Repr. EUROSIM	Emilio Jiminez, *emilio.jimenez@unirioja.es*
Edit. Board SNE	Emilio Jiminez, *emilio.jimenez@unirioja.es*
Web EUROSIM	Mercedes Perez *mercedes.perez@unirioja.es*

Last data update March 2016

CROSSIM – Croatian Society for Simulation Modelling

CROSSIM-*Croatian Society for Simulation Modelling* was founded in 1992 as a non-profit society with the goal to promote knowledge and use of simulation methods and techniques and development of education. CROSSIM is a full member of **EUROSIM** since 1997.

→ *www.eurosim.info*

vdusak@foi.hr

✉ CROSSIM / Vesna Dušak
Faculty of Organization and
Informatics Varaždin, University of Zagreb
Pavlinska 2, HR-42000 Varaždin, Croatia

CROSSIM Officers	
President	Vesna Dušak, *vdusak@foi.hr*
Vice president	Jadranka Božikov, *jbozikov@snz.hr*
Secretary	Vesna Bosilj-Vukšić, *vbosilj@efzg.hr*
Executive board members	Vlatko Čerić, *vceric@efzg.hr*
	Tarzan Legović, *legovic@irb.hr*
Repr. EUROSIM	Jadranka Božikov, *jbozikov@snz.hr*
Edit. Board SNE	Vesna Dušak, *vdusak@foi.hr*
Web EUROSIM	Jadranka Bozikov, *jbozikov@snz.hr*

Last data update December2012

CSSS – Czech and Slovak Simulation Society

CSSS -The *Czech and Slovak Simulation Society* has about 150 members working in Czech and Slovak national scientific and technical societies (*Czech Society for Applied Cybernetics and Informatics*, *Slovak Society for Applied Cybernetics and Informatics*). The main objectives of the society are: development of education and training in the field of modelling and simulation, organising professional workshops and conferences, disseminating information about modelling and simulation activities in Europe. Since 1992, CSSS is full member of **EUROSIM**.

→ *www.fit.vutbr.cz/CSSS*

snorek@fel.cvut.cz

✉ CSSS / Miroslav Šnorek, CTU Prague
FEE, Dept. Computer Science and Engineering,
Karlovo nam. 13, 121 35 Praha 2, Czech Republic

CSSS Officers	
President	Miroslav Šnorek, *snorek@fel.cvut.cz*
Vice president	Mikuláš Alexík, *alexik@frtk.fri.utc.sk*
Treasurer	Evžen Kindler, *ekindler@centrum.cz*
Scientific Secr.	A. Kavička, *Antonin.Kavicka@upce.cz*
Repr. EUROSIM	Miroslav Šnorek, *snorek@fel.cvut.cz*
Deputy	Mikuláš Alexík, *alexik@frtk.fri.utc.sk*
Edit. Board SNE	Mikuláš Alexík, *alexik@frtk.fri.utc.sk*
Web EUROSIM	Petr Peringer, peringer@fit.vutbr.cz

Last data update December2012

DBSS – Dutch Benelux Simulation Society

The Dutch Benelux Simulation Society (DBSS) was founded in July 1986 in order to create an organisation of simulation professionals within the Dutch language area. DBSS has actively promoted creation of similar organisations in other language areas. DBSS is a member of **EUROSIM** and works in close cooperation with its members and with affiliated societies.

→ `www.eurosim.info`

a.w.heemink@its.tudelft.nl

✉ DBSS / A. W. Heemink
Delft University of Technology, ITS - twi,
Mekelweg 4, 2628 CD Delft, The Netherlands

www.DutchBSS.org

DBSS Officers	
President	A. Heemink, *a.w.heemink@its.tudelft.nl*
Vice president	M. Mujica Mota, *m.mujica.mota@hva.nl*
Treasurer	M. Mujica Mota, *m.mujica.mota@hva.nl*
Secretary	P. M. Scala, p.m.scala@hva.nl
Repr. EUROSIM	M. Mujica Mota, *m.mujica.mota@hva.nl*
Edit. SNE/Web	M. Mujica Mota, *m.mujica.mota@hva.nl*

Last data update March 2016

FRANCOSIM – Société Francophone de Simulation

FRANCOSIM was founded in 1991 and aims to the promotion of simulation and research, in industry and academic fields. Francosim operates two poles.

- Pole Modelling and simulation of discrete event systems. Pole Contact: *Henri Pierreval, pierreva@imfa.fr*
- Pole Modelling and simulation of continuous systems. Pole Contact: *Yskandar Hamam, y.hamam@esiee.fr*

→ *www.eurosim.info*

y.hamam@esiee.fr

✉ FRANCOSIM / Yskandar Hamam
Groupe ESIEE, Cité Descartes,
BP 99, 2 Bd. Blaise Pascal,
93162 Noisy le Grand CEDEX, France

FRANCOSIM Officers	
President	Karim Djouani, *djouani@u-pec.fr*
Treasurer	François Rocaries, *f.rocaries@esiee.fr*
Repr. EUROSIM	Karim Djouani, *djouani@u-pec.fr*
Edit. Board SNE	Karim Djouani, *djouani@u-pec.fr*

Last data update December2012

HSS – Hungarian Simulation Society

The Hungarian Member Society of EUROSIM was established in 1981 as an association promoting the exchange of information within the community of people involved in research, development, application and education of simulation in Hungary and also contributing to the enhancement of exchanging information between the Hungarian simulation community and the simulation communities abroad. HSS deals with the organization of lectures, exhibitions, demonstrations, and conferences.

→ *www.eurosim.info*

javor@eik.bme.hu

✉ HSS / András Jávor,
Budapest Univ. of Technology and Economics,
Sztoczek u. 4, 1111 Budapest, Hungary

HSS Officers	
President	András Jávor, *javor@eik.bme.hu*
Vice president	Gábor Szűcs, *szucs@itm.bme.hu*
Secretary	Ágnes Vigh, *vigh@itm.bme.hu*
Repr. EUROSIM	András Jávor, *javor@eik.bme.hu*
Deputy	Gábor Szűcs, *szucs@itm.bme.hu*
Edit. Board SNE	András Jávor, *javor@eik.bme.hu*
Web EUROSIM	Gábor Szűcs, *szucs@itm.bme.hu*

Last data update March 2008

ISCS – Italian Society for Computer Simulation

The Italian Society for Computer Simulation (ISCS) is a scientific non-profit association of members from industry, university, education and several public and research institutions with common interest in all fields of computer simulation.

→ *www.eurosim.info*

Mario.savastano@uniina.at

✉ ISCS / Mario Savastano,
c/o CNR - IRSIP,
Via Claudio 21, 80125 Napoli, Italy

ISCS Officers	
President	M. Savastano, *mario.savastano@unina.it*
Vice president	F. Maceri, *Franco.Maceri@uniroma2.it*
Repr. EUROSIM	F. Maceri, *Franco.Maceri@uniroma2.it*
Secretary	Paola Provenzano, *paola.provenzano@uniroma2.it*
Edit. Board SNE	M. Savastano, *mario.savastano@unina.it*

Last data update December2010

LIOPHANT Simulation

Liophant Simulation is a non-profit association born in order to be a trait-d'union among simulation developers and users; Liophant is devoted to promote and diffuse the simulation techniques and methodologies; the Association promotes exchange of students, sabbatical years, organization of International Conferences, courses and internships focused on M&S applications.

→ *www.liophant.org*

info@liophant.org

✉ LIOPHANT Simulation, c/o Agostino G. Bruzzone,
DIME, University of Genoa, Savona Campus
via Molinero 1, 17100 Savona (SV), Italy

LIOPHANT Officers	
President	A.G. Bruzzone, *agostino@itim.unige.it*
Director	E. Bocca, *enrico.bocca@liophant.org*
Secretary	A. Devoti, *devoti.a@iveco.com*
Treasurer	Marina Masseimassei@itim.unige.it
Repr. EUROSIM	A.G. Bruzzone, *agostino@itim.unige.it*
Deputy	F. Longo, *f.longo@unical.it*
Edit. Board SNE	F. Longo, *f.longo@unical.it*
Web EUROSIM	F. Longo, *f.longo@unical.it*

Last data update March 2016

LSS – Latvian Simulation Society

The Latvian Simulation Society (LSS) has been founded in 1990 as the first professional simulation organisation in the field of Modelling and simulation in the post-Soviet area. Its members represent the main simulation centres in Latvia, including both academic and industrial sectors.

→ *briedis.itl.rtu.lv/imb/*

merkur@itl.rtu.lv

LSS / Yuri Merkuryev, Dept. of Modelling and Simulation Riga Technical University Kalku street 1, Riga, LV-1658, LATVIA

LSS Officers	
President	Yuri Merkuryev, *merkur@itl.rtu.lv*
Secretary	Artis Teilans, *Artis.Teilans@exigenservices.com*
Repr. EUROSIM	Yuri Merkuryev, *merkur@itl.rtu.lv*
Deputy	Artis Teilans, *Artis.Teilans@exigenservices.com*
Edit. Board SNE	Yuri Merkuryev, *merkur@itl.rtu.lv*
Web EUROSIM	Vitaly Bolshakov, *vitalijs.bolsakovs@rtu.lv*

Last data update March 2016

PSCS – Polish Society for Computer Simulation

PSCS was founded in 1993 in Warsaw. PSCS is a scientific, non-profit association of members from universities, research institutes and industry in Poland with common interests in variety of methods of computer simulations and its applications. At present PSCS counts 257 members.

→ *www.ptsk.man.bialystok.pl*

leon@ibib.waw.pl

PSCS / Leon Bobrowski, c/o IBIB PAN, ul. Trojdena 4 (p.416), 02-109 Warszawa, Poland

PSCS Officers	
President	Leon Bobrowski, *leon@ibib.waw.pl*
Vice president	Tadeusz Nowicki, *Tadeusz.Nowicki@wat.edu.pl*
Treasurer	Z. Sosnowski, *zenon@ii.pb.bialystok.pl*
Secretary	Zdzislaw Galkowski, *Zdzislaw.Galkowski@simr.pw.edu.pl*
Repr. EUROSIM	Leon Bobrowski, *leon@ibib.waw.pl*
Deputy	Tadeusz Nowicki, *tadeusz.nowicki@wat.edu.pl*
Edit. Board SNE	Zenon Sosnowski, z.sosnowski@pb.ed.pl
Web EUROSIM	Magdalena Topczewska *m.topczewska@pb.edu.pl*

Last data update December2013

SIMS – Scandinavian Simulation Society

SIMS is the *Scandinavian Simulation Society* with members from the four Nordic countries Denmark, Finland, Norway and Sweden. The SIMS history goes back to 1959. SIMS practical matters are taken care of by the SIMS board consisting of two representatives from each Nordic country (Iceland one board member).

SIMS Structure. SIMS is organised as federation of regional societDjouaniies. There are FinSim (Finnish Simulation Forum), DKSIM (Dansk Simuleringsforening) and NFA (Norsk Forening for Automatisering).

→ *www.scansims.org*

esko.juuso@oulu.fi

SIMS / SIMS / Erik Dahlquist, School of Business, Society and Engineering, Department of Energy, Building and Environment, Mälardalen University, P.O.Box 883, 72123 Västerås, Sweden

SIMS Officers	
President	Erik Dahlquist, *erik.dahlquist@mdh.se*
Vice president	Bernd Lie, *lie@hit.noe*
Treasurer	Vadim Engelson, *vadim.engelson@mathcore.com*
Repr. EUROSIM	Erik Dahlquist, *erik.dahlquist@mdh.se*
Edit. Board SNE	Esko Juuso, *esko.juuso@oulu.fi*
Web EUROSIM	Vadim Engelson, *vadim.engelson@mathcore.com*

Last data update March 2016

SLOSIM – Slovenian Society for Simulation and Modelling

SLOSIM - Slovenian Society for Simulation and Modelling was established in 1994 and became the full member of **EUROSIM** in 1996. Currently it has 69 members from both slovenian universities, institutes, and industry. It promotes modelling and simulation approaches to problem solving in industrial as well as in academic environments by establishing communication and cooperation among corresponding teams.

→ www.slosim.si

slosim@fe.uni-lj.si

SLOSIM / Vito Logar, Faculty of Electrical Engineering, University of Ljubljana, Tržaška 25, 1000 Ljubljana, Slovenia

SLOSIM Officers	
President	Vito Logar, *vito.logar@fe.uni-lj.si*
Vice president	Božidar Šarler, *bozidar.sarler@ung.si*
Secretary	Aleš Belič, *ales.belic@sandoz.com*
Treasurer	Milan Simčič, *milan.simcic@fe.uni-lj.si*
Repr. EUROSIM	B. Zupančič, *borut.zupancic@fe.uni-lj.si*
Deputy	Vito Logar, *vito.logar@fe.uni-lj.si*
Edit. Board SNE	B. Zupančič, *borut.zupancic@fe.uni-lj.si* Vito Logar, *vito.logar@fe.uni-lj.si* Blaž Rodič, *blaz.rodic@fis.unm.si*
Web EUROSIM	Vito Logar, *vito.logar@fe.uni-lj.si*

Last data update March 2016

UKSIM - United Kingdom Simulation Society

The UK Simulation Society is very active in organizing conferences, meetings and workshops. UKSim holds its annual conference in the March-April period. In recent years the conference has always been held at Emmanuel College, Cambridge. The Asia Modelling and Simulation Section (AMSS) of UKSim holds 4-5 conferences per year including the EMS (European Modelling Symposium), an event mainly aimed at young researchers, organized each year by UKSim in different European cities.

Membership of the UK Simulation Society is free to participants of any of our conferences and thier co-authors.

→ *www.uksim.org.uk*

david.al-dabass@ntu.ac.uk

✉ UKSIM / Prof. David Al-Dabass
Computing & Informatics,
Nottingham Trent University
Clifton lane, Nottingham, NG11 8NS
United Kingdom

UKSIM Officers	
President	David Al-Dabass, *david.al-dabass@ntu.ac.uk*
Secretary	A. Orsoni, *A.Orsoni@kingston.ac.uk*
Treasurer	A. Orsoni, *A.Orsoni@kingston.ac.uk*
Membership chair	G. Jenkins, *glenn.l.jenkins@smu.ac.uk*
Local/Venue chair	Richard Cant, *richard.cant@ntu.ac.uk*
Repr. EUROSIM	A. Orsoni, *A.Orsoni@kingston.ac.uk*
Deputy	G. Jenkins, *glenn.l.jenkins@smu.ac.uk*
Edit. Board SNE	A. Orsoni, *A.Orsoni@kingston.ac.uk*

Last data update March 2016

RNSS – Russian Simulation Society

NSS - The Russian National Simulation Society (Национальное Общество Имитационного Моделирования – НОИМ) was officially registered in Russian Federation on February 11, 2011. In February 2012 NSS has been accepted as an observer member of **EUROSIM**, and in 2014 RNSS has become full member.

→ *www.simulation.su*

yusupov@iias.spb.su

✉ RNSS / R. M. Yusupov,
St. Petersburg Institute of Informatics and Automation
RAS, 199178, St. Petersburg, 14th lin. V.O, 39

RNSS Officers	
President	R. M. Yusupov, *yusupov@iias.spb.su*
Chair Man. Board	A. Plotnikov, *plotnikov@sstc.spb.ru*
Secretary	M. Dolmatov, *dolmatov@simulation.su*
Repr. EUROSIM	R.M. Yusupov, *yusupov@iias.spb.su* Y. Senichenkov, senyb@dcn.icc.spbstu.ru
Deputy	B. Sokolov, *sokol@iias.spb.su*
Edit. Board SNE	Y. Senichenkov, senyb@dcn.icc.spbstu.ru

Last data update March 2016

EUROSIM OBSERVER MEMBERS

KA-SIM Kosovo Simulation Society

Kosova Association for Modeling and Simulation (KA – SIM, founded in 2009), is part of Kosova Association of Control, Automation and Systems Engineering (KA – CASE). KA – CASE was registered in 2006 as non Profit Organization and since 2009 is National Member of IFAC – International Federation of Automatic Control. KA-SIM joined EUROSIM as Observer Member in 2011. In 2016, KA-SIM has applied for full membership KA-SIM has about 50 members, and is organizing the international conference series International Conference in Business, Technology and Innovation, in November, in Durrhes, Albania, an IFAC Simulation workshops in Pristina.

→ *www.ubt-uni.net/ka-case*

ehajrizi@ubt-uni.net

✉ MOD&SIM KA-CASE; Att. Dr. Edmond Hajrizi
Univ. for Business and Technology (UBT)
Lagjja Kalabria p.n., 10000 Prishtina, Kosovo

KA-SIM Officers	
President	Edmond Hajrizi, *ehajrizi@ubt-uni.net*
Vice president	Muzafer Shala, *info@ka-sim.com*
Secretary	Lulzim Beqiri, *info@ka-sim.com*
Treasurer	Selman Berisha, *info@ka-sim.com*
Repr. EUROSIM	Edmond Hajrizi, *ehajrizi@ubt-uni.net*
Deputy	Muzafer Shala, *info@ka-sim.com*
Edit. Board SNE	Edmond Hajrizi, *ehajrizi@ubt-uni.net*
Web EUROSIM	Betim Gashi, *info@ka-sim.com*

Last data update March 2016

ROMSIM – Romanian Modelling and Simulation Society

ROMSIM has been founded in 1990 as a non-profit society, devoted to theoretical and applied aspects of modelling and simulation of systems. ROMSIM currently has about 100 members from Romania and Moldavia.

→ *www.ici.ro/romsim/*

sflorin@ici.ro

✉ ROMSIM / Florin Hartescu,
National Institute for Research in Informatics, Averescu Av. 8 – 10, 71316 Bucharest, Romania

ROMSIM Officers	
President	
Vice president	Florin Hartescu, *flory@ici.ro* Marius Radulescu, *mradulescu@ici.ro*
Repr. EUROSIM	Florin Stanciulescu, *sflorin@ici.ro*
Deputy	Marius Radulescu, *mradulescu@ici.ro*
Edit. Board SNE	
Web EUROSIM	Zoe Radulescu, *radulescu@ici.ro*

Last data update partly March 2016

MIMOS – Italian Modelling and Simulation Association

MIMOS (Movimento Italiano Modellazione e Simulazione – Italian Modelling and Simulation Association) is the Italian association grouping companies, professionals, universities, and research institutions working in the field of modelling, simulation, virtual reality and 3D, with the aim of enhancing the culture of 'virtuality' in Italy, in every application area.

MIMOS has submitted application for membership in **EUROSIM** (Observer Member).

→ *www.mimos.it*

roma@mimos.it – info@mimos.it

✉ MIMOS – Movimento Italiano Modellazione e Simulazione; via Ugo Foscolo 4, 10126 Torino – via Laurentina 760, 00143 Roma

MIMOS Officers	
President	Paolo Proietti, *roma@mimos.it*
Secretary	Davide Borra, *segreteria@mimos.it*
Treasurer	Davide Borra, *segreteria@mimos.it*
Repr. EUROSIM	Paolo Proietti, *roma@mimos.it*
Deputy	Agostino Bruzzone, *agostino@itim.unige.it*
Edit. Board SNE	Paolo Proietti, *roma@mimos.it*

Last data update March 2016

Albanian Simulation Society

At department of Statistics and Applied Informatics, Faculty of Economy, University of Tirana, Prof. Dr. Kozeta Sevrani at present is setting up an Albanian Simulation Society. Kozeta Sevrani, professor of Computer Science and Management Information Systems, and head of the Department of Mathematics, Statistics and Applied Informatic, has attended a EUROSIM board meeting in Vienna and has presented simulation activities in Albania and the new simulation society.

The society – constitution and bylaws are at work - will be involved in different international and local simulation projects, and will be engaged in the organisation of the conference series ISTI – Information Systems and Technology. The society intends to become a EUROSIM Observer Member.

kozeta.sevrani@unitir.edu.al

✉ Albanian Simulation Goup, attn. Kozeta Sevrani
University of Tirana, Faculty of Economy
rr. Elbasanit, Tirana 355 Albania

Albanian Simulation Society- Officers (Planned)	
President	Kozeta Sevrani, *kozeta.sevrani@unitir.edu.al*
Secretary	
Treasurer	
Repr. EUROSIM	Kozeta Sevrani, *kozeta.sevrani@unitir.edu.al*
Edit. Board SNE	Albana Gorishti, *albana.gorishti@unitir.edu.al* Majlinda Godolja, majlinda.godolja@fshn.edu.al

Last data update March 2016

ASIM - Buchreihen / ASIM Book Series

Proceedings

Simulation in Production und Logistics 2015 - 16. ASIM-Fachtagung Simulation in Produktion und Logistik
M. Raabe, U. Clausen (Hrsg.); ISBN 978-3-8396-0936-1, Stuttgart: Fraunhofer Verlag, 2015. (O. P.)

Simulation in Produktion und Logistik 2013: Entscheidungsunterstützung von der Planung bis zur Steuerung
W. Dangelmaier, C. Laroque, A. Klaas (Hrsg.); ISBN 978-3-942647-35-9, HNI-Verlagsschriftenreihe, Heinz Nixdorf Institut, Paderborn, 2013 (O. P.)

Modellierung, Regelung und Simulation in Automotive und Prozessautomation – Proc. 5. ASIM-Workshop Wismar 2011. C. Deatcu, P. Dünow, T. Pawletta, S. Pawletta (eds.), ISBN 978-3-901608-36-0, ASIM/ARGESIM, Wien, 2011 (O. A.)

Simulation in Produktion und Logistik 2010: Integrationsaspekte der Simulation - Technik, Organisation und Personal. G. Zülch, P. Stock, (Hrsg.), ISBN 978-3-86644-558-1, KIT Scientific Publ. Karlsruhe, 2010 (O.P.)

Monographs

Simulation und Optimierung in Produktion und Logistik – Praxisorientierter Leitfaden mit Fallbeispielen.
L. März, W. Krug, O. Rose, G. Weigert , G. (Hrsg.); ISBN 978-3-642-14535-3, Springer, 2011 (O.P.)

Verifikation und Validierung für die Simulation in Produktion und Logistik - Vorgehensmodelle und Techniken.
M. Rabe, S. Spieckermann, S. Wenzel (eds.); ISBN: 978-3-540-35281-5, Springer, Berlin, 2008 (O. P.)

Qualitätskriterien für die Simulation in Produktion und Logistik – Planung und Durchführung von Simulationsstudien. S. Wenzel, M. Weiß, S. Collisi – Böhmer, H. Pitsch, O. Rose (Hrsg.); ISBN: 978-3-540-35281-5, Springer, Berlin, 2008

Series Fortschrittsberichte Simulation

P. Einzinger: **A Comparative Analysis of System Dynamics and Agent-Based Modelling for Health Care Reimbursement Systems.**
FBS 25, ASIM/ARGESIM Vienna, 2014; ISBN 978-3-901608-75-9, ARGESIM Report 75 (O. A.)

M. Bruckner: **Agentenbasierte Simulation von Personenströmen mit unterschiedlichen Charakteristiken**
FBS 24, ASIM/ARGESIM Vienna, 2014; ISBN 978-3-901608-74-2, ARGESIM Report 74 (O. A.)

S. Emrich: **Deployment of Mathematical Simulation Models for Space Management**
FBS 23, ASIM/ARGESIM Vienna, 2013; ISBN 978-3-901608-73-5, ARGESIM Report 73 (O. A.)

G. Maletzki: **Rapid Control Prototyping komplexer und flexibler Robotersteuerungen auf Basis des SBC-Ansatzes.** FBS 22, ASIM/ARGESIM Vienna, 2014; ISBN 978-3-901608-72-8, ARGESIM Report 72 (O. A.)

X. Descovich: **Lattice Boltzmann Modeling and Simulation of Incompressible Flows in Distensible Tubes for Applications in Hemodynamics**
FBS 21, ASIM/ARGESIM Vienna, 2012; ISBN 978-3-901608-71-1, ARGESIM Report 71 (O. A.)

F. Miksch: **Mathematical Modeling for New Insights into Epidemics by Herd Immunity and Serotype Shift**
FBS 20, ASIM/ARGESIM Vienna, 2012; ISBN 978-3-901608-70-4, ARGESIM Report 70 (O. A.)

S. Tauböck: **Integration of Agent Based Modelling in DEVS for Utilisation Analysis: The MoreSpace Project at TU Vienna;** FBS 19, ASIM/ARGESIM Vienna, 2012; ISBN 978-3-901608-69-8, ARGESIM Report 69 (O. A.)

Ch. Steinbrecher: **Ein Beitrag zur prädiktiven Regelung verbrennungsmotorischer Prozesse**
FBS 18, ASIM/ARGESIM Vienna, 2010; ISBN 978-3-901608-68-1, ARGESIM Report 68 (O. A.)

O. Hagendorf: **Simulation-based Parameter and Structure Optimisation of Discrete Event Systems**
FBS 17, ASIM/ARGESIM Vienna, 2010; ISBN 978-3-901608-67-4, ARGESIM Report 67 (O. A.)

Orders via ASIM (O. A.) **or via Publisher** (O. P.)**:**
ASIM/ARGESIM Office Germany, Hochschule Wismar, PF 1210, 23952 Wismar, Germany
ASIM/ARGESIM Geschäftsstelle Österreich, c/o DWH, Neustiftgasse 57, 1040 Vienna, Austria
Download (some books) via ASIM webpage in preparation
Info: www.asim-gi.org, info@asim-gi.org

Parlez-vous MATLAB?

Über eine Million Menschen weltweit sprechen MATLAB. Ingenieure und Wissenschaftler in allen Bereichen – von der Luft- und Raumfahrt über die Halbleiterindustrie bis zur Biotechnologie, Finanzdienstleistungen und Geo- und Meereswissenschaften – nutzen MATLAB, um ihre Ideen auszudrücken. Sprechen Sie MATLAB?

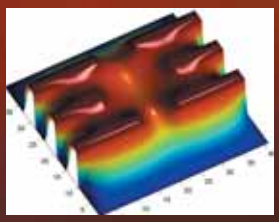

Modellierung eines elektrischen Potentials in einem Quantum Dot.

Dieses Beispiel finden Sie unter: www.mathworks.de/ltc

Image: Kim Young-Sang, Jung HeeJun, Quantum Device Lab, Hanyang Univ.

MATLAB®

The language of technical computing